

The Immunomodulatory Effects of the Garlic Organosulfur Compounds allicin and Z-Ajoene in an *in vitro* Murine Model of LPS-Induced Inflammation

Jessica Kaari Hitchcock

Thesis Presented for the Degree of
MASTER OF SCIENCE IN MEDICINE

in the Department of Medical Biochemistry

Faculty of Health Sciences

UNIVERSITY OF CAPE TOWN

February 2015

Supervisors:

Dr. Georgia Schäfer

Prof. Ariele A. Katz

Dr. Catherine H. Kaschula



The financial assistance of the National Research Foundation (NRF) towards this research is hereby acknowledged. Opinions expressed and conclusions arrived at, are those of the author and are not necessarily to be attributed to the NRF

The copyright of this thesis vests in the author. No quotation from it or information derived from it is to be published without full acknowledgement of the source. The thesis is to be used for private study or non-commercial research purposes only.

Published by the University of Cape Town (UCT) in terms of the non-exclusive license granted to UCT by the author.

Declaration

I, Jessica Kaari Hitchcock, hereby declare that the work on which this dissertation/thesis is based is my original work (except where acknowledgements indicate otherwise) and that neither the whole work nor any part of it has been, is being, or is to be submitted for another degree in this or any other university.

I empower the university to reproduce for the purpose of research either the whole or any portion of the contents in any manner whatsoever.

Signature: _____

Date: _____

Acknowledgements

I would like to formally thank the following people and institutions:

My supervisors Georgia Schäfer, Catherine Kaschula and Arie Katz for their advice, guidance and financial support for the past two years.

George Cooper and Aron Abera for their support and technical advice.

Jacqueline Meyer from the Centre for Proteomic and Genomic Research (CPGR) for her assistance with Biogazelle qBase plus analysis software.

Jonathon Cotton and Daniel Kuzsa for synthesising the garlic organosulfur compounds used in this study.

The International Centre for Genetic Engineering and Biotechnology (ICGEB) for the use of their facilities and technical equipment.

Graham Christians, Roshan Ebrahim and Xolani Nonzinyana for the day-to-day running of our laboratory.

Paul Kennedy and my parents for their continued emotional support.

The University of Cape Town and the National Research Foundation for financial support.

The Cancer Association of South Africa (CANSA) for funding this project.

Abstract

Cancer is a leading cause of death in the modern world. Chronic inflammation facilitates tumourigenesis and cancer progression by providing an environment conducive to cancer. Dysregulation of the immune response, and particularly inflammation, is an important part of this process.

Garlic (*Allium sativum*) has been used for centuries as both a prophylactic and therapeutic medicinal agent, more recent epidemiological and experimental evidence shows that garlic has both cancer-preventative and immune system-enhancing effects. While garlic contains many bioactive compounds, garlic organosulfur compounds (OSCs) have been most widely studied for their anti-cancer properties. In this study, we hypothesize that garlic OSCs modulate the inflammatory immune response by downregulating pro-inflammatory while stimulating anti-inflammatory responses, preventing the formation of a cancer-friendly chronic inflammatory environment. To test this hypothesis we established and optimised an *in vitro* inflammatory model using lipopolysaccharide-stimulated RAW264.7 murine macrophages.

Expression analysis of selected inflammatory genes was performed by qPCR on RNA harvested 4 h and 8 h post treatment, while protein expression was analysed by ELISA using cell culture supernatant samples harvested 8 h and 24 h post treatment. These experiments were complemented by gene and protein arrays. Results showed that allicin had a more pronounced upregulatory effect on LPS-induced gene expression 4 h post-LPS treatment. In contrast, Z-ajoene generally had mild downregulatory effects on the expression of LPS-induced genes. Conversely, Z-ajoene had pronounced downregulatory effects on LPS-induced inflammatory proteins after 24 h, while allicin showed mild up- or downregulatory effects. Overall, we found that allicin induced an initial pro-inflammatory gene response, while Z-ajoene induced a longer-lasting anti-inflammatory response at a protein level.

Finally, as many of the inflammatory genes investigated are regulated by the transcription factor STAT3, we investigated the effects of allicin and Z-ajoene on STAT3 phosphorylation and hence activation. Western blot analyses showed that allicin increased LPS-induced STAT3 phosphorylation (2-8 h), while Z-ajoene was found to decrease the phosphorylation of STAT3 after 4 h. These effects on STAT3 phosphorylation are in agreement with the early pro-inflammatory effect of allicin and the later anti-inflammatory effect of Z-ajoene on LPS-induced gene and protein expression. Further, using Western blotting we showed that *E/Z*-ajoene directly interacts with and reversibly alkylates STAT3 via a thiol-disulfide reaction with a cysteine thiolate on STAT3.

We propose that the covalent modification of STAT3 by *E/Z*-ajoene may provide the chemical basis for the observed decrease in STAT3 phosphorylation. This is the first time that a garlic OSC has been shown to modulate the immune system by directly interacting with STAT3. Our findings therefore support the use of dietary garlic containing Z-ajoene and allicin as an immunomodulatory agent which may have implications in the prevention of inflammatory diseases.

Table of Contents

| | |
|---|-----|
| Declaration..... | i |
| Acknowledgements..... | ii |
| Abstract..... | iii |
| Abbreviations and Symbols..... | vii |
| Chapter 1 Literature Review..... | 1 |
| 1.1. Cancer | 1 |
| 1.2. Inflammation and cancer | 1 |
| 1.2.1. The role of NF- κ B and STAT3 in tumourigenesis and cancer progression | 3 |
| 1.2.2. Use of NSAIDs in cancer prevention | 6 |
| 1.2.3. Immunomodulatory and anti-inflammatory properties of natural dietary compounds | 7 |
| 1.3. Medicinal use of garlic | 9 |
| 1.3.1. Epidemiological evidence for garlic consumption protecting against cancer | 9 |
| 1.4. Chemical structures of naturally occurring garlic organosulfur compounds..... | 9 |
| 1.5. Garlic organosulfur compound chemistry and metabolism | 13 |
| 1.6. Evidence for the effects of garlic on inflammatory cytokine and chemokine expression.... | 14 |
| 1.7. Evidence for the effects of garlic on inflammatory enzymes | 16 |
| 1.8. Evidence for the effects of garlic on inflammatory signalling pathways | 17 |
| 1.9. Possible chemical biology behind the biological activity of garlic OSCs | 19 |
| 1.10. Significance | 21 |
| 1.10.1. Hypothesis..... | 21 |
| 1.10.2. Aim | 21 |
| 1.10.3. Objectives..... | 21 |
| Chapter 2 Materials and Methods..... | 23 |
| 2.1. Cell culture | 23 |
| 2.1.1. Cell lines and cell culture media | 23 |
| 2.1.2. Cell plating and splitting..... | 23 |
| 2.1.3. Cell counting | 23 |
| 2.2. Garlic organosulfur compounds..... | 24 |
| 2.3. Thin layer chromatography..... | 26 |
| 2.4. Cell viability assay (MTT assay) | 27 |
| 2.5. <i>In vitro</i> inflammatory model | 28 |
| 2.6. Gene and protein nomenclature | 28 |
| 2.7. Gene expression analysis | 29 |
| 2.7.1. RNA extraction | 29 |
| 2.7.2. DNase I treatment..... | 30 |
| 2.7.3. Ethanol precipitation of RNA oligonucleotides..... | 30 |

| | | |
|------------|---|----|
| 2.7.4. | RNA integrity analysis | 30 |
| 2.7.5. | Reverse transcription of RNA..... | 31 |
| 2.7.6. | Quantitative real-time PCR (qPCR) | 31 |
| 2.8. | RT ² Profiler PCR Arrays..... | 35 |
| 2.8.1. | Reverse transcription | 35 |
| 2.8.2. | Quantitative real-time PCR (qPCR) | 36 |
| 2.9. | Protein expression analysis..... | 36 |
| 2.9.1. | Enzyme-Linked Immunosorbent Assay | 36 |
| 2.9.2. | SDS-PAGE and Western blot analysis..... | 37 |
| 2.10. | Proteome Profiler™ Mouse Cytokine Array | 39 |
| 2.11. | Protein alkylation by dansylated-ajoene | 39 |
| 2.12. | Statistical analysis | 40 |
| Chapter 3 | Results | 41 |
| 3.1. | MTT colorimetric cell viability assays..... | 41 |
| 3.2. | Establishing an <i>in vitro</i> inflammatory model | 41 |
| 3.2.1. | Optimizing LPS concentration and stimulation time | 43 |
| 3.3. | Gene and protein expression of selected cytokines and inflammatory mediators..... | 47 |
| 3.3.1. | Cytokines downregulated by garlic OSC treatment..... | 55 |
| 3.3.2. | Cytokines and inflammatory mediators upregulated by garlic OSC treatment..... | 56 |
| 3.3.3. | Cytokines and inflammatory mediators affected differently by garlic OSCs | 57 |
| 3.3.4. | Selecting optimal timepoints for gene and protein array experiments | 57 |
| 3.4. | RT ² Profiler PCR Array for Inflammatory Response and Autoimmunity | 58 |
| 3.4.1. | Allicin treatment | 59 |
| 3.4.2. | Z-ajoene treatment | 62 |
| 3.5. | Proteome Profiler Mouse Cytokine Array..... | 65 |
| 3.6. | The effect of selected garlic OSCs on LPS-induced STAT3 phosphorylation..... | 72 |
| 3.7. | STAT3 alkylation by <i>E/Z</i> -ajoene..... | 74 |
| Chapter 4 | Discussion..... | 76 |
| 4.1. | Establishment of a well-defined <i>in vitro</i> inflammatory model | 76 |
| 4.2. | Experiments investigating immune and inflammatory responses | 78 |
| 4.2.1. | Allicin and Z-ajoene regulate interleukins to prevent inflammation..... | 78 |
| 4.2.2. | Allicin and Z-ajoene differentially modulate chemokine expression..... | 80 |
| 4.2.3. | Differential effects on inflammatory enzymes | 81 |
| 4.2.4. | Effects on TNF and TNF ligand superfamily cytokines | 82 |
| 4.3. | Garlic OSCs may affect STAT3 phosphorylation and activity through posttranslational modification of cysteine residues | 84 |
| 4.4. | Potential garlic OSC-target proteins in inflammatory signalling pathways | 87 |
| Conclusion | | 89 |

| | | |
|------------|---|-----|
| Appendix A | Reagent Recipes..... | 90 |
| Appendix B | Literature Review Supplementary Tables..... | 92 |
| Appendix C | MIQE Guidelines Checklist and qPCR Optimisation and Quality Control | 94 |
| References | | 102 |

Abbreviations and Symbols

| | |
|-----------------------|---|
| <i>Actb</i> /ACTB | β-actin |
| AGE | aged garlic extract |
| AM | allyl mercaptan |
| AMDS | allyl methyl disulfide |
| AMS | allyl methyl sulfide |
| AMTS | allyl methyl trisulfide |
| ANOVA | analysis of variance |
| AP1 | activator protein-1 |
| AST | aspartate amino transferase |
| <i>B2m</i> /B2M | β2-microglobulin |
| <i>Bcl2</i> /BCL2 | B-cell lymphoma-2 |
| CAT | catalase |
| <i>Ccl11</i> /CCL11 | chemokine C-C motif ligand 11 |
| <i>Ccl2</i> /CCL2 | chemokine C-C motif ligand 2 |
| <i>Ccl3</i> /CCL3 | chemokine C-C motif ligand 3 |
| <i>Ccl4</i> /CCL4 | chemokine C-C motif ligand 4 |
| <i>Ccl5</i> /CCL5 | chemokine C-C motif ligand 5 |
| <i>Ccl8</i> /CCL8 | chemokine C-C motif ligand 8 |
| <i>Cd40l</i> /CD40L | CD40 ligand |
| cDNA | complementary deoxyribonucleic acid |
| COX | cyclooxygenase |
| <i>Cox2</i> /COX2 | cyclooxygenase 2 |
| CPGR | Centre for Proteomic and Genomic Research |
| Cq | quantification cycle |
| <i>Csf2</i> /CSF2 | colony stimulating factor 2 |
| <i>Csf3</i> /CSF3 | colony stimulating factor 3 |
| <i>Cxcl1</i> /CXCL1 | chemokine C-X-C motif ligand 1 |
| <i>Cxcl10</i> /CXCL10 | chemokine C-X-C motif ligand 10 |
| <i>Cxcl11</i> /CXCL11 | chemokine C-X-C motif ligand 11 |
| <i>Cxcl12</i> /CXCL12 | chemokine C-X-C motif ligand 12 |
| <i>Cxcl16</i> /CXCL16 | chemokine C-X-C motif ligand 16 |
| <i>Cxcl2</i> /CXCL2 | chemokine C-X-C motif ligand 2 |
| <i>Cxcl3</i> /CXCL3 | chemokine C-X-C motif ligand 3 |
| <i>Cxcl8</i> /CXCL8 | chemokine C-X-C motif ligand 8 |
| <i>Cxcl9</i> /CXCL9 | chemokine C-X-C motif ligand 9 |
| <i>Cxcr4</i> /CXCR4 | chemokine C-X-C motif receptor 4 |
| CYP1A2 | cytochrome P450, family 1, subfamily A, polypeptide 2 |
| CYP2E1 | cytochrome P450, family 2, subfamily E, polypeptide 1 |
| Cys | cysteine |
| DADS | diallyl disulfide |
| DAS | diallyl sulfide |
| DATS | diallyl trisulfide |
| DBD | DNA-binding domain |
| DEN | diethylnitrosamine |
| DMDS | dimethyl disulfide |
| DMEM | Dulbecco's-Modified Eagle Medium |
| DMSO | dimethyl sulfoxide |
| DNA | deoxyribonucleic acid |

| | |
|--------------------------|---|
| dsDNA | double-stranded DNA |
| DTT | dithiothretinol |
| <i>E.coli</i> | <i>Escherichia coli</i> |
| EDTA | ethylenediaminetetraacetic acid |
| ELISA | enzyme-linked immunosorbent assay |
| ERK | extracellular signal-regulated kinase |
| EtOAc | ethyl acetate |
| <i>Fas</i> / <i>FASL</i> | Fas ligand |
| FBS | foetal bovine serum |
| <i>Gapdh</i> /GAPDH | glyeraldehyde-3-phosphate dehydrogenase |
| GMCSF | Granulocyte macrophage colony stimulating factor |
| GPE | garlic powder extract |
| GPX | glutathione peroxidase |
| GSSG | oxidised glutathione |
| H | hour |
| HO1 | heme oxygenase-1 |
| HRP | horse radish peroxidase |
| HSD | honest significant difference |
| HUVECs | human umbilical vein endothelial cells |
| ICAM1 | intercellular adhesion molecule-1 |
| <i>Ifng</i> /IFNG | interferon- γ |
| IKK α | inhibitory I κ B kinase- α |
| IKK β | inhibitory I κ B kinase- β |
| <i>Il10</i> /IL10 | interleukin-10 |
| <i>Il12</i> /IL12 | interleukin-12 |
| <i>Il12b</i> /IL12B | interleukin-12 subunit- β |
| <i>Il13</i> /IL13 | interleukin-13 |
| <i>Il18</i> /IL18 | interleukin-18 |
| <i>Il1a</i> /IL1A | interleukin-1 α |
| <i>Il1b</i> /IL1B | interleukin-1 β |
| <i>Il1rn</i> /IL1RN | interleukin-1 receptor antagonist |
| <i>Il22</i> /IL22 | interleukin-22 |
| <i>Il23</i> /IL23 | interleukin-23 |
| <i>Il23r</i> /IL23R | interleukin-23 receptor |
| <i>Il27</i> /IL27 | interleukin-27 |
| <i>Il4</i> /IL4 | interleukin-4 |
| <i>Il6</i> /IL6 | interleukin-6 |
| <i>Il8</i> /IL8 | interleukin-8 |
| I κ B | inhibitory NF- κ B |
| JAK | Janus kinase |
| JAK/STAT | Janus kinase/signal transducer and activator of transcription |
| JNK | c-Jun N-terminal kinase |
| kcal | kilocalories |
| LDH | lactate dehydrogenase |
| LPS | lipopolysaccharide |
| <i>Lta</i> /LTA | lymphotoxin- α |
| <i>Ltb</i> /LTB | lymphotoxin- β |
| MAPK | mitogen-activated protein kinase |
| MDSCs | myeloid-derived suppressor cells |
| mg | milligrams |
| MHz | megahertz |

| | |
|-----------------------|---|
| min | minutes |
| MIQE | minimum information for publication of quantitative real-time PCR experiments |
| ml | millilitre |
| MTT | 3-[4,5-dimethylthiazol-2-yl]-2,5-diphenyltetrazolium bromide |
| NCBI | National Center for Biotechnology Information |
| NCI | National Cancer Institute |
| NF- κ B | nuclear factor κ -light-chain-enhancer of activated B cells |
| ng | nanogram |
| NMR | nuclear magnetic resonance |
| NO | nitric oxide |
| <i>Nos2</i> /NOS2 | nitric oxide synthase 2 |
| NQO1 | NAD(P)H:quinone acceptor oxidoreductase 1 |
| NRF2 | nuclear factor (erythroid-derived 2)-like 2 |
| NRQ | normalised relative quantities |
| ns | not significant |
| NSAIDs | non-steroidal anti-inflammatory drugs |
| °C | degrees Celsius |
| OSCs | organosulfur compounds |
| PAMPs | pattern-associated molecular patterns |
| PBMCs | peripheral blood mononuclear cells |
| PBS | phosphate-buffered saline |
| PBST | phosphate buffered saline Tween-20 |
| PCR | polymerase chain reaction |
| PEN-STREP | penicillin-streptomycin |
| pg | pictogram |
| PGE2 | prostaglandin E2 |
| PI3K | phosphoinositide-3-kinase |
| pK _a | acid-dissociation constant |
| PKB | protein kinase B |
| PMA | phorbol myristate |
| p-STAT3 | phosphorylated STAT3 |
| <i>Ptgs2</i> /PTGS2 | prostaglandin-endoperoxide synthase-2 |
| qPCR | quantitative real-time polymerase chain reaction |
| QR | quinone reductase |
| <i>Rantes</i> /RANTES | regulated on activation, normal T cell expressed and secreted |
| R _f | retardation factor |
| RIN | ribonucleic acid integrity number |
| RNA | ribonucleic acid |
| RNS | reactive nitrogen species |
| ROS | reactive oxygen species |
| rpm | rotations per minute |
| RTPrimerDB | Real Time Primer Database |
| s | seconds |
| SAC | S-allyl cysteine |
| SAMC | S-allyl mercaptocysteine |
| SD | standard deviation |
| SDS | sodium dodecyl sulfate |
| SDS-PAGE | sodium dodecyl sulfate-polyacrylamide gel electrophoresis |
| <i>Sele</i> /SELE | E-selectin |
| SEM | standard error of the mean |

| | |
|-------------------------|--|
| SOD | superoxide dismutase |
| STAT1 | signal transducer and activator of transcription 1 |
| STAT3 | signal transducer and activator of transcription 3 |
| TAD | trans-activating domain |
| TAK1 | activated kinase-1 |
| TAMs | tumour-associated macrophages |
| TBS | Tris-buffered saline |
| TBST | Tris-buffered saline Tween-20 |
| <i>Tgfb</i> /TGFB | tumour growth factor- β |
| TIMP1 | tissue inhibitor of metalloprotease-1 |
| TLC | thin-layer chromatography |
| TLR | toll-like receptor |
| TLR3 | toll-like receptor 3 |
| TLR4 | toll-like receptor 4 |
| T _m | melting temperature |
| <i>Tnf</i> /TNF | tumour necrosis factor |
| TNFSF | TNF ligand superfamily |
| <i>Tnfsf10</i> /TNFSF10 | TNF ligand superfamily, member 10 |
| <i>Tnfsf2</i> /TNFSF2 | TNF ligand superfamily, member 2 |
| <i>Tnfsf2</i> /TNFSF6 | TNF ligand superfamily, member 6 |
| <i>Tnfsf3</i> /TNFSF3 | TNF ligand superfamily, member 3 |
| <i>Tnfsf5</i> /TNFSF5 | TNF ligand superfamily, member 5 |
| Tyr | tyrosine |
| <i>Vegf</i> /VEGF | vascular endothelial growth factor |
| WHO | World Health Organisation |
| μ g | microgram |
| μ M | micromolar |

Chapter 1 Literature Review

1.1. Cancer

Cancer is a collective term for diseases characterised by groups of cells with abnormal or uncontrolled growth, called tumours. Tumourigenesis is a multistep process which involves the sequential acquisition of genetic and epigenetic mutations in cells which may confer a proliferative advantage to these cells. In the past 15 years, researchers have identified a number of acquired biological capabilities inherent in cancer, which have been termed the “Hallmarks of Cancer”^{1,2}. These capabilities are described as the ability to sustain proliferative signalling; evade growth suppressors; avoid immune destruction; enable replicative immortality; activate tumour invasion and metastasis; induce angiogenesis; resist cell death; and modify cellular metabolism². Two characteristics recognised to facilitate or enable the acquisition and maintenance of the aforementioned hallmarks include genomic instability (and mutability) and tumour-promoting inflammation².

Significantly, cancer is a leading cause of death worldwide, with approximately 7.6 million deaths occurring in the year 2008, and 13.1 million cancer-related deaths projected for the year 2030³. Despite medical advances in early cancer detection methods and the development of new anti-cancer drugs, limited access to healthcare and the high cost of cancer treatments obstructs early cancer diagnosis and effective treatment in low income groups^{3,4}. This explains why 70% of world cancer deaths occur in low- and middle-income countries^{3,4}. In recent years there has been a growing awareness that cancer prevention is of utmost importance^{5,6}: it has been described by the World Health Organisation (WHO) as the “most cost-effective and long-term strategy for the control of cancer”⁴, as many cancers are preventable with environmental or exogenous causative agents playing a role^{4,6}. Some exogenous factors include tobacco and alcohol use; a lack of exercise; an unhealthy diet; obesity; chemical carcinogens; radiation; and bacterial and viral infections^{4,6}.

1.2. Inflammation and cancer

The causative agents or risk factors in cancer are often associated with changes to the immune system. The mammalian immune system consists of two components: the innate and adaptive immune responses⁷⁻⁹. The innate immune response is the first line of defence against microbial invasion and immediately recognises and counters infections while the slower, but more specific, adaptive response is mounted. The cellular components of the innate immune response comprise macrophages, dendritic cells, mast cells, neutrophils, eosinophils, and natural killer cells which can directly activate effector mechanisms of innate immunity. These include phagocytosis and activation

of pro-inflammatory pathways that induce the expression of a set of endogenous signals in the form of inflammatory cytokines and chemokines. These signals control the recruitment of leukocytes to the sites of infection and regulate the activation of appropriate effector mechanisms, for example by controlling differentiation of T lymphocytes into effector cells of a particular type. The acute inflammatory response and innate immune cells then secrete factors and activate multiple signalling pathways which promote wound healing⁷⁻⁹.

Acute inflammation is short-lived and forms an essential part of the innate immune response. However, chronic inflammation (due to persistent infection or long-term exposure to chemical irritants) leads to dysregulation of the inflammatory response and results in immunosuppression^{10,11}. Research suggests that chronic or tumour-associated inflammation may facilitate the acquisition of some cancer hallmark capabilities^{2,12,13}. This is because chronic inflammation leads to a cancer-friendly environment through sustained exposure of cells to growth and pro-angiogenic factors; anti-apoptotic regulators; extracellular matrix-remodelling enzymes; and damaging antimicrobial factors including defensins and reactive oxygen and nitrogen species (ROS and RNS)^{2,12,13}. This leads to a pro-proliferative, pro-angiogenic, anti-apoptotic, potentially DNA-damaging and immune surveillance-compromised environment conducive to tumourigenesis^{2,12,13}. Inflammation has thus been described as a double-edged sword in neoplasia: as an acute response to insult it can initiate the immune response and promote anti-tumour immunity, but under sustained chronic conditions it may facilitate immunosuppression and provide an environment conducive to tumour initiation, promotion and progression¹⁴. This has led to tumours being described as “wounds that do not heal”¹⁵.

The presence of inflammatory immune cells, particularly tumour-associated macrophages (TAMs) and myeloid-derived suppressor cells (MDSCs) (a heterogeneous population of myeloid progenitor cells and immature innate immune cells) is closely associated with malignancy and all stages of tumourigenesis and tumour progression^{16,17}. Indeed, there is a strong correlation between TAM and MDSC density within a tumour and poor patient prognosis^{16,17}. While TAMs appear to have a symbiotic relationship with cancer cells¹⁶, under certain conditions these cells can also display tumouricidal activities¹⁸.

The paradoxical nature of the immune response extends to the effector molecules/proteins which include inflammatory cytokines, chemokines and enzymes. These effector proteins are largely produced by innate immune cells to induce inflammation and recruit immune cells⁷⁻⁹. While the classification of cytokines and chemokines as either pro- or anti-inflammatory mediators has been criticised for being overly simplistic¹⁹, it is still of value to consider their predominant activity. Typical

cytokines generally considered to exert pro-inflammatory effects include interleukin-1 β (IL1 β), interleukin-6 (IL6), interleukin-12 (IL12), interleukin-18 (IL18), interleukin-23 (IL23), interleukin-27 (IL27) tumour necrosis factor (TNF) and interferon- γ (IFNG)^{19–22} *. On the other hand, interleukin-4 (IL4), interleukin-10 (IL10), interleukin-13 (IL13) and tumour growth factor- β (TGFB) are generally considered to exert anti-inflammatory effects^{19,23}. Chemokines are chemoattractant cytokines that facilitate chemotaxis of immune cells that express complementary receptors²⁴. In this way, chemokines secreted in the inflammatory or tumour microenvironment selectively regulate the recruitment of immune cells to the site of injury⁹. Significantly, TAMs have been shown to have constitutive and elevated expression levels of many chemokines including chemokine C-C motif ligand 2 (CCL2), chemokine C-C motif ligand 5 (CCL5), chemokine C-X-C motif ligand 9 (CXCL9), chemokine C-X-C motif ligand 10 (CXCL10), chemokine C-X-C motif ligand 12 (CXCL12) and chemokine C-X-C motif ligand 16 (CXCL16), as well as chemokine receptors which facilitate their recruitment to tumour sites²⁵. Important inflammatory enzymes include the cyclooxygenase (COX) enzymes which convert arachidonic acid into prostaglandins (hormone-like lipid signalling molecules), which regulate a variety of functions including vascular permeability, epithelial-barrier function and inflammation^{26,27}. Another enzyme involved in the inflammatory response is the inducible nitric oxide synthase 2 (NOS2) which produces nitric oxide (NO); a reactive nitrogen species (RNS) involved in inflammatory signalling^{28,29}. The expression and secretion of these inflammatory effector molecules or proteins is regulated by diverse cell signalling networks which are activated in response to cellular or exogenous stresses⁸.

1.2.1. The role of NF- κ B and STAT3 in tumourigenesis and cancer progression

Transcription factors nuclear factor κ -light-chain-enhancer of activated B cells (NF- κ B) and signal transducer and activator of transcription 3 (STAT3) are central regulators of the immune response and have been shown to facilitate tumourigenesis and cancer progression^{30–32}. NF- κ B and STAT3 have been shown to regulate the expression of cytokines and chemokines as well as genes involved in cell survival, growth, angiogenesis and tissue remodelling³⁰. Indeed, these transcription factors are often both constitutively active in cancer cells, and recent evidence suggests that they cooperate to promote tumourigenesis and cancer progression^{12,33–36}. NF- κ B and STAT3 likely facilitate tumourigenesis and cancer progression through their gene products which can re-activate inflammatory signalling pathways, resulting in feedback signalling loops that maintain a chronic inflammatory land, thus

*According to “The Guidelines for Human Nomenclature”¹⁶⁶, human genes and proteins are represented by symbols written in uppercase Latin letters and Arabic numerals. Genes are distinguished from proteins by the use of italics. For further information see Section 2.6

ch
attention from cancer researchers. It has since been recognised as a master regulator of cellular development and the stress-induced immune response⁴¹. NF- κ B is a heterodimeric protein consisting of different combinations of the five members of the REL-homology domain family of proteins: RELA

(also known as p65), RELB, c-REL, p50 and p52⁴². In the cell, cytoplasmic NF-κB heterodimers remain inactive while complexed with inhibitory NF-κB (IκB) proteins³⁰. NF-κB signalling is induced by the engagement of pattern recognition receptors (e.g. toll-like receptors (TLRs)), cytokine receptors or antigen receptors which activate signalling pathways and thereby mediate phosphorylation and consequent activation of IκB kinases (IKKα or IKKβ). IKKα or IKKβ phosphorylate IκB proteins, which induces ubiquitin-mediated degradation of IκB and allows NF-κB heterodimers to translocate into the nucleus and facilitate gene transcription. NF-κB gene transcription is further regulated by NF-κB post-translational modifications (such as acetylation and S-glutathionylation) and through interactions with transcription factors or co-factors³⁰. Some NF-κB target genes include cytokines such as *IL1B*, *IL6*, *IL12* subunit β (*IL12B*), *IL10* and *IL27*; chemokines including *CCL2*, *CCL3*, *CCL4*, *CCL5*, *CCL20*, *CXCL1*, *CXCL2*, *CXCL3* and *CXCL10*; TNF superfamily ligands (*TNFSF*) including *TNF* (also known as *TNFSF2*) and TNF-related apoptosis inducing ligand (*TRAIL*, also known as *TNFSF10*); growth or differentiation factors including colony stimulating factor 2 (*CSF2*) and colony stimulating factor 3 (*CSF3*); and inflammatory enzymes *COX2* and *NOS2* (reviewed by Pahl (1999)⁴³).

As previously mentioned, NF-κB plays a central role in tumourigenesis where it is often constitutively active in cells in the chronic inflammatory environment^{32,38,44}. In an established tumour, however, NF-κB activation and function is often inhibited in TAMs while remaining active in tumour cells²⁵. This suggests that during tumourigenesis, prolonged activation of NF-κB in both pre-malignant and immune cells can facilitate tumour initiation and promotion, while in the tumour microenvironment constitutively active NF-κB in tumour cells and compromised NF-κB activation in TAMs maintains inflammatory conditions but compromises immune surveillance. NF-κB activation, therefore, has complex context-dependent effects in the tumour microenvironment, especially with regards to the tumourigenic stage and cell type.

STAT3 is another transcription factor involved in immune system regulation and implicated in cancer⁴⁵. It is a member of the evolutionarily-conserved signal transducer and activator of transcription (STAT) protein family that regulates diverse cellular functions including cell growth, proliferation, differentiation and survival⁴⁶. STAT3 is activated in response to a variety of factors including intrinsic cytokines and growth factors (often NF-κB target gene products such as IL6 and IL10) and extrinsic chemical carcinogens, pathogens and UV radiation³¹. These factors regulate STAT3 activation by inducing receptor and non-receptor tyrosine kinase-mediated phosphorylation of STAT3 at Tyr705 (reviewed by Aggarwal et al. (2009)⁴⁷). STAT3 Tyr705 phosphorylation induces homo- or heterodimer (with STAT1) formation and subsequent nuclear translocation, where STAT3 regulates the transcription of multiple gene targets involved in the immune response⁴⁷. Target genes include inflammatory cytokines, such as *IL6*, *IL10*, *IL11*, *IL17*, *IL23*; chemokines including *CXCL12*⁴⁸; pro-

proliferative growth factors and cell cycle proteins including vascular endothelial growth factor (*VEGF*)⁴⁹ and cyclin D1/D2⁵⁰; and anti-apoptotic mediators such as B-cell lymphoma-2 (*BCL2*)⁴⁹.

Interestingly, differences in the duration of STAT3 activation have profound effects on the inflammatory response^{51,52}. A transient peak in STAT3 activation (generally induced by IL6-family cytokines) results in a pro-inflammatory immune response, while sustained STAT3 activation (induced by IL10-family cytokines) induces the expression of anti-inflammatory and immunosuppressive genes^{51,52}. Like NF- κ B, STAT3 gene targets can either promote or repress tumourigenesis. The IL6-induced pro-inflammatory STAT3 signalling, for example, has been shown to protect against tumourigenesis by promoting the acute inflammatory response and hence immunosurveillance, but dysregulation of this pathway can result in excessive inflammation and the formation of a chronic inflammatory and tumour-promoting microenvironment⁵³. The IL10-induced anti-inflammatory and immunosuppressive response, on the other hand, plays an important role in resolving inflammation by dampening the immune response in order to promote wound healing and restore normal tissue function^{23,54–56}. In addition, IL10-mediated STAT3 signalling protects against inappropriate immune responses which can result in autoimmune diseases^{23,54–56}. Colitis, for example, can result from an overactive immune response mounted against commensal gut microflora⁵⁷. These IL10/STAT3-mediated immunosuppressive and wound-healing mechanisms, however, can also be co-opted in a tumour to promote excessive cell proliferation and safeguard premalignant cells from apoptosis and immune surveillance^{31,58,59}.

While NF- κ B and STAT3 are both fast-acting transcription factors which respond to intrinsic and extrinsic cell stress signals to initiate the transcription of important immune-regulating genes, they are clearly regulated by distinct signalling mechanisms³⁰. It is important to note that as STAT3 and NF- κ B activator mutations are rare, constitutive activation of NF- κ B and STAT3 during chronic inflammation and in the tumour microenvironment is generally mediated by dysregulation of upstream signalling proteins or through cytokine activation of signalling pathways^{30,60}. Significantly, NF- κ B transcriptional activity can indirectly activate STAT3 by inducing the transcription of STAT3 signalling molecules, and vice versa³⁰. In addition, NF- κ B and STAT3 have been shown to directly interact and this interaction can regulate the expression of NF- κ B target genes^{33–35,61,62}. This NF- κ B-STAT3 complex preferentially transcribes genes with binding sites for both NF- κ B and STAT3 over genes with only NF- κ B binding sites³⁵. This complex web of regulation has significant implications in chronic inflammatory conditions and in the tumour microenvironment where both transcription factors are active, as their interaction has been shown to enhance the transcription of tumour-promoting genes, while suppressing NF- κ B-mediated transcription of immunostimulatory and

tumour-suppressing genes^{33,35,63}. STAT3 and NF-κB are therefore attractive therapeutic targets for inflammatory diseases as well as cancer.

Therapeutic attempts to prevent cancer via NF-κB or STAT3 inhibition have had mixed outcomes in animal models of tumourigenesis. In some cases, inhibition of NF-κB^{64,65} or STAT3^{49,53,66–70} signalling can prevent tumour formation, induce apoptosis in cancer cells and thereby decrease tumour size. Inhibition of either NF-κB^{71,72} or STAT3^{23,55,73} signalling, however, has also been shown to promote inflammation, tumourigenesis and tumour progression. Grivennikov and Karin (2010) suggest that the different outcomes observed from the use of NF-κB or STAT3 inhibitors are a result of differential responses from immune cells and epithelial cells³⁰. It is thus important to consider all cell types present in the inflammatory or tumour microenvironment when developing drugs to target these important transcription factors with a view to prevent or treat cancer. An alternative strategy to directly targeting NF-κB or STAT3 pathways is to target inflammatory cytokines, enzymes and mediators which facilitate the activation and maintenance of NF-κB and STAT3 signalling. Examples of these kind of drugs include non-steroidal anti-inflammatory drugs (NSAIDs) (e.g. aspirin)^{74,75} and cytokine and chemokine inhibitors^{76,77}. Further, drugs which inhibit NF-κB and STAT3 interaction could prevent the preferential transcription of many tumour-promoting gene products with NF-κB and STAT3 binding sites, without compromising the acute inflammatory immune response³⁰.

1.2.2. Use of NSAIDs in cancer prevention

NSAIDs, such as aspirin (acetylsalicylic acid) and ibuprofen, are anti-inflammatory, anti-analgesic and anti-pyretic drugs used to treat rheumatoid diseases as well as general pain and inflammation⁷⁴. Further, many of these drugs have shown a protective effect against cancer development as well as cancer progression by downregulating the inflammatory response and preventing the formation and maintenance of a chronic inflammatory and tumour-promoting microenvironment (reviewed by Ulrich et al. (2006)⁷⁴). Regular, long-term (>5 years) intake of aspirin has been shown to protect against tumourigenesis, progression and metastasis of gastrointestinal tract cancers, most significantly colorectal cancer⁷⁸.

NSAIDs act through inhibition of COX enzyme activity⁷⁴. As previously mentioned, COX enzymes convert arachidonic acid into prostaglandins which regulate a variety of functions including platelet aggregation (blood-clotting), inflammation, vascular permeability, mucus production and control of mucosal pH²⁷. These functions are essential for maintaining the integrity of the gastrointestinal tract mucosa, which protects the body against stresses present in the lumen of the digestive tract such as gastric acid, changes in osmolarity, cytotoxic substances and pathogens (reviewed by Wallace (2008)²⁷). Unsurprisingly, the long term use of COX enzyme-inhibiting NSAIDs has been shown to

increase the risk of gastrointestinal bleeding⁷⁹, ulcers⁸⁰, and liver damage⁸¹. Due to these unwanted side-effects, the long-term use of NSAIDs in cancer prevention has limited therapeutic application. These findings have led to a shift towards the use of natural anti-inflammatory compounds, often present in the diet, to aid in the prevention and control of cancer⁸².

1.2.3. Immunomodulatory and anti-inflammatory properties of natural dietary compounds

A number of natural compounds derived from dietary sources have been shown to have anti-inflammatory and chemopreventative activities similar to those seen for NSAIDs^{74,82}. Interestingly, comparisons of various epidemiological studies report that the duration and continuity of NSAID use is more significant than the dosage with regards to cancer prevention⁷⁵. The benefits of natural dietary anti-inflammatory and chemopreventative compounds are that they are non-toxic, inexpensive, and can be consumed on a daily basis with little or no side effects. Natural compounds therefore provide a sustainable, cost-effective and healthy alternative to NSAIDs for cancer prevention. Figure 1.1 shows the source and chemical structure of a number of naturally occurring dietary anti-inflammatory compounds⁸².

While the prophylactic and/or therapeutic effects of the individual compounds listed in Figure 1.1⁸² are too numerous to discuss here, many of these compounds have been shown to downregulate the expression of inflammatory cytokines including IL1B, IL6, IL12 and TNF and the inflammatory enzymes; COX2 and NOS2⁸². These compounds likely act by modulating proteins or enzymes from diverse inflammatory signalling pathways including NF-κB, c-Jun N-terminal kinase (JNK), STAT3, phosphoinositide 3-kinase/protein kinase B (PI3K/PKB) and mitogen-activated protein kinases (MAPK) (reviewed by Pan et al. (2009)⁸²). While it does not appear in Figure 1.1, dietary garlic has been used for thousands of years to treat and prevent infections, heart disease and cancer⁸³.

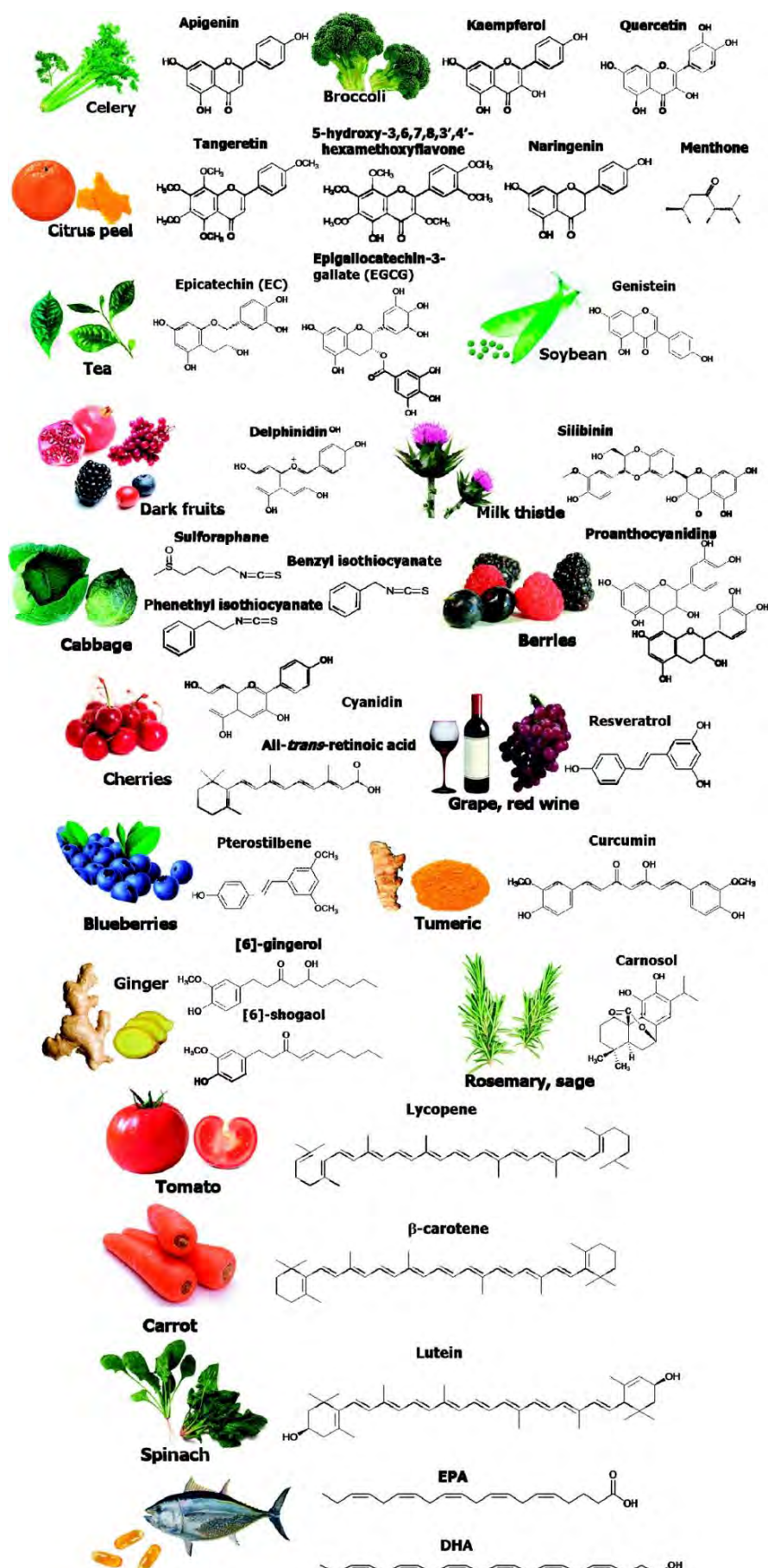


Figure 1.1: Sources and chemical structures of some natural anti-inflammatory and immunomodulating compounds. Reproduced with permission from Pan et al, (2009)⁸² © American Chemical Society, 2009.

1.3. Medicinal use of garlic

Garlic (*Allium sativum*) has been used for over 3000 years for both culinary and medicinal purposes⁸³. The Papyrus Ebers, which dates back to 1500BC, and is the oldest extant medical text, advocates garlic for the treatment of asthma, headaches, tumours and infections⁸³. Today's research has shown garlic to display anti-inflammatory^{84–86}, antibacterial^{87–89}, antifungal^{90,91}, antiviral⁹², antithrombotic⁹³, lipid-lowering⁹⁴ and anti-oxidant⁹⁵ properties. In addition, garlic has been shown to elicit both cancer preventative and therapeutic effects^{96–99}.

1.3.1. Epidemiological evidence for garlic consumption protecting against cancer

Modern epidemiological studies have shown an inverse relationship between dietary garlic consumption and cancer incidence, especially cancers of the gastrointestinal tract^{100–103}. One of the first studies to address the relationship between garlic consumption and gastric cancer was a population-based study in China that showed a 40% decrease in gastric cancer risk in individuals with a diet rich in *Allium* vegetables (the *Allium* genus includes onions, garlic, chives, scallions, shallots, leeks)¹⁰³. Meta-analyses of the available epidemiological literature have supported this early finding, showing an inverse relationship between garlic or *Allium* consumption and the incidence of gastric cancer^{104–106}. In contrast, another meta-analysis study conducted by Kim and Kwon (2009) found no credible evidence in support of a relationship between garlic intake and reduced risk of cancers¹⁰⁷. More controversial, however, is the protective effect of garlic or *Allium* vegetable consumption against colorectal cancer. While earlier meta-analyses conducted by Fleischauer and Arab (2001)¹⁰⁶ and Ngo et al. (2007)¹⁰⁸ showed protective effects of garlic or *Allium* vegetable consumption against colorectal cancer, more recent meta-analyses conducted by Hu et al. (2014)¹⁰⁹ and Zhu et al. (2014)¹¹⁰ have suggested that garlic consumption does not protect against colorectal cancer.

1.4. Chemical structures of naturally occurring garlic organosulfur compounds

Garlic contains many bioactive compounds which are reported to have beneficial health effects including lectins¹¹¹, steroid saponins⁹⁰, flavonoids¹¹², organoselenium compounds, and organosulfur compounds (OSCs)^{96,113}. Of these, garlic OSCs have been the most widely studied for their role as anti-cancer agents (reviewed by Amagase (2006)). Figure 1.2 shows the chemical structures of a number of predominant garlic OSCs.

The major sulfur-containing compound found in intact garlic cloves is alliin, which upon crushing, cutting or grinding comes into contact with the cell vacuole enzyme alliinase¹¹⁴. Alliinase converts alliin

into pyruvic acid, ammonia and sulfenic acid. The sulfenic acid is a reactive intermediate which can readily dimerise through hydrolysis into diallyl thiosulfinate (allicin) (Figure 1.3A)¹¹⁴. Allicin, which gives garlic its typical pungent smell and strong garlic taste, is a highly reactive compound with potent anti-microbial activity. The production of allicin therefore protects the plant from pathogenic invasion and discourages pests from eating it¹¹⁵. Being unstable, allicin rapidly degrades into a number of oil- and water-soluble polysulfides (Figure 1.2), primarily via two types of chemical reactions, β -elimination and S-thiolation (Figure 1.3)¹¹⁶.

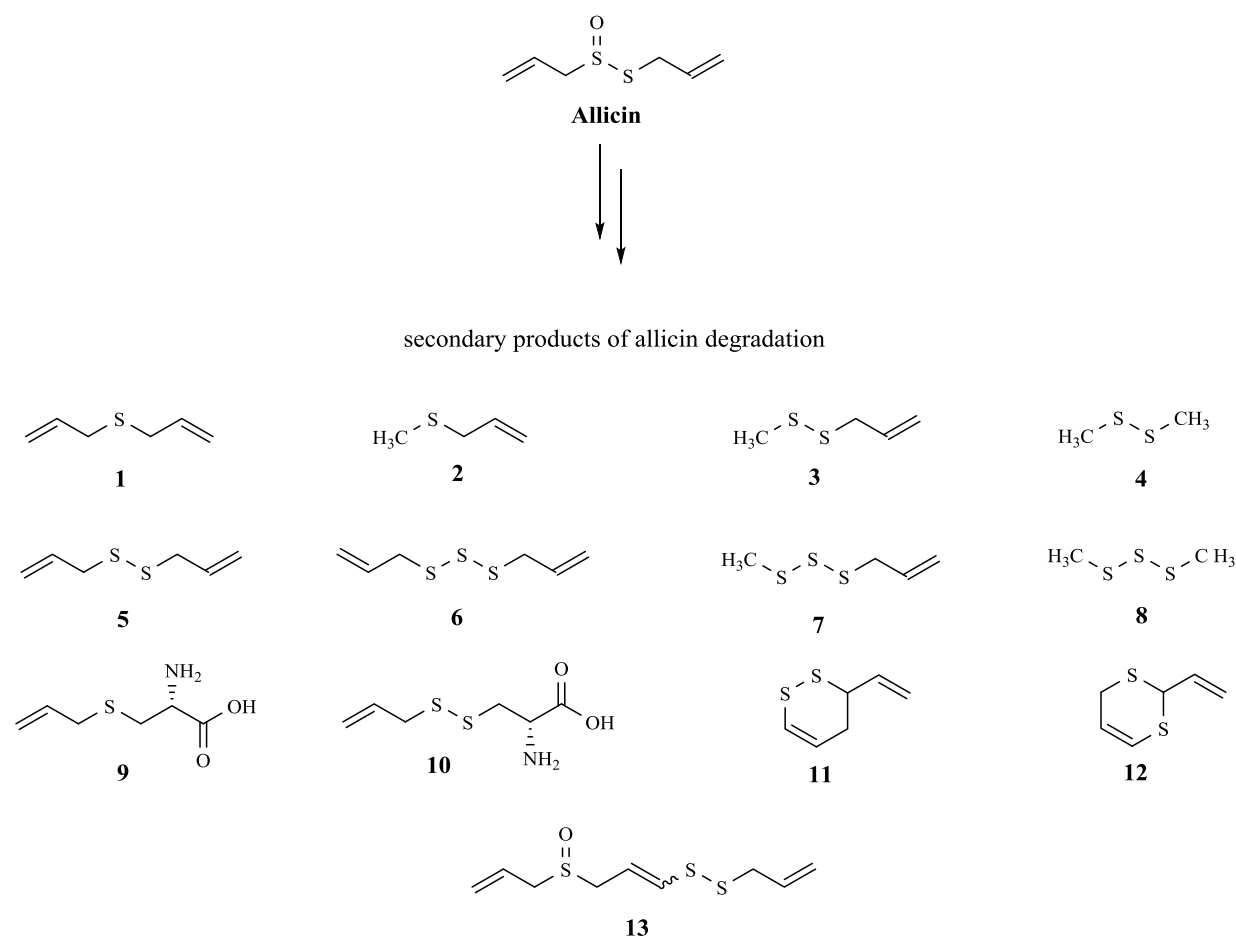


Figure 1.2: The predominant secondary products of allicin degradation in crushed garlic. (1) diallyl sulfide (DAS), (2) allyl methyl sulfide (AMS), (3) allyl methyl disulfide (AMDS), (4) dimethyl disulfide (DMDs), (5) diallyl disulfide (DADS), (6) diallyl trisulfide (DATS), (7) allyl methyl trisulfide (AMTS), (8) dimethyl trisulfide (DMTS), (9) S-allyl cysteine (SAC), (10) S-allyl mercaptocysteine (SAMC), (11) 2-vinyl-2,4-dihydro-1,3-dithiin, (12) 3-vinyl-3,4-dihydro-1,2-dithiin, (13) *E/Z*-4,5,9-trithiadodeca-1,6,11-triene 9-oxide (*E/Z*-ajoene). Note that compounds 9 and 10 are the only water soluble compounds. Reproduced with permission from Schäfer and Kaschula (2014)¹¹⁷.

The secondary garlic OSCs derived from allicin include dithiins, ajoenes and allyl sulfides (e.g. diallyl sulfide (DAS), diallyl disulfide (DADS) and diallyl trisulfide (DATS))¹¹⁸. Figure 1.3B-E show the formation of some of the bioactive allicin rearrangement products as elucidated by Block et al. (1984, 1986)^{93,116}. Dithiins are proposed to be formed from the dimerisation of two thioacroleins, which are formed through β -elimination of allicin (Figure 1.3B). The *E/Z*-isomers of ajoene are formed when two molecules of allicin combine to form a sulfonium ion, which can then undergo β -elimination followed by γ -addition of 2-propenesulfenic acid to yield a mixture of *E*- and *Z*-isomers of ajoene⁹³ (Figure 1.3C). DADS can be formed through an *S*-thiolation reaction between allyl mercaptan (AM) and allicin (Figure 1.3D), while DATS is proposed to be formed via hydrolysis of the sulfonium ion followed by addition of AM coupled with the expulsion of 2-propenesulfenic acid (Figure 1.3E). All of these interconversion reactions are proposed to occur naturally in damaged garlic cells. Therefore the exact chemical composition of a garlic preparation varies widely depending on the mode and age of the preparation. Fresh preparations contain higher concentrations of allicin, whereas aged preparations contain higher concentrations of the second generation compounds DADS, DATS and *E/Z*-ajoene.

Studies investigating the metabolism of allicin from human breath, plasma and gastric fluid samples show that allicin is also a highly reactive and metabolically unstable compound when consumed^{119,120}. Sample analysis has revealed that allicin is never detected; however the products of allicin degradation are detected, including DADS, DATS, allyl methyl sulfide (AMS) and allyl methyl disulfide (AMDS)^{119,120}. The presence of these products indicates that allicin *S*-thiolation and β -elimination reactions occur within the body. There are many potential thiol nucleophiles in living systems which could be the target of allicin *S*-thiolation. These include susceptible cysteine thiols in proteins which could potentially become alkylated through *S*-thiolation by allicin¹²¹. Significantly, Miron et al. (2000) showed that allicin not only interacts with thiol-containing molecules in the cell, but that it can easily permeate membrane lipid bilayers without causing membrane fusion, aggregation or leakage. This suggests that allicin may rapidly exert its therapeutic effects within the intracellular environment by *S*-thiolating thiol-containing proteins and molecules¹²².

The second-generation allyl sulfides formed from allicin degradation are more stable than allicin and are reported to be found in blood and breath samples after garlic ingestion¹¹⁹. These compounds appear to remain in circulation in the body for longer periods than allicin although it is likely that they succumb to the same fate as they are also excellent thiolating agents¹¹⁹. Therefore, although the chemical composition of consumed garlic varies in the exact distribution of organosulfur compounds, they are likely to act via a similar mechanism i.e. via protein thiolation.

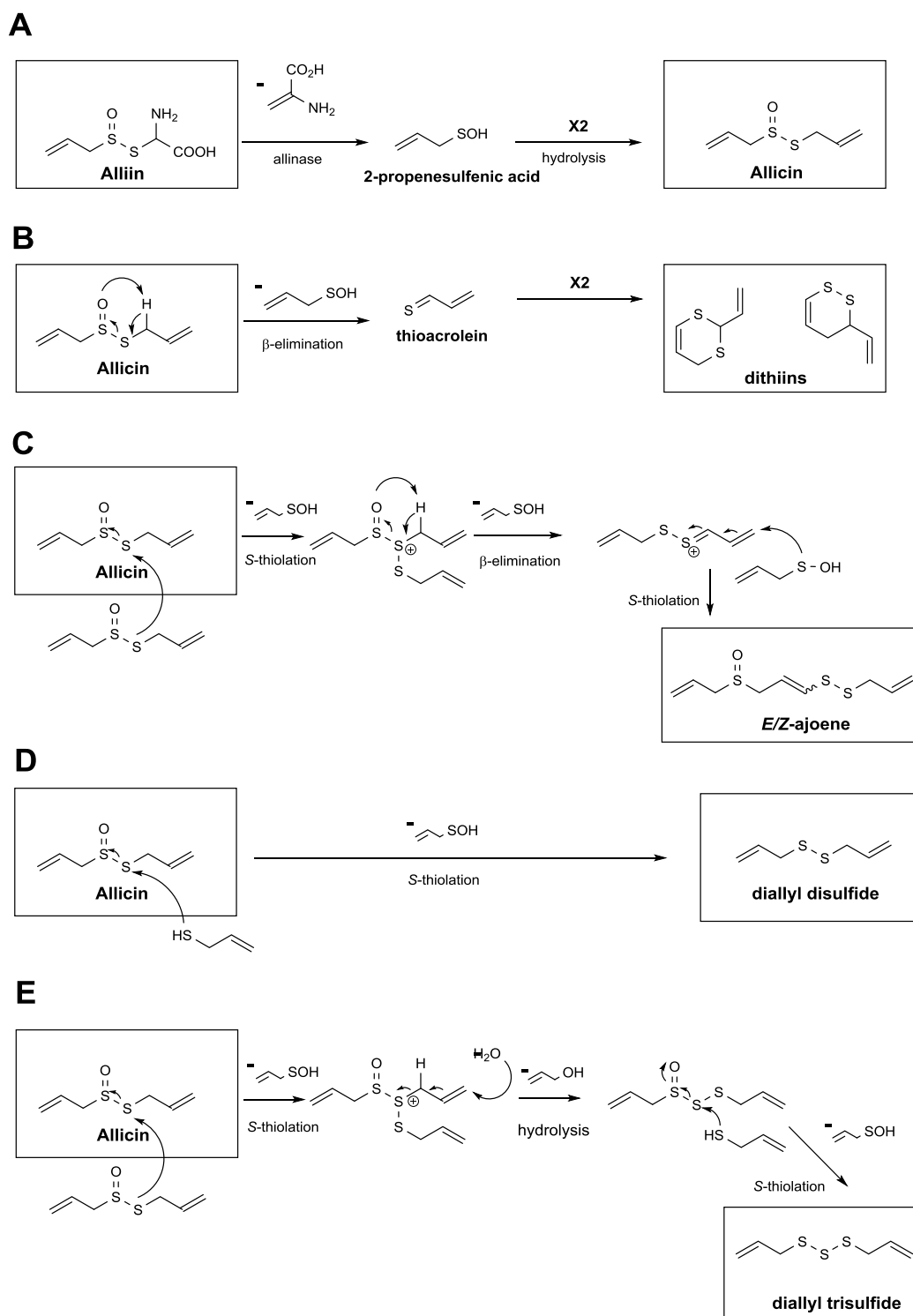


Figure 1.3: The formation of alliin and some bioactive alliin rearrangement products by β -elimination and S-thiolation reactions in crushed garlic cloves. A. The formation of alliin from alliin is catalysed by the enzyme alliinase **B.** Dithiins are formed from the alliin β -elimination product thioacrolein. **C.** *E/Z*-ajoenes are formed from addition of two alliin molecules to generate the sulfonium ion, which undergoes β -elimination and subsequent γ -addition of 2-propenesulfenic acid. **D.** Diallyl disulfide is formed via S-thiolation of alliin by allyl mercaptan. **E.** Diallyl trisulfide is formed by hydrolysis of the sulfonium ion in (C) and subsequent S-thiolation by allyl mercaptan. These mechanisms of chemical interconversion were elucidated by Block et al. (1984, 1986)^{93,116}.

1.5. Garlic organosulfur compound chemistry and metabolism

Garlic OSCs are reported to be active both as cancer preventative and therapeutic agents^{123–129}. On a therapeutic level, garlic compounds have been shown to inhibit proliferation and induce apoptosis in cancer cells, both in culture and in animal models^{123–127} (Supplementary Table B1, Appendix B). In addition, garlic has been shown to protect against free radical (ROS and RNS) damage by upregulating the expression of anti-oxidant enzymes (Supplementary Table B2, Appendix B). In cancer prevention, garlic compounds have been shown to be active anti-mutagenic agents capable of inhibiting induction of cancer through chemical carcinogens^{128,129}. While this very likely contributes to the cancer preventative potential of garlic, it may also be attributed to their underlying effects on the immune system^{85,130–132}. Research groups to date have used several different experimental approaches and various garlic preparations – including garlic powder extract, garlic oil and purified garlic OSCs – to study the effect of garlic on numerous aspects of the immune system^{88,97,132,133}. The variability in experimental design, especially regarding the chemical composition of different garlic extracts, has made comparison between studies challenging (reviewed by (Schäfer and Kaschula (2014)¹¹⁷). The principle components of different garlic extracts as well as methods of preparation have been summarised by Trio et al., (2014)¹³⁴. Generally, garlic essential oils are reported to contain high quantities of the allyl sulfides (DADS, DATS and allyl methyl trisulfide (AMTS)); garlic powder is reported to contain alliin and allyl sulfides (DADS and DATS); aged garlic extract (AGE) is reported to contain high concentrations of the water soluble S-allyl cysteine (SAC) and S-allyl mercaptocysteine (SAMC) compounds; while freshly crushed garlic contains allicin, allyl sulfides, ajoenes and dithiins¹³⁴. Some important papers which report on the effect of garlic compounds and preparations on inflammatory cytokines and chemokines; inflammatory enzymes; and signalling pathways and transcription factors are summarised in Tables 1.1-1.3, respectively, and are described in detail in the following section.

1.6. Evidence for the effects of garlic on inflammatory cytokine and chemokine expression

Table 1.1 summarises the literature reporting the effects of garlic extract or garlic OSC treatment on the induced expression of a number of pro- and anti-inflammatory cytokines and chemokines.

Table 1.1: A summary of the literature reporting the effects of garlic OSC and garlic extract on induced expression of inflammatory cytokines and chemokines. All abbreviations and symbols used in this table can be found in the list of Abbreviations and Symbols.

| Functional Component | Concentration | Experimental System | Reported effect | Ref |
|----------------------|---|--|--|-----|
| Alliin | 0.05-3 µg/ml | LPS-induced PBMCs (<i>in vitro</i>) | Increased IL1B and TNF expression. Decreased IL6 expression. | 135 |
| Garlic extract | 0.1-10 µg/ml | PMA-, ionomycin- or LPS-stimulated whole blood PBMCs (<i>in vitro</i>) | Increased IL10 expression. Decreased IL1A, IL2, IL6, CXCL8 (IL8), IL12, TNF, IFNG expression. | 84 |
| Garlic extract | 20 mg/kg per day x 14 days | <i>Leishmania major</i> -infected BALB/c mice (<i>in vivo</i>) | Increased IL2 and IFNG. Decreased IL4 expression. | 136 |
| Allicin | 5-80 µM | TNF-stimulated HT-29 and Caco-2 adenocarcinoma cells (<i>in vitro</i>) | Decreased IL1B, CXCL8 (IL8), CXCL9 and CXCL10. | 137 |
| Garlic extract | 10-1000 µg/ml | Placenta and pre-eclampsic placenta explants (<i>in vitro</i>) | Decreased IL6 (normal placental explants) and TNF (pre-eclampsic placental explants). Increased IL10 (for 10 µg/ml) in normal placental explants. Decreased IL10 (for 1000 µg) in normal and pre-eclampsic placental explants. | 86 |
| Alliin | 0.1 mM | LPS-induced 3T3-L1 cells (<i>in vitro</i>) | Decreased IL6 expression. | 138 |
| DATS | 100-200 µM | LPS-stimulated RAW264.7 macrophages (<i>in vitro</i>) | Decreased IL6, IL10, IL12, CXCL1, CCL2 & TNF expression. | 139 |
| Allicin | 1-100ng/ml | Thioglycollate-induced murine peritoneal macrophages (<i>in vitro</i>) | Increased IL1, IL6 and TNF expression. | 132 |
| DAS, DADS, AMS | 1-10 µM, 0.1-0.5 µM, 2-20 µM | LPS-stimulated RAW264.7 macrophages (<i>in vitro</i>) | DAS: Decreased IL1B, IL6, IL10, TNF expression. DADS: Decreased IL10, TNF and increased IL1B and IL6 expression. AMS: Decreased TNF and increased IL10 expression. | 140 |
| DADS | 100 µM | TNF-stimulated MDA-MB-231 breast cancer cells (<i>in vitro</i>) | Decreased CCL2 expression. | 141 |
| DAS | 15 µM | TNF- or histamine-stimulated A7r5 aortic smooth rat muscle cells (<i>in vitro</i>) | Decreased IL1B and TNF expression. | 142 |
| E/Z-ajoene | 20 µM | LPS-stimulated RAW264.7 macrophages (<i>in vitro</i>) | Decreased IL1B, IL6 and TNF expression. | 143 |
| GPE, DADS | 10-100 mg/L, 1-100 µmol/L | LPS-induced human whole blood (<i>in vitro</i>) | Decreased IL1B and TNF expression. | 85 |
| GPE | 1 g-3 g | Healthy human volunteers (<i>in vivo</i>) | Increased IL12 expression and no change in IL8 and TNF expression in urine samples. | 144 |
| AGE | 1-3 doses of 20 mg/kg every 2 nd day | BALB/c mice with allergic airway inflammation (<i>in vivo</i>) | Increased IFNG expression and decreased airway inflammation. | 145 |
| DAS | 150 mg/kg x 6 days | Gentamicin-induced nephrotoxicity in Wistar rats (<i>in vivo</i>) | Decreased expression of TNF. | 95 |

Much of the literature suggests that treatment with garlic OSCs or garlic extract decreases the inflammation-induced expression of IL1B, IL6 and TNF (Table 1.1). The downregulatory effect of garlic treatment was also seen for IL12, but these results are less reliable as only 2 out of 3 studies are in agreement. The expression of IL12 in LPS-stimulated PBMCs⁸⁴ and RAW264.7 macrophages¹³⁹ was found to be reduced by both garlic extract and DATS treatment, respectively. In contrast, an increase in IL12 was seen in urine collected from healthy human volunteers administered with 1-3 g of garlic powder extract (GPE)¹⁴⁴. This suggests that garlic may elevate IL12 expression in the absence of inflammation, but decreases IL12 expression by monocytes and macrophages during the inflammatory response.

The effect of garlic treatment on IL10 expression appears to differ between studies. Hodge et al. (2002) showed that treatment of LPS-stimulated whole blood peripheral blood mononuclear cells (PBMCs) with ≥ 1 $\mu\text{g/ml}$ garlic extract resulted in a significant increase in IL10 production⁸⁴. Similarly, Chang et al. (2005) showed that IL10 expression in LPS-stimulated RAW264.7 macrophages was increased by AMS but decreased by DAS and DADS treatment. Interestingly, a study conducted by Makris et al. (2005) looked at the expression of cytokines in explants of placentas with or without pre-eclampsia (a hypertensive disorder in pregnant women which can develop into eclampsia, which is life-threatening to the mother and infant) and found that treatment with lower concentrations of garlic extract (10 $\mu\text{g/ml}$) increased IL10 expression, while higher concentrations of garlic extract (1000 $\mu\text{g/ml}$ garlic extract) decreased IL10 expression. This discrepancy is likely a result of garlic compound toxicity at higher concentrations.

Interferon- γ (IFNG) expression was shown to be increased following treatment with both fresh or aged garlic extract in two independent studies looking at inflammation in BALB/c mice^{136,145}. Conversely, Hodge et al. (2002) showed that the expression of IFNG in phorbol myristate (PMA)- or ionomycin-stimulated T-cells was significantly decreased following treatment with 1-10 $\mu\text{g/ml}$ garlic extract⁸⁴.

While there are few studies reporting the effects of garlic treatment on the expression of chemokines, all studies included in Table 1.1 show a downregulatory effect on the expression of all reported chemokines including CCL2^{139,141}, CXCL1¹³⁹, CXCL8 (also known as IL8)^{84,137}, CXCL9¹³⁷ and CXCL10¹³⁷.

Taken together, the majority of papers reviewed show a consistent downregulatory effect for garlic treatment on the expression of IL1B (5 out of 7 studies)^{85,137,140,142,143}, IL6 (7 out of 8 studies)^{84,86,135,138-140,143} and TNF (8 out of 11 studies)^{84-86,95,139,140,142,143}. There is less evidence for the downregulatory effect of garlic treatment on IL12 (2 out of 3 studies)^{84,139} and the upregulatory effect on IFNG (2 out of 3 studies)^{136,145}. Finally, the modulation of IL10 expression by garlic treatment appears to be

dependent on the garlic OSC and the concentration used, although it may also be due to toxicity of the garlic OSC at the high concentrations used.

1.7. Evidence for the effects of garlic on inflammatory enzymes

Cyclooxygenase-2 (COX2) and NOS2 enzymes are involved in generating inflammation-promoting prostaglandins (especially prostaglandin E₂ (PGE2))²⁶ and NO²⁸, a signalling molecule important in inflammation. There is significant evidence to suggest that garlic OSCs inhibit inflammation by downregulating the expression of COX2 and NOS2 enzymes (Table 1.2).

Table 1.2: A summary of the literature reporting the effects of garlic OSCs or garlic extract on inflammatory enzymes. All abbreviations and symbols used in this table can be found in the list of Abbreviations and Symbols.

| Functional Component | Concentration | Experimental System | Reported effect | Ref |
|------------------------------|------------------------------|--|--|-----|
| Allicin; <i>E/Z</i> -ajoene, | 1-100 µM; 0.1-20 µM | LPS-stimulated RAW264.7 macrophages (<i>in vitro</i>) | Decreased NOS2 expression and NO accumulation. | 146 |
| <i>E/Z</i> -ajoene | 10 µM | LPS-stimulated RAW264.7 macrophages (<i>in vitro</i>) | Increased COX2 expression, but inhibited enzyme activity and release of PGE2. | 147 |
| DAS, DADS, AMS | 1-10 µM, 0.1-0.5 µM, 2-20 µM | LPS-stimulated RAW264.7 macrophages (<i>in vitro</i>) | DAS: decreased COX2 and PGE2. DAS, DADS, AMS: decreased NO accumulation. DAS, DADS: decreased NOS2 expression. | 148 |
| DAS, DADS, AMS | 1-10 µM, 0.1-0.5 µM, 2-20 µM | LPS-stimulated RAW264.7 macrophages (<i>in vitro</i>) | Decreased PGE2 and NO levels. | 140 |
| <i>E/Z</i> -ajoene | 20 µM | LPS-stimulated RAW264.7 macrophages (<i>in vitro</i>) | Decreased COX2 and NOS2 expression and decreased NO and PGE2 production. | 143 |
| DADS | 100 mg/kg | Ethanol-induced gastric ulceration in Sprague-Dawley rats (<i>in vivo</i>) | Decreased NOS2 expression. | 149 |
| DADS DATS | 200-400 µM 100-200 µM | LPS-stimulated RAW264.7 macrophages (<i>in vitro</i>) | DADS and DATS inhibited expression of COX2, NOS2. DATS inhibited production of PGE2 and NO. | 139 |
| Allicin | 1-100 ng/ml | Thioglycollate-induced murine peritoneal macrophages (<i>in vitro</i>) | Increased NO expression. | 132 |

Table 1.2 shows that the inflammatory enzymes COX2 and NOS2 and their products PGE2 and NO were generally downregulated by garlic OSC treatment. The expression of NOS2 was decreased by garlic OSC treatment in all studies reporting the effect of garlic OSC treatment on NOS2^{95,139,146,148,149}, while NO expression was decreased in 5 out of 6 studies^{139,140,143,146,148}. COX2 expression was decreased in 3 of 4 studies^{139,143,147,148} while PGE2 was decreased in all 5 studies^{139,140,143,147,148} reporting the effects of garlic OSC treatment. Dirsch and Vollmar (2001) treated cells with 1 µg/ml LPS (which simulates a bacterial infection) and 10 µM *E/Z*-ajoene and found an increase in LPS-induced COX2 expression, but showed a decrease in PGE2 (the major product of COX2 conversion of arachidonic acid into prostaglandins) and thus showed a decrease in COX2 enzyme activity¹⁴⁷. Conversely, Lee et al. (2012) also stimulated RAW264.7 macrophages with 1 µg/ml LPS but used a higher concentration of *E/Z*-

ajoene (20 μ M) and found a decrease in LPS-induced COX2 expression as well as a decrease in COX2-dependent PGE2 production¹⁴³. Therefore, while lower concentrations of *E/Z*-ajoene increase LPS-induced COX2 expression (as compared to a decrease in expression seen for higher doses), *E/Z*-ajoene treatment inhibited the COX2 enzyme directly thereby resulting in a decrease in PGE2 production.

According to the literature, garlic OSC treatment appears to reduce the inflammation-induced expression of pro-inflammatory enzymes NOS2 and COX2 with a concomitant decrease in the production of the pro-inflammatory signalling molecules PGE2 and NO.

1.8. Evidence for the effects of garlic on inflammatory signalling pathways

As discussed in Section 1.2.1, the transcription factors NF- κ B and STAT3 play important roles in mediating immune responses and have been implicated in tumourigenesis and cancer progression. NF- κ B gene targets include inflammatory cytokines and chemokines; inflammatory enzymes; growth factors and anti-apoptotic mediators. Similarly STAT3, while regulating the expression of inflammatory mediators, is also involved in downregulating the inflammatory responses via IL10-STAT3 pathway signalling. IL10-STAT3 pathway is, however, also involved in immunosuppression, which can promote tumourigenesis and cancer progression. A review of the literature indicates that garlic OSCs affect many proteins involved in inflammatory signalling and immune regulatory pathways. Table 1.3 summarises the literature reporting the effects of garlic OSCs on a number of different signalling pathways activated during the immune response.

Table 1.3: A summary of the literature reporting the effects of garlic OSC and garlic extract on inflammatory signalling pathways and transcription factors. All abbreviations and symbols used in this table can be found in the list of Abbreviations and Symbols.

| Functional Component | Concentration | Experimental System | Reported effect | Ref |
|----------------------|--------------------------------|---|---|-----|
| Allicin | 5-80 μ M | TNF-stimulated HT-29 and Caco-2 colorectal adenocarcinoma cells (<i>in vitro</i>) | Suppressed degradation of I κ B. | 137 |
| DADS, AM | 1-100 μ M | TNF-stimulated HUVECs (<i>in vitro</i>) | No effect on TNF-induced NF- κ B activation or NF- κ B-regulated E-selectin. | 130 |
| Alliin | 0.1 mM | LPS-induced 3T3-L1 adipocytes (<i>in vitro</i>) | Decreased ERK phosphorylation. | 138 |
| <i>E/Z</i> -ajoene | 5-40 μ M | Human promyeloleukemic cells (<i>in vitro</i>) | Apoptosis induced by stimulated NF- κ B activation. | 99 |
| GPE, DADS | 10-100 mg/L, 1-100 μ mol/L | LPS-induced human whole blood (<i>in vitro</i>) | Decreased NF- κ B activity. | 85 |
| DATS | 20-40 μ M | IL6-stimulated DU145 and LNCaP prostate cancer cells (<i>in vitro</i>) | Decreased IL6-induced STAT3 phosphorylation and nuclear translocation. | 150 |
| DATS | 100-200 μ M | LPS-stimulated RAW264.7 macrophages (<i>in vitro</i>) | Downregulated NF- κ B & MAPK signalling. Prevented PKB and TAK1 phosphorylation. | 139 |
| DATS | 40 mg/kg x 5 days per week | Immunohistochemistry of orthotopically implanted PC-3 prostate cancer-cell tumours in nude BALB/c mice (<i>in vivo</i>) | Inhibited activation of PKB and NF- κ B pathways, and downregulated associated gene expression. | 124 |
| DAS | 15 μ M | TNF- or histamine-stimulated A7r5 aortic smooth rat muscle cells (<i>in vitro</i>) | Inhibited PI3K/PKB, AP1 and NF- κ B signalling. Prevented NF- κ B p65 nuclear accumulation. | 142 |

Five out of seven studies reporting effects of garlic treatment on NF- κ B show a downregulatory effect on NF- κ B activation and/or nuclear accumulation^{85,124,137,139,142}. In contrast, Dirsch et al. (2004) showed no effect of DADS or AM treatment on TNF-induced NF- κ B activation in human umbilical vein endothelial cells (HUVECs)¹³⁰, while the same research group showed that *E/Z*-ajoene treatment induced apoptosis in human promyeloleukemic cells via NF- κ B activation⁹⁹. The downregulation of NF- κ B signalling may be a result of inhibition of PI3K/PKB activation via DAS or DATS treatment, as reported in 3 studies^{124,139,142}. Ho et al. (2014) reported that DAS decreased the LPS-induced phosphorylation of PKB as well as activated kinase-1 (TAK1); the latter forms part of the MAPK signalling pathway¹⁴². In addition, Quintero-Fabián et al. (2013) saw a decrease in the phosphorylation of extracellular signal-regulated kinases (ERKs) (also involved in the MAPK pathway) in LPS-induced 3T3-L1 adipocytes following treatment with alliin¹³⁸. There is only one study in which an effect on STAT3 has been reported. Here, DATS was found to decrease Tyr705 phosphorylation and nuclear translocation of the STAT3 transcription factor in IL6-stimulated prostate cancer cells¹⁵⁰.

In summary, the literature appears to support the general downregulation by garlic OSCs of multiple NF- κ B pathway signalling proteins and inhibition of NF- κ B activation. There is a single study reporting an inhibitory effect of DATS treatment on STAT3 activation in cancer cells¹⁵⁰, but no literature reports on the effect of garlic OSC treatment on STAT3 activation in immune cells.

1.9. Possible chemical biology behind the biological activity of garlic OSCs

In cells, the antioxidant molecule GSH can form mixed disulfide bonds with redox-sensitive (low acid-dissociation constant (pK_a)) cysteine thiols on proteins via a process called *S*-glutathionylation (Figure 1.4A)^{151,152}. The addition of GSH to cysteines via *S*-glutathionylation is a post-translational modification of proteins which can protect against ROS-mediated damage, regulate protein function or enzyme activity and can play a role in cell signalling (reviewed by Dalle-Donne et al. (2007) and Klatt and Lamas (2000)^{151,152}).

Currently there are about 150 prokaryote and eukaryote proteins known to be *S*-glutathionylated¹⁵³. Among these are apoptotic mediators (e.g. caspase-3¹⁵⁴ and Fas¹⁵⁵), cytoskeletal proteins (β -tubulin¹⁵⁶ and actin¹⁵⁷) and signalling proteins and transcription factors (e.g. NF- κ B subunits^{158,159}, I κ B kinase (IKK)¹⁶⁰, and STAT3¹⁶¹). A more comprehensive list of *S*-glutathionylation protein targets can be seen in the review by Pastore and Piemonte (2012). As cysteine thiols in proteins are evolutionarily conserved, and are important in protein folding (and thus conformation) and activity, the reversible modification of cysteine thiols in proteins by *S*-glutathionylation has important implications in cell signalling (reviewed by Klatt and Lamas (2000)). For example, *S*-glutathionylation of the transcription factors NF- κ B p50¹⁵⁸, NF- κ B RELA (p65)¹⁵⁹ and STAT3¹⁶¹ have been shown to affect DNA binding and hence transcriptional activity of these proteins. *S*-glutathionylation is thus functionally analogous to protein phosphorylation, which is a well-known post-translational modification that regulates protein conformation and activity.

S-glutathionylation is considered a mechanism through which the intracellular redox state of cells is transduced into a functional response¹⁵². Significantly, *S*-glutathionylation reactions are redox sensitive: changes in the ratio of reduced GSH and oxidised GSH (GSSG) (GSH as a mixed disulfide) and changes in the levels of ROS and RNS can dictate whether cysteine thiolates form mixed-disulfide bonds with GSH or are oxidised into sulfenates or *S*-nitrothiols by ROS and RNS, respectively. *S*-glutathionylation and antioxidant thiol-transferase enzymes can reduce sulfenates and *S*-nitrothiols in proteins back into cysteine thiols and thereby restore protein function. Under conditions of oxidative stress however, when there is an increase in GSSG relative to GSH, these sulfenates and *S*-nitrothiols

can be irreversibly oxidised by ROS and RNS resulting in permanent loss of protein activity and even cell death¹⁵².

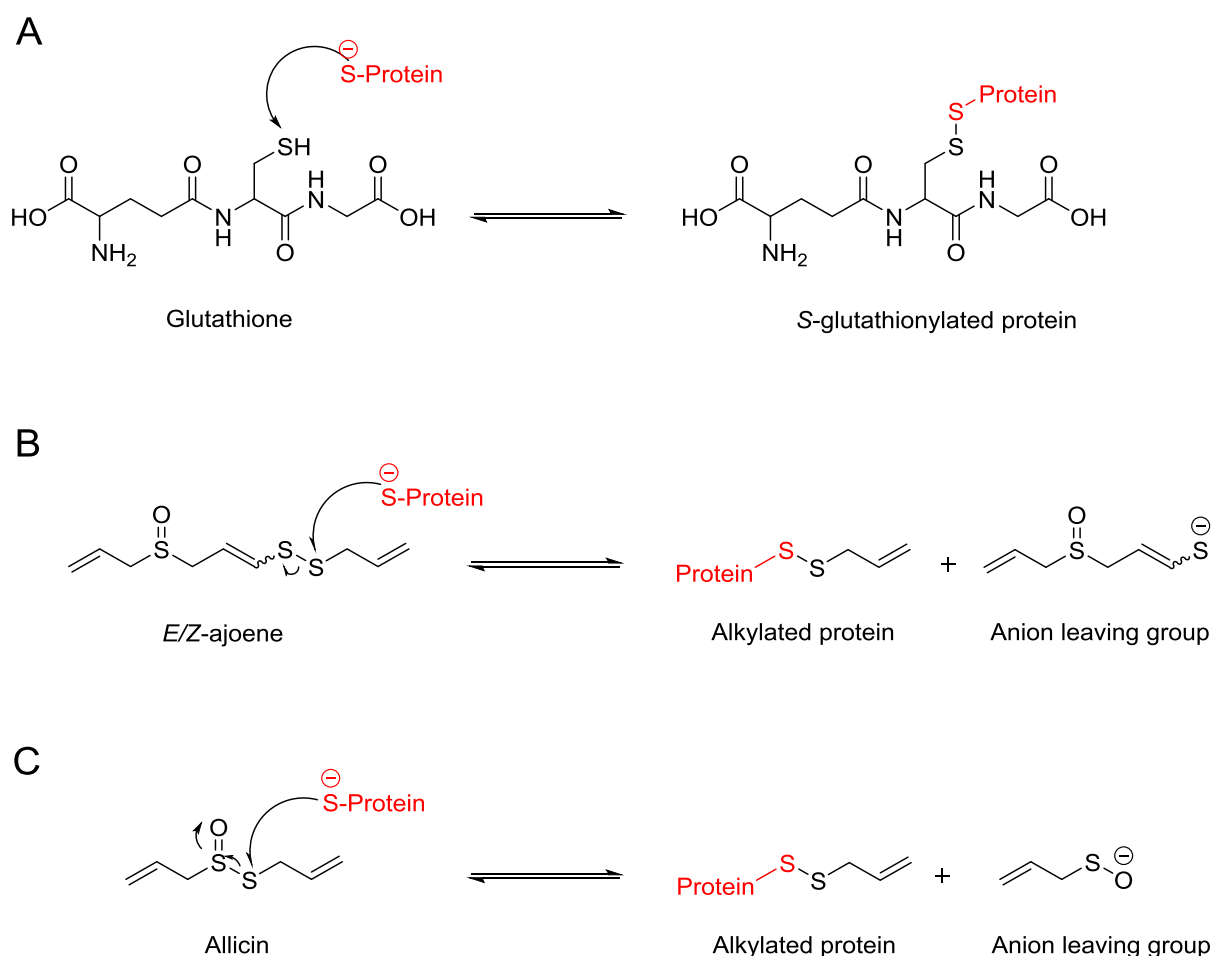


Figure 1.4: S-thiolation of protein cysteine thiols by glutathione, *E/Z*-ajoene and allicin. **A.** A cysteine thiol of a protein is S-glutathionylated by reduced glutathione. A cysteine thiol of a protein is S-thiolated or alkylated by **B.** *E/Z*-ajoene and **C.** allicin.

Garlic OSCs have been proposed to exert biological effects similar to S-glutathionylation through S-thiolation/disulfide exchange with cysteine thiols on proteins¹⁶³, as illustrated in Figure 1.4. It is thus likely that proteins susceptible to S-glutathionylation are also susceptible to S-thiolation/disulfide-exchange with garlic OSCs. In support of this, a number of *in vitro* studies demonstrate that garlic OSCs can alkylate and inhibit the activity of thiol-containing enzymes. Allicin, for example, has been shown to alkylate and inactivate papain and alcohol dehydrogenase in a cell-free system¹⁶⁴. Another study demonstrated that *E/Z*-ajoene inhibits glutathione reductase enzyme activity by alkylating an active site cysteine (Cys58)¹⁶⁵. In addition, Hosono et al. (2005) demonstrated that DATS alkylates two β -tubulin cysteines (Cys12 β and Cys354 β) and this inhibits tubulin polymerisation and induces apoptosis in cultured human colon cancer HCT-1 and DLD-1 cells¹²⁷.

As many proteins involved in inflammatory signalling pathways are known to be targets of S-glutathionylation^{158–161}, garlic OSCs may modulate immune function by targeting (and alkylating) these proteins.

1.10. Significance

Based on the evidence in Tables 1.1-1.3, it is clear that garlic OSCs affect a number of cellular processes involved in the immune response. The variability in experimental design, however, has made comparisons between these studies challenging. For example, some studies used pure garlic OSCs while others used garlic extracts with unknown or unspecified chemical composition. The concentrations of garlic OSCs or garlic extracts used greatly varied across studies, and many studies did not first determine compound toxicity in the chosen cell line or model. In addition, the studies used many different cell types (e.g. cancerous, epithelial or myeloid cells) which may respond differently to garlic OSC or garlic extract treatment. For these reasons, it is unclear which garlic OSCs elicit the immunomodulating effects of garlic, whether the concentrations used are biologically relevant, and whether the same effects seen on cancer and normal epithelial cells apply to immune cells. With this in mind, we developed an *in vitro* model to ascertain the effects of sub-toxic doses of pure garlic OSCs on immune system function and signalling in cultured macrophages.

1.10.1. Hypothesis

We hypothesise that garlic OSCs counterbalance the establishment of a chronic inflammatory microenvironment, which is critical to the initiation, promotion and progression of many cancers. In this way garlic OSCs may aid in cancer prevention. Garlic OSCs may act on a chemical level by S-thiolating redox susceptible cysteine residues in proteins, which inhibit enzyme activity or modulate cell signalling pathway. Further, as S-thiolation is similar to the well-known post-translational modification S-glutathionylation, we hypothesise that the targets of S-glutathionylation are targets of garlic OSCs.

1.10.2. Aim

To determine whether pure garlic OSCs are able to modulate the inflammatory response *in vitro*.

1.10.3. Objectives

Using pure synthesised garlic OSCs we will determine compound toxicity using cell viability assays in cultured RAW264.7 murine macrophages. In order to determine the effects of garlic-OSC treatment on LPS-induced inflammation, we will establish a well-defined *in vitro* inflammatory model that simulates regular dietary consumption of garlic. Once this has been achieved we will assess the effects

of garlic OSC treatment on the induced inflammatory response in these cells using quantitative real-time PCR (qPCR) gene expression and enzyme-linked immunosorbent assay (ELISA) protein expression analysis. If we find that the selected garlic OSCs modulate the inflammatory response, we will look at associated transcription factors or signalling proteins to see if garlic OSCs directly affect protein function through mixed-disulfide bond formation. These experiments will serve as the basis for the *in vitro* proof-of-concept required for an ethics application for future *in vivo* experiments to determine the effects of garlic OSC gavage on induced gastrointestinal- and colorectal inflammation in BALB/c mice.

Chapter 2 Materials and Methods

All solutions used are described in detail in Appendix A.

2.1. Cell culture

2.1.1. Cell lines and cell culture media

Abelson murine leukaemia virus-transformed murine macrophages (RAW264.7) (TIB-71™, ATCC®) were cultured in Dulbecco's-modified Eagle Medium (DMEM, Lonza, BioWhittaker®) supplemented with 10% foetal bovine serum (FBS Superior Cat. No. S0615, Biochrom AG), 1% PEN-STREP (Lonza, BioWhittaker®, 100U/ml penicillin and 100 µg/ml streptomycin), also referred to as "complete medium". The cells were grown in a humidified atmosphere (5% CO₂) at 37°C. Media was changed every 2-3 days and cells were routinely checked for mycoplasma contamination.

2.1.2. Cell plating and splitting

Cell lines were cultured in 25 cm² or 50 cm² culture flasks (Corning®, Sigma-Aldrich) and were split when 80% confluent. Medium was removed and cells were incubated with 5 ml lidocaine-ethylenediaminetetraacetic acid (EDTA) (Appendix A) for 2 min at 37°C. Lidocaine-EDTA suspended cells were transferred into 15 ml tubes and centrifuged at 1500 xg for 3 min. The supernatant was removed and the cells were resuspended in complete medium, transferred to a fresh culture flask and incubated at 37°C (5% CO₂). Thereafter, the medium was changed every 2-3 days. Cells were cultured for up to 10 passages after which they were discarded and a new frozen cell stock was thawed and cultured. Preliminary experiments were conducted which confirmed that there was no detectible difference in cell morphology and LPS-induced cytokine expression following cell splitting with lidocaine-EDTA or using a cell scraper (data not shown).

2.1.3. Cell counting

For counting purposes, 10 µl of the resuspended cells (Section 2.1.2) was added to 90 µl Trypan blue (Celtic Molecular Diagnostics (Pty) Ltd), of which 10 µl was pipetted onto a haemocytometer slide (Neubauer) covered by a coverslip. The number of cells was determined using the method described in the Neubauer manual. To determine the volume of cells needed, the following formula was used:

$$\text{Volume (ml)} = \frac{\text{Number of cells required}}{\text{Number of live cells (per ml)}}$$

2.2. Garlic organosulfur compounds

Chemically pure DATS (98%) supplied in acetone was purchased from the Cayman Chemical Company, while technical grade (80%) DADS in oil form was purchased from Sigma-Aldrich and purified by distillation (performed in the Chemistry Department at the University of Cape Town) prior to use.

Both allicin and *E*- and *Z*-ajoene were synthesised by Daniel Kuzsa, in the Chemistry Department at the University of Cape Town (UCT) according to the previously published method described by Block et al. (1986)¹¹⁶. Allicin was prepared via the oxidation of DADS in peracetic acid and purified at 4°C by flash silica gel chromatography.

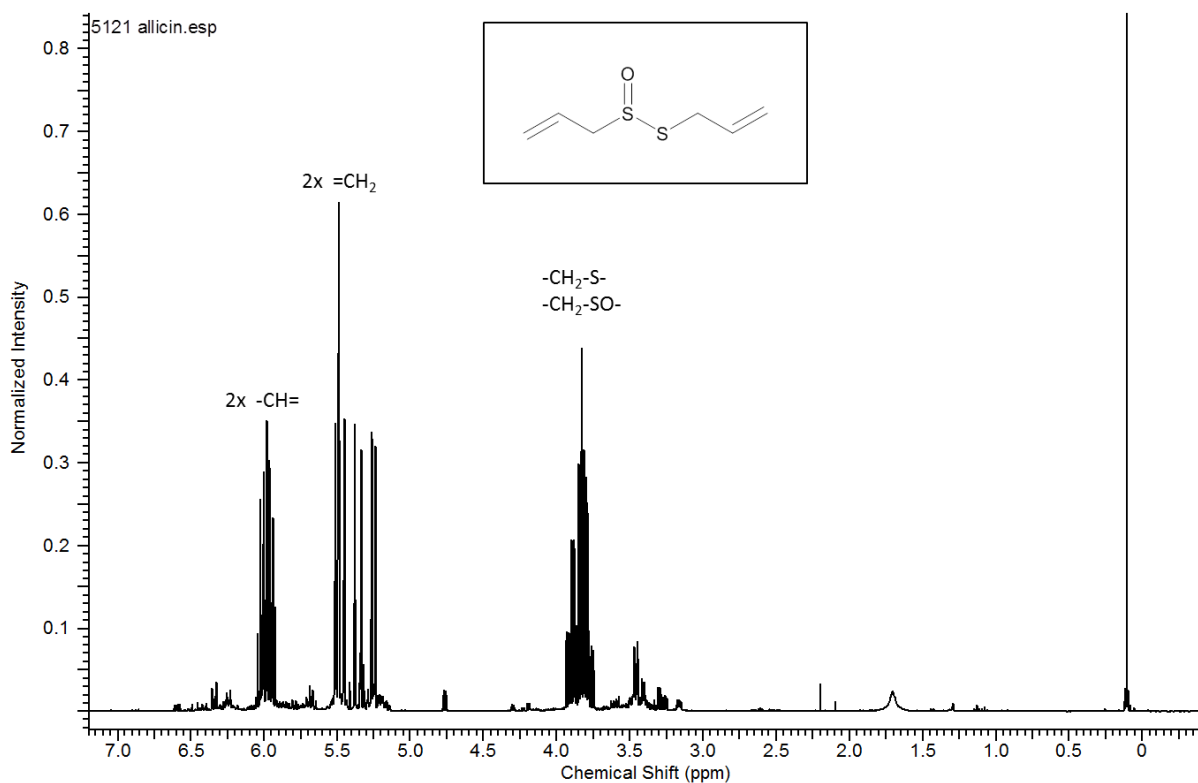


Figure 2.1: Characterisation of allicin by ¹H nuclear magnetic resonance spectroscopy. ¹H NMR δ_H (400MHz, CDCl₃) 3.83 (1H, S-CH₂-C, dd, *J* 14.1, *J* 7.2) 3.85 (1H, S-CH₂-C, dd, *J* 14.1, *J* 7.2) 3.91 (1H, SO-CH₂-C, dd, *J* 13.2, *J* 7.0) 4.01 (1H, SO-CH₂-C, dd, *J* 13.2, *J* 7.0) 5.26 (1H, S-CH₂-CH=CH₂, d, *J* = 10), 5.36 (1H, S-CH₂-CH=CH₂, d, *J* = 10), 5.48 (1H, CH₂=CH-CH₂-SO, d, *J* = 16), 5.50 (1H, CH₂=CH-CH₂-SO, d, *J* = 16), 5.95-6.02 (2H, CH₂-CH-CH₂, ddt, *J* = 16, *J* = 10, *J* = 7.2)

Ajoene was synthesised from allicin by thermal rearrangement in refluxing acetone and the *E*- and *Z*-geometric isomers were separated by slow silica gel chromatography. Compound purity was assessed by ^1H nuclear magnetic resonance (NMR) spectroscopy and silica-gel thin layer chromatography (TLC) (Section 2.3).

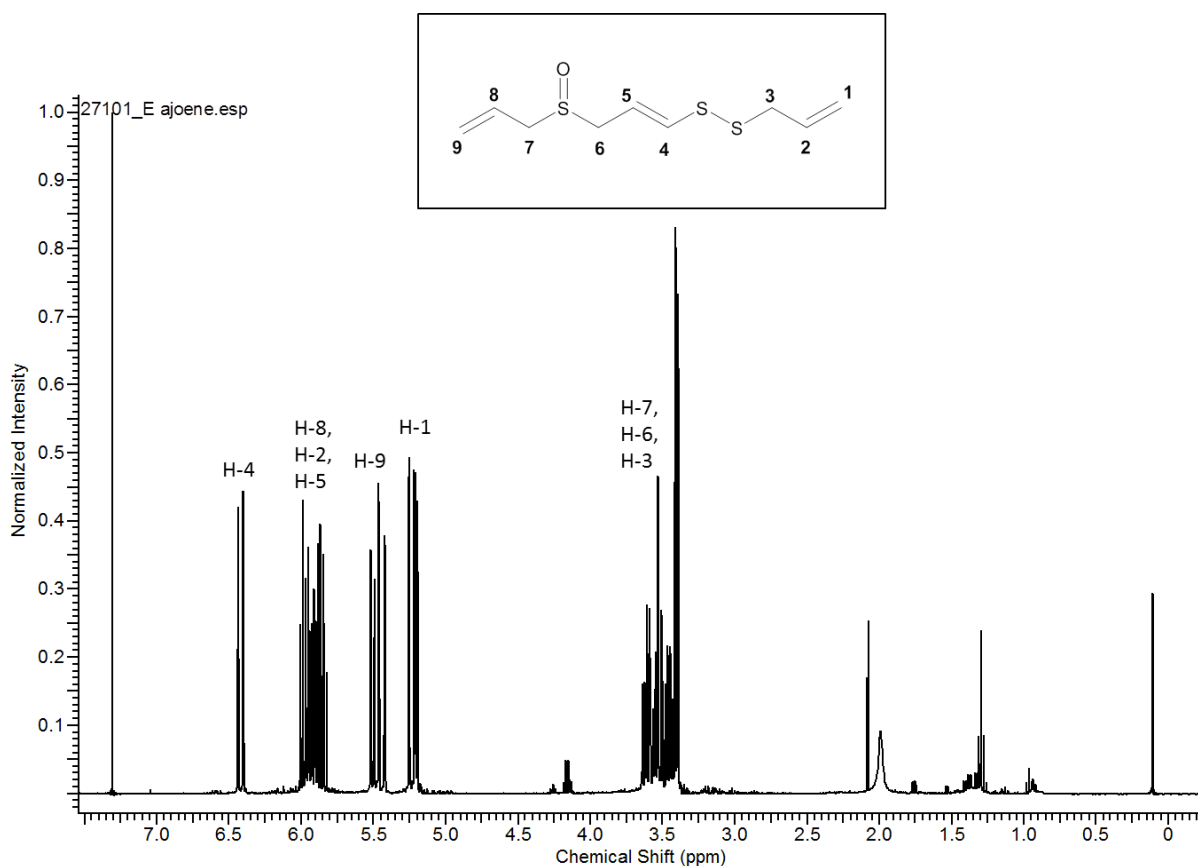


Figure 2.2: Characterisation of *E*-ajoene by ^1H nuclear magnetic resonance spectroscopy. ^1H NMR δ_{H} (400MHz, CDCl_3) 6.3 (1H, d, J 14.6, H-4); 5.9 – 5.7 (3H, m, H-8, H-2 and H-5); 5.4 (2H, m, H-9); 5.1 (2H, m, H-1); 3.6 - 3.3 (6H, m, H-7, H-6, H-3).

Allicin, which is known to be unstable, was stored as a 1 mg/ml solution in water at -80°C . DADS, *E*- and *Z*-ajoene were stored as pure oil or diluted in dimethyl sulfoxide (DMSO, Sigma-Aldrich) and stored at -80°C . DATS was diluted in acetone and stored at -20°C . Regular TLC analysis (Section 2.3) of these compounds showed that allicin, DADS, DATS and *E*- and *Z*-ajoene were not prone to degradation when stored under these conditions.

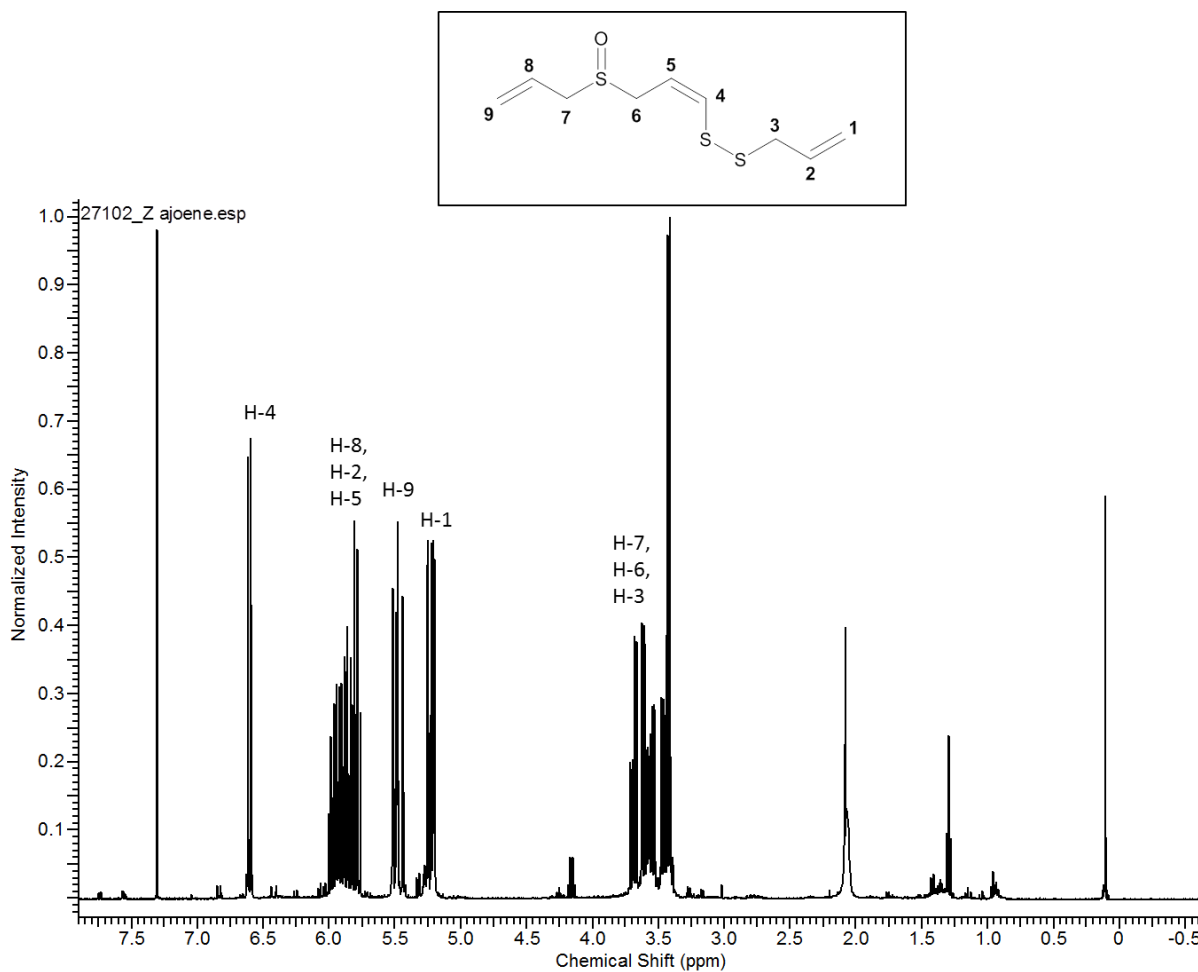


Figure 2.3: Characterisation of Z-ajoene by ^1H nuclear magnetic resonance spectroscopy. ^1H NMR δ_{H} (400MHz, CDCl_3) 6.56 (1H, d, $J = 9.5$, H-4); 5.97 – 5.70 (3H, m, H-8, H-2 and H-5); 5.4 (2H, m, H-9); 5.1 (2H, m, H-1); 3.7 - 3.4 (6H, m, H-7, H-6, H-3).

2.3. Thin layer chromatography

Silica-gel thin layer chromatography (TLC) was used to test for compound purity prior to the use of the garlic OSCs in experiments. While TLC can detect trace amounts of impurity, this method is limited to qualitative detection. As ^1H NMR was used to characterise and demonstrate purity of the selected garlic OSCs, TLC was used to test for OSC degradation which may occur subsequently over time during storage. This technique was used instead of ^1H NMR as it is an easy and rapid technique sensitive enough to reveal trace amounts of impurities and hence degradation. In addition TLC could be performed in the laboratory at the UCT Medical School whereas ^1H NMR would need to be performed at the UCT Chemistry Department. Silica-gel TLC allows for separation of compounds due to differences in attraction to the stationary phase (silica gel) and solvent, usually a mixture of ethyl acetate and hexanes. The garlic OSCs solubilised in water, acetone or DMSO were spotted 0.5 cm from the bottom of a TLC Silica gel 60 F254 aluminium plate (Merck) using a Hirschmann micropipette (Sigma-Aldrich) and left to dry. The TLC plate was then placed in a sealed development tank containing

a mixture of ethyl acetate (EtOAc) and hexanes (20% EtOAc and 80% hexanes was used for allicin; 80% EtOAc and 20% hexanes was used for *E*- and *Z*-ajoene; and 50% EtOAc to 50% hexanes was used for DADS and DATS). After the EtOAc/hexane solvent mixture had migrated approximately 3cm, the solvent front was marked and the TLC plate was visualised under a 254 nm ultraviolet lamp. The 'spots' on the plate were circled using a pencil and the compound was considered pure if there was a single 'spot' on the plate. The retardation factor (R_f) value was calculated by dividing the distance travelled by the compound or 'spot' by the distance travelled by the solvent. R_f values were then compared to previously determined R_f values for the pure compounds and purity could be confirmed if the R_f values were similar.

2.4. Cell viability assay (MTT assay)

To determine cytotoxicity of the selected garlic compounds on RAW264.7 murine macrophages, thiazolyl blue tetrazolium bromide (MTT) colourimetric viability assays were performed. Actively-metabolising cells convert the MTT reagent (yellow tetrazolium salt) into a purple formazan product. This reaction involves electron transfer from pyrimidine nucleotide co-factors NADH and NADPH to the MTT reagent which is in turn reduced to a purple formazan product. The crystalline formazan is solubilised and the absorbance is measured at 595 nm with a spectrophotometer. As the amount of formazan produced is directly proportional to the number of viable cells, this assay can be used to measure the cytotoxicity of various garlic OSCs on treated cells.

Briefly, 96-well plates were seeded with 6000 cells per well, suspended in 90 μ l of complete DMEM. After 24 h, cells were treated with 10 μ l of the garlic OSC at a range of concentrations at 2-fold dilutions varying from 0-100 μ M (and 0-100 mM for DADS). After a 24 h treatment period, the cells were treated with MTT reagent (3-[4,5-dimethylthiazol-2-yl]-2,5-diphenyltetrazolium bromide, Cat. No. M2128, Sigma-Aldrich) at a final concentration of 0.5 mg/ml for 4 h. Thereafter, Solubilisation Reagent (Appendix A) was added to a final concentration of 5% and incubated at 37°C for 24 h. Absorbance at 595 nm was measured using a plate-reading spectrophotometer (VersaMax™ Tuneable Microplate Reader, Molecular Devices). The negative control for these experiments was cells treated with 0.1% of either DMSO (for DADS, *E*-ajoene and *Z*-ajoene), acetone (DATS) or water (Allicin), diluted in DMEM. Each data point had 8 technical repeats. As previous studies have shown that the MTT reagent can be reduced by redox-sensitive compounds, a preliminary experiment was performed to ascertain whether the garlic OSCs used in this study, namely DADS, DATS, *E*-ajoene, *Z*-ajoene or allicin were able to reduce MTT to formazan in a system without cells. None of these compounds were found to reduce MTT to formazan (data not shown).

The data was analysed using GraphPad Prism 5.00 (GraphPad Software, <http://www.graphpad.com>) and fitted using a non-linear regression with a sigmoidal dose-response curve (variable slope). The average IC₅₀, defined as the concentration of the compound found to inhibit cell viability by 50% after 24 h, was obtained from 4 independent experiments.

2.5. *In vitro* inflammatory model

Briefly, 400 000 cells per well were plated in 6-well plates, allowed to settle/adhere overnight. Thereafter, cells were pre-treated with ½ IC₅₀ concentrations of the chosen garlic OSC. In order to simulate regular dietary consumption, cells were given a second dose after 24 h. In conjunction with the second dose, cells were stimulated with 10 ng/ml LPS (*E. coli* serotype O55:B5, Cat. No. L4005, Sigma-Aldrich) (unless otherwise indicated). Total RNA was extracted from cells 4 h and 8 h post LPS addition (or as indicated) for qPCR analysis for selected cytokines and inflammatory mediators. Additionally, supernatants and cell lysates were collected 8 h and 24 h post LPS addition or as indicated and analysed by sandwich ELISA and Western blot, respectively, for secretion of selected cytokines and inflammatory mediators.

Table 2.1: A summary of the experimental design for the *in vitro* inflammatory model with two independent treatment variables and four treatment groups.

| Variables | Untreated | LPS-treated |
|--------------------|-----------|-------------|
| Untreated | Group A | Group B |
| Garlic OSC-treated | Group C | Group D |

Table 2.1 summarises the experimental design with two independent variables, LPS treatment and garlic OSC treatment, and four treatment groups. Group A (untreated cells) served as a control for Group B (LPS-treated cells) and Group C (garlic OSC-treated cells), while Group B and Group C served as controls for Group D (garlic OSC- and LPS-treated cells).

Note that a minimum of three independent experiments (biological repeats) were performed with treatment groups run in triplicate (technical repeats) in each individual experiment.

2.6. Gene and protein nomenclature

In this thesis standardised abbreviations (referred to as symbols) have been used to refer to genes and proteins. According to the Human Gene Nomenclature Committee, human genes and proteins are represented by symbols written in uppercase Latin letters and Arabic numerals, and genes are distinguished from proteins by the use of italics¹⁶⁶. Human interleukin-1β, for example is written as *IL1B* (gene) or IL1B (protein). In contrast, mouse gene symbols start with a capital letter, followed by

lowercase letters and are also italicised¹⁶⁷. Mouse protein symbols are written in the same format as human proteins¹⁶⁷. Mouse interleukin-1 β is written as *Il1b* (gene) and IL1B (protein). Within the literature review, human gene and protein symbols have been used for consistency. As the experimental work for this thesis was conducted using the murine macrophage cell line RAW264.7, symbols used in the rest of this thesis refer to the mouse, unless otherwise indicated. When gene and protein expression of selected cytokines and inflammatory mediators were referred to together, both abbreviations were used i.e. *Il1b*/IL1B.

2.7. Gene expression analysis

mRNA was extracted from treated cells as described in Section 2.5, treated with DNase I to remove DNA contaminants, and reverse transcribed into complementary DNA (cDNA). cDNA was used to determine relative gene expression of selected cytokines and inflammatory mediators after LPS-stimulation using qPCR.

2.7.1. RNA extraction

Prior to RNA extraction, all surfaces and pipettes were cleaned with RNase Zap™ (Sigma-Aldrich) in order to remove RNase contaminants. The pipettes were then treated with 10 % bleach and placed under an ultraviolet lamp to degrade any contaminating DNA. Media was removed and adherent cells were washed with 1 ml PBS. 500 μ l PBS was added to each well in the 6-well plate, and adherent cells were removed by scraping with a sterile cell scraper (Corning®, Sigma-Aldrich) and transferred into a 2 ml microcentrifuge tube. Cells were pelleted by centrifugation (250xg for 5 min), the supernatant was removed and RNA was extracted using the GeneJET™ RNA Purification kit (Thermo Scientific) according to manufacturer's instructions. Briefly, the cell pellet was resuspended in Lysis Buffer supplemented with 40 mM dithiothreitol (DTT, Sigma) and vortexed for 10 s. To ensure complete cell homogenisation, cell lysates were passed through a blunt 21-gauge needle fitted to an RNase-free syringe, after which 360 μ l of 96 % ethanol was added to each sample cell lysate. The GeneJET™ RNA Purification Column was loaded with 700 μ l of lysate and centrifuged at 12000 xg for 1 min. The flow-through was discarded and loading was repeated until all lysate was loaded onto the column. The column was then transferred to a new 2 ml collection tube and washed 3x (with 700 μ l of Wash Buffer 1, 600 μ l Wash Buffer 2 and finally 250 μ l of Wash Buffer 2) and centrifuged at 12000 xg for 1 min between each wash step. The column was then inserted into a 1.5 ml microcentrifuge tube and 100 μ l of nuclease-free water (Thermo Scientific) was added to the column, followed by a 1 min centrifugation at 12000 xg. The flow-through containing the extracted RNA was collected and the concentration was measured using a Thermo Scientific NanoDrop 2000 Spectrophotometer. RNA

purity was checked by ensuring that sample ratios of absorbance 260/280 and 260/230 were above 1.8 and 2, respectively.

2.7.2. DNase I treatment

In order to remove genomic DNA from extracted RNA samples, samples were treated with DNase I endonuclease (Thermo Scientific). Briefly, 1 µg of RNA was combined with 1 µl of 10x Reaction Buffer containing Mg²⁺ and 1U of DNase I. The sample volume was then made up to 10 µl with nuclease-free water (Thermo Scientific). When higher concentrations of RNA were required, the reaction was scaled up. Samples were then incubated at 37°C for 30 min. After which, samples were either cleaned by ethanol precipitation (Section 2.7.3) or – if the RNA was intended for use with the RT² Profiler PCR Array Plates (Qiagen) (Section 2.8) – samples were repurified using GeneJET™ RNA Purification Columns as previously described (Section 2.7.1) with the exception that the Lysis Buffer was not supplemented with DTT and samples were not homogenised through a needle.

2.7.3. Ethanol precipitation of RNA oligonucleotides

Ethanol precipitation was performed in order to remove DNase I endonuclease from RNA samples. RNA samples in 2 ml microcentrifuge tubes were made up to 400 µl with nuclease-free water (Thermo Scientific) after which 50 µl of 3 M sodium acetate and 1.5 ml of 96% ethanol was added. Samples were then vortexed for 10 s and stored at -80°C overnight. Thereafter, samples were centrifuged at 13000 xg for 20 min at 4°C. Supernatants were removed and 200 µl of cold 96% ethanol (stored at -20°C) was added to each tube. The ethanol was poured off, samples were left to dry for 20 min after which 10 µl of nuclease-free water was added to the pellet and the RNA was resuspended by pipetting. RNA concentration and purity was then measured using a Thermo Scientific NanoDrop 2000 Spectrophotometer. Only RNA samples with ratios of absorbance for 260/280 and 260/230 that were above 1.8 and 2, respectively, were used for reverse transcription.

2.7.4. RNA integrity analysis

Representative RNA samples were sent to the Centre for Proteomic and Genomic Research (CPGR) to be analysed on an Agilent 2100 Bioanalyzer (Agilent Technologies) for RNA quality and integrity. The Agilent 2100 Bioanalyzer software assigns an RNA Integrity Number (RIN) based on the measured electrophoretic trace of the entire RNA sample. RINs between 7 and 10 indicate mRNA of acceptable quality for reverse-transcription PCR and downstream qPCR analysis. All samples sent for RNA integrity analysis returned RIN values of ≥ 8 , indicating that the RNA extraction and sample processing methods used return high quality RNA and that samples are not prone to RNA degradation.

2.7.5. Reverse transcription of RNA

DNase I-treated RNA was reverse transcribed using the High Capacity cDNA Reverse Transcription Kit (Applied Biosystems™), according to manufacturer's instructions. A 2x Reverse Transcription master mix was prepared containing 2 µl of 10x RT Buffer, 0.8 µl of 100 mM dNTP mix, 2 µl of 10x RT Random Primers, 1 µl of MultiScribe™ Reverse Transcriptase (50 U/µl) and 4.2 µl of nuclease-free water. For each reaction, 1 µg of total RNA was made up to a 10 µl volume with nuclease-free water in 8-well PCR stripettes. 10 µl of 2x Reverse Transcription master mix was added to 10 µl of RNA sample and mixed by pipetting. The PCR stripettes were sealed and briefly centrifuged in a desktop centrifuge and placed on ice. The following program was set up on the Applied Biosystems Gene Amp® PCR system 2700 thermal cycler set for a 20 µl reaction volume: 25°C for 10 min (annealing step), 37°C for 120 min (elongation step) and 85°C for 5 min (denaturation step). Samples were stored at -20°C until further use. For large experiments, the reverse transcription reaction was scaled up accordingly.

2.7.6. Quantitative real-time PCR (qPCR)

The Minimum Information for Publication of Quantitative Real-Time PCR Experiments (MIQE) guidelines describe the minimum information required to allow for peer-review of qPCR experiments¹⁶⁸. These reporting guidelines encourage better experimental practice by improving the accuracy, repeatability and reliability of qPCR experiments. A MIQE checklist can be found in Appendix C. This checklist was used for all qPCR experiments performed.

2.7.6.1. Primer oligonucleotide design

qPCR experiments were performed for the following genes; cyclooxygenase-2 (*Cox2*) (official gene name Prostaglandin-endoperoxide synthase 2 (*Ptgs2*)), *Il1b*, *Il6*, *Il10*, *Il12b*, *Nos2*, *Tnf*, and *Trail/Tnfsf10*. Primer sequences for selected genes were either designed using Primer3Plus free online software¹⁶⁹ or obtained from the Real Time Primer DataBase (RTPrimerDB)¹⁷⁰, with the exception of primers for *Il12b*, which were purchased from Qiagen (Cat. No. 330001 PPM03020E). Primer suitability was analysed using OligoAnalyzer 3.1 software (Integrated DNA Technologies, Inc) for oligonucleotide melting temperature (T_m) (Supplementary Table C2, Appendix C) possible hairpin loop structures (max T_m recorded in Supplementary Table C2, Appendix C) and homodimers and heterodimers. Default parameters were used with the exception of the Mg^{2+} concentration, which was set at 3 mM. The spontaneity of the formation of homodimers and heterodimers is measured as Gibbs Free energy (ΔG) (kcal/mole); the smaller the ΔG value, the more spontaneous the formation of the structure. In order to control for highly spontaneous homodimers and heterodimers, a cut off of the difference between the ΔG value for the oligonucleotide binding to its perfect complement (Maximum ΔG) and the most spontaneous homodimer or heterodimer was chosen to be less than

-30 kcal/mol. In other words, the spontaneity of the oligonucleotide binding to its perfect complement was always -30 kcal/mol more spontaneous than any other structure (Supplementary Table C2, Appendix C). Further, all primers were tested for alignment with NCBI sequences using NCBI Primer BLAST (www.ncbi.nlm.nih.gov/tools/primer-blast/) against *Mus musculus* with default settings. Accession numbers of matching sequences were recorded in Supplementary Table C2, Appendix C. Primers which met the aforementioned standards, were synthesised in the UCT Molecular and Cellular Biology DNA Synthesis Laboratory using an Applied Biosystems 394 DNA Synthesizer.

Table 2.2: Primer oligonucleotides used for qPCR analysis of relative gene expression. Further information regarding primer amplification efficiency; amplicon positions on coding sequences; primer melting temperatures; NCBI Blast results; transcript variants; and homo- and heterodimer formation can be found in Supplementary Table C2, Appendix C.

| Target Type | Target Gene Name | Gene Symbol | Sequence Accession number | Entrez ID | RT-Primer DB ID | F / R | Primer Sequence 5'-3' | Length (bp) | Amplicon Length (bp) |
|-------------------|--|--------------------------------------|---------------------------|-----------|-----------------|-------|--------------------------|-------------|----------------------|
| Reference Genes | β-actin | <i>Actb</i> | NM_007393 | 11461 | 168 | F | AGAGGGAAATCGTGCCTGAC | 20 | 138 |
| | | | | | | R | CAATAGTGATGACCTGGCCGT | 21 | |
| | β2-microglobulin | <i>B2m</i> | NM_009735 | 12010 | 1192 | F | ATTCACCCCACTGAGACTGA | 21 | 86 |
| | | | | | | R | CTCGATCCCAGTAGACGGTC | 20 | |
| | Glyceraldehyde-3-phosphate dehydrogenase | <i>Gapdh</i> | NM_008084 | 14433 | N/A | F | CCAATGTGTCCGTCGTGGATCT | 22 | 149 |
| | | | | | | R | GTTGAAGTCGAGGAGACAACC | 22 | |
| Genes of interest | Prostaglandin-endoperoxide synthase 2 | <i>Ptgs2</i> (also <i>Cox2</i>)* | NM_011198 | 17709 | N/A | F | CCAGCACTTCACCCATCAGTT | 21 | 53 |
| | | | | | | R | ACCCAGGTCCTCGCTTATGA | 20 | |
| | Interleukin-1β | <i>Il1b</i> | NM_008361 | 16176 | N/A | F | CAGGCAGGCAGTATCACTCA | 20 | 350 |
| | | | | | | R | AGGCCACAGGTATTTGTCTG | 20 | |
| | Interleukin-6 | <i>Il6</i> | NM_031168 | 16193 | 138 | F | GAGGATACCACTCCCAACAGACC | 23 | 141 |
| | | | | | | R | AAGTGCACTCATCGTTGTTCAACA | 24 | |
| | Interleukin-10 | <i>Il10</i> | NM_010548 | 16153 | 140 | F | GGTTGCCAAGCCTTATCGGA | 20 | 192 |
| | | | | | | R | ACCTGCTCCACTGCCTTGCT | 20 | |
| | Nitric oxide synthase 2 | <i>Nos2</i> | NM_010927 | 18126 | 151 | F | CAGCTGGGCTGTACAAACCTT | 21 | 95 |
| | | | | | | R | CATTGGAAGTGAAGCGTTTCG | 21 | |
| | Tumour Necrosis Factor | <i>Tnf</i> | NM_013693 | 21926 | 3747 | F | CAAAATTCGAGTGACAAGCCTG | 22 | 114 |
| | | | | | | R | GAGATCCATGCCGTTGGC | 18 | |
| | TNF superfamily member 10 | <i>Tnfsf10</i> (also <i>Trail</i>)* | NM_009425 | 22035 | N/A | F | TCTTGAACAGACCCTGCTTG | 20 | 179 |
| | | | | | | R | CCGAGTGATCCCAGTAATGTG | 21 | |

*While prostaglandin-endoperoxide synthase 2 (*Ptgs2*/PTGS2) is the official name, this gene/protein is widely referred to as cyclooxygenase-2 (*Cox2*/COX2) in the literature. For clarity we refer to this gene as *Cox2*/*Ptgs2* and protein as COX2/PTGS2 from here onwards. While, *TNF* superfamily member 10 (*Tnfsf10*/TNFSF10) is the official name, this gene/protein is widely referred to as *TNF*-related apoptosis inducing ligand (*Trail*/TRAIL) in the literature. For clarity we refer to this gene as *Trail*/*Tnfsf10* and protein as TRAIL/TNFSF10 from here onwards. When written out in full we refer to these genes or proteins as cyclooxygenase-2 and *TNF*-related apoptosis-inducing ligand.

2.7.6.2. Confirmation of primer specificity: melt curves and gel electrophoresis

Melt curve analysis was used to control for primer specificity and was checked for a single peak indicative of a single qPCR product (amplicon). Melt curve analysis makes use of SYBR Green I dye which is an asymmetrical cyanine dye that preferentially binds to double stranded DNA. (dsDNA) The DNA-dye complex absorbs light at 497 nm and emits light at 520 nm, and can thus be used to measure the quantity of DNA in qPCR. In order to determine whether there was a single amplicon product, a

melt curve analysis was performed, where the temperature of the sample is increased incrementally while the instrument continues to measure fluorescence (Supplementary Figure C1, Appendix C). As the dsDNA dissociates, so will the SYBR Green I dye resulting in a decrease in fluorescence. The change in slope of the fluorescence is plotted against the temperature to create a melt curve. A single peak on a melt curve indicates that all dsDNA dissociated at the same temperature, suggesting that there is a single amplicon. In order to verify the presence of a single product, qPCR samples and 5 µl O'GeneRuler 50 bp DNA Ladder (Thermo Scientific) were loaded onto a 3% agarose gel and subjected to gel electrophoresis in 1x TBE (Appendix A) for 2 h at 100V to separate products by size (Supplementary Figure C1, Appendix C).

2.7.6.3. qPCR reagents and reaction conditions

qPCR experiments were carried out using the SensiMix™ SYBR®-No-ROX Kit (BioLine). A master mix for each gene target was prepared for the required number of reactions. A 1x master mix contained 5 µl of 2x SensiMix™ SYBR® No-ROX (final concentration of 3 mM MgCl₂), 1 µl of 10 µM forward primer (final concentration 1 µM), 1 µl of 10 µM reverse primer (final concentration 1 µM) and 2 µl of nuclease-free water. Using a multichannel pipette, 9 µl of the master mix was loaded per well into either a 96-well or 384-well white polypropylene LightCycler® 480 Multiwell plate (Roche), followed by 1 µl cDNA (prepared as described in Section 2.7.5) to make a final reaction volume of 10 µl. The plate was sealed with Optical Adhesive Film (Roche) and centrifuged for 3 min at room temperature in an Eppendorf® 5810R centrifuge to remove air bubbles. Each sample for each gene target was performed in duplicate including negative controls; the no-template control and no-reverse transcription control were included to control for DNA contamination. The samples were considered free of DNA contamination if the difference between the negative control quantification cycle (C_q) and the lowest concentration unknown sample (that would have the highest C_q value of the unknown samples) was > 5 C_qs. In addition, a 10-fold serial dilution of cDNA, pooled from all samples within a given experiment, was included in each experiment from which primer target and run-specific amplification efficiency was calculated (Section 2.7.6.5). The qPCR reaction conditions for the Roche LightCycler 480II are detailed in Table 2.3.

Table 2.3: Quantitative real time PCR thermal cycling conditions.

| Cycles | Temperature (°C) | Time | Notes |
|--------|---------------------------|--------|--------------------------------------|
| 1 | 95 | 10 min | Polymerase activation |
| 45 | 95 | 30 s | Denaturation |
| | 64* (see Section 2.7.6.4) | 30 s | Annealing |
| | 72 | 90 s | Extension & Fluorescence Acquisition |
| 1 | Range | set | Melt curve analysis |

2.7.6.4. Optimisation of qPCR annealing temperature

In order to determine the ideal conditions for qPCR using the primers listed in Table 2.2, a temperature gradient qPCR was performed using a gradient qPCR machine, the CFX96 Touch™ Real-Time PCR System (Bio-Rad Laboratories, Inc). Reaction conditions used are described in Table 2.3, with the following annealing temperatures: 58, 59, 60, 61, 62, 63, 64 and 65°C. The annealing temperature which on average yields the lowest C_q values for the targets tested is the optimal temperature. In this case the optimum annealing temperature was 64°C (Supplementary Figure C3, Appendix C) and thus the annealing temperature for all subsequent qPCR experiments was set to 64°C. Note as this experiment used a different qPCR machine, compatible white polypropylene Hard-Shell® 96-Well PCR Plates (Bio-Rad Laboratories, Inc) were used for this experiment only.

2.7.6.5. PCR efficiency correction

Conversion of C_q values to normalised relative quantities (NRQ) is required in order to determine relative gene expression. Relative quantification of gene expression was achieved by normalising the expression of a gene of interest to the expression of stable reference genes using qBase plus software (Biogazelle). qBase plus software utilises a modified version of the PCR efficiency-corrected method¹⁷¹, which makes use of a serial dilution curve to calculate the amplification efficiency of the primer oligonucleotides. The qBase plus method as described by Hellemans et al. (2007)¹⁷² allows for PCR efficiency-correction as well as normalisation to multiple reference genes. Amplification efficiencies from a representative experiment for primer oligonucleotides are included in Supplementary Table C2 (Appendix C).

2.7.6.6. Reference gene stability and selection using geNorm geometric normalisation factor

The conventional use of a single reference gene for normalisation in relative qPCR experiments can result in inaccurate interpretation of relative gene expression data¹⁷³. This is especially true when a reference gene is not stably expressed in tissues, cell lines or across experimental conditions¹⁷³. It is therefore important to assess the stability of reference genes prior to normalisation. It has also been shown that normalising a gene of interest to a normalisation factor (calculated as the geometric mean of multiple stably-expressed reference genes) provides more accurate and reliable results¹⁷³. In order to determine reference gene stability and the minimum number of reference genes required for accurate normalisation, three reference genes - β -actin (*Actb*), glyceraldehyde -3 phosphate dehydrogenase (*Gapdh*), and β 2-microglobulin (*B2m*) - were analysed using qBase plus software

(Biogazelle) (see Hellemans et al. (2007) and Vandesompele et al. (2002)^{172,173} for details on formulae) (Table 2.4). All three reference genes analysed had acceptable geometric normalisation factor (geNorm M) (<0.5) and coefficient of variation (CV) (<0.2) values. While *Gapdh* and *B2m* were the two most stable of these genes, the amplification efficiency determined for *B2m* (Supplementary Table C2, Appendix C) did not fall within the acceptable 90–110% range. *Actb* and *Gapdh* were therefore chosen to determine the normalisation factor for all future experiments.

Table 2.4: Reference gene stability and selection. Potential reference genes β -actin (*Actb*), β -microglobulin (*B2m*) and glyceraldehyde-3-phosphate dehydrogenase (*Gapdh*) were assayed for stability across treatment conditions. The geNorm M (geometric normalisation factor) and CV (coefficient of variation) values were determined by the qBase plus software (Biogazelle) geNorm function. Acceptable values are geNorm M and CV values below 0.5 and 0.2, respectively.

| Reference gene | geNorm M | CV |
|----------------|----------|-------|
| <i>Actb</i> | 0.358 | 0.159 |
| <i>B2m</i> | 0.341 | 0.135 |
| <i>Gapdh</i> | 0.311 | 0.114 |

2.8. RT² Profiler PCR Arrays

Murine Inflammatory Response and Autoimmunity RT² Profiler PCR Arrays (Cat. No. PAMM-077Z, Qiagen) were performed to determine the effect of selected garlic OSCs on LPS-induced inflammatory gene expression for 84 different genes. Samples were processed and analysed for RNA integrity as described under Sections 2.7.1, 2.7.2 and 2.7.4. A pooled sample, consisting of three technical repeats, was used for each treatment group.

2.8.1. Reverse transcription

Total RNA was reverse transcribed into cDNA using the RT² First Strand Kit (Qiagen) according to manufacturer's instructions. Briefly, 500ng of RNA was added to 2 μ l Genomic DNA Elimination Buffer, made up to 10 μ l with RNase-free water and mixed by pipetting. Samples were incubated at 42°C for 5 min and then transferred to ice. A 10x reverse transcription mix was made for four reactions containing 16 μ l of 5x Buffer BC3, 4 μ l Control P2, 8 μ l RE3 Reverse Transcriptase Mix and 12 μ l RNase-free water. 10 μ l of the reverse transcription mix was added to each sample and mixed by pipetting. Samples were then incubated at 42°C for 15 min and the reaction was stopped by incubating at 95°C for 5 min. Samples were then made up to 111 μ l by adding 91 μ l of RNase-free water and stored at -20°C.

2.8.2. Quantitative real-time PCR (qPCR)

A PCR components mixture was made for each sample containing 650 µl 2x RT² SYBR Green Mastermix, 102 µl cDNA and 548 µl of RNase-free water. The PCR components mixture for each sample was then transferred into a 50 ml reagent reservoir (Axygen®, Corning, Sigma-Aldrich) and 10 µl was loaded onto the Roche Lightcycler compatible 384-well RT² Profiler PCR Array plates. The provided 384EZLoad covers were used to guide pipetting of samples into the correct wells. The plate was then sealed using the Optical Adhesive Film and centrifuged at 1000 xg for 1 min at room temperature in an Eppendorf® 5810R centrifuge. qPCR was performed using the Roche LightCycler 480II and cycling conditions are detailed in Table 2.5. Cq values were exported to Microsoft Excel and analysed using qBase plus software with the assumption that the oligonucleotide primer efficiencies were 100%. Results are shown as the average of two independent experiments.

Table 2.5: RT² Profiler PCR Array thermal cycling conditions

| Cycles | Temperature (°C) | Time | Notes |
|--------|------------------|--------|--|
| 1 | 95 | 10 min | Polymerase activation |
| 45 | 95 | 15 s | Denaturation |
| | 60 | 1 min | Annealing, elongation and fluorescence acquisition |
| 1 | Range | set | Melt curve analysis |

2.9. Protein expression analysis

2.9.1. Enzyme-Linked Immunosorbent Assay

Cell culture supernatants from cells treated as described in Section 2.5 were assayed for concentrations of the following cytokines: IL1B, IL6, IL10, TNF and IL12B using sandwich ELISAs (BD OptEIA™, BD Biosciences). A murine TRAIL (TNFSF10) ELISA kit was purchased from Komabiotech.

2.9.1.1. Sample preparation

RAW 264.7 murine macrophages were treated as described in Section 2.5 and cell culture supernatants were collected 24 h after addition of LPS. The supernatants were centrifuged at 350 xg for 5 min at 4°C to remove floating cells and debris after which the supernatants were transferred into new microcentrifuge tubes and either used immediately for ELISA analysis or stored at -80°C until use.

2.9.1.2. Protocol

A 96-well high-binding polystyrene ELISA plate (Microlon®, Greiner Bio-One) was coated with 100 µl of capture antibody (1:250) diluted in 1x PBS. The plate was covered with a lid, placed in a sealed humidified container and stored at 4°C overnight. (Note that for all subsequent incubation steps, the

plate was covered with a lid and incubated at room temperature inside a humidified container to minimise evaporation.) The following day, the wells were aspirated and washed 3x with ELISA Wash Buffer 1 (Appendix A). The wells were blocked with 200 µl of Assay Diluent (BD OptEIA™, BD Biosciences) for 1 h. The plate was washed 3x with ELISA Wash Buffer 2 (Appendix A). Standards were prepared as 2-fold serial dilutions in Assay Diluent (BD OptEIA™, BD Biosciences) with the following highest concentrations: 1000 pg/ml for *IL6*, *TNF*, *IL12B* and 2000 pg/ml for *IL1B* and *IL10*. Blank Assay Diluent served as the zero standard (0 pg/ml). Wells were loaded with 100 µl of standard or sample in duplicate and incubated for 2 h. The plate was then washed 5x with ELISA Wash Buffer 1, after which 100 µl of the working detector (detection antibody at kit-specified concentration and streptavidin-horseradish peroxidase (HRP) (1:250) diluted in Assay Diluent) was added to each well and incubated for 1 h. The plate was then washed 7x with ELISA Wash Buffer 1, 100 µl of Substrate Solution (BD Pharmingen™ TMB Substrate Reagent Set, BD Biosciences) was added to each well and the plate was then incubated in the dark for 30 min. The enzyme reaction was stopped using 100 µl of 1 M H₂SO₄. The plate was briefly heated with a flame to remove any air bubbles and absorbance was measured using a plate-reading spectrophotometer (VersaMax™ Tuneable Microplate Reader, Molecular Devices) at 450 nm (within 30 min after stopping the reaction). Protein concentration of samples was determined by plotting the concentration of the standards against the corresponding OD reading to generate a standard curve.

2.9.2. SDS-PAGE and Western blot analysis

2.9.2.1. Preparation of cell lysates and determination of protein concentration

Cell lysates were collected from adherent cells by adding 200 µl Cell Lysis Buffer (1x Cell Culture Lysis 5x Reagent (Promega) supplemented with 1x Halt™ Protease Inhibitor Cocktail (100x) (Thermo Scientific)) and scraping with the back of a pipette tip. Cell lysates were transferred into microcentrifuge tubes and incubated on ice for 5 min, centrifuged at 13 000 xg for 5 min and the supernatants were collected and stored at -20°C until further use. Protein concentration was determined using the Pierce™ BCA Assay Kit (Pierce Biotechnologies) according to manufacturer's instructions.

2.9.2.2. SDS-Polyacrylamide Gel Electrophoresis (PAGE)

10 µg total protein per sample was mixed with 2 µl of 5x Non-Reducing Lane Marker (Thermo Scientific) containing 0.1 M DTT and incubated at 95°C for 5 min in order to linearise proteins. Samples were then loaded onto 1.5 mm thick 10% sodium dodecyl sulphate (SDS)-polyacrylamide gels (Appendix A) along with 5 µl of PageRuler™ Plus Prestained Protein Ladder (Thermo Scientific). SDS-

polyacrylamide gel electrophoresis (PAGE) gels were electrophoresed in 1x SDS-PAGE Running Buffer (Appendix A) in a Mini PROTEAN II™ system (BioRad) at 100 V for approximately 90 min.

2.9.2.3. Western blotting

SDS-PAGE separated proteins were then transferred onto a nitrocellulose membrane (Hybond™, Amersham) in 1x SDS-PAGE Transfer Buffer (Appendix A) at 100 V for 1 h. Equal loading and protein transfer was confirmed by Ponceau staining (Appendix A) of the nitrocellulose membranes. Nitrocellulose membranes were then blocked at room temperature for 1 h on a rocking platform shaker with 5% w/v bovine serum albumin (BSA, Sigma-Aldrich) in TBS (Appendix A) with 0.1% Tween in TBS (TBST) for phospho-STAT3, otherwise in 5% w/v non-fat powdered milk in PBS (Appendix A) with 0.1% Tween (PBST) .

Table 2.6: Primary antibodies used in Western blotting.

| Primary Antibody | Target MW (kDa) | Organism raised in | Monoclonal/ Polyclonal | Dilution used | Source | Cat. No. |
|------------------------------|-----------------|--------------------|------------------------|---------------|-----------------------------|----------|
| Dansyl | N/A* | Rabbit | monoclonal | 1:7500 | Life Technologies | A-6398 |
| COX-2 (C-20) | 70-72 | Goat | polyclonal | 1:1000 | Santa Cruz Biotechnology | sc-1746 |
| GAPDH(FL-335) | 37 | Rabbit | polyclonal | 1:1000 | Santa Cruz Biotechnology | sc-25778 |
| Phospho-STAT3 (Tyr705)(D3A7) | 80 | Rabbit | monoclonal | 1:2000 | Cell Signalling Technology® | 9145 |
| STAT3 (124H6) | 80 | Mouse | monoclonal | 1:1000 | Cell Signalling Technology® | 9139 |

* The dansyl antibody was used to detect dansylated proteins and therefore the MW of interest was that of the protein of interest.

After membrane blocking, the primary antibody at the concentration listed in Table 2.6 was added to 10 ml of the appropriate blocking solution and the membranes were incubated at 4°C on a rocking platform shaker overnight. The membrane was then washed 3x in 10 ml TBST or PBST, after which a secondary HRP-conjugated antibody against the organism the antibody was raised in was added in 5% w/v BSA-TBST or 5% w/v milk-PBST and incubated at room temperature for 1 h. The blot was washed 3x in 10 ml TBST or PBST, thereafter 1 ml of LumiGlo® Chemiluminescent substrate (KPL) was pipetted onto the membrane and chemiluminescence was visualised using the VisionWorks LS Biospectrum™ 500 Imaging system (UVP). In order to probe the membrane for another protein, the blot was stripped in 1 M glycine pH2.2 for 10 min and washed 1x in PBST. Blocking was repeated using 5% non-fat milk PBST for 1 h prior to the addition of the primary antibody and the procedure was repeated as described above. Relative quantification of protein bands was performed using the UVP densitometry tool.

2.10. Proteome Profiler™ Mouse Cytokine Array

A Proteome Profiler™ mouse cytokine Array (Cat. No. ARY006, R&D Systems) for 40 mouse cytokines and chemokines was performed to obtain a more comprehensive overview of the effects of selected garlic OSCs on LPS-induced cytokine expression. This array consists of four nitrocellulose membranes spotted with 40 different anti-cytokine antibodies. Incubation of these membranes with cell culture supernatants, followed by addition of Streptavidin-HRP and chemiluminescent detection reagents allows for relative quantitation of cytokine concentration. Briefly, nitrocellulose membranes were blocked with 2 ml of Array Buffer 6 in the provided 4-Well Multidish for 1 h on a rocking platform shaker. Samples were prepared by adding 500 µl of cell culture supernatant to 500 µl of Array Buffer 4 and 500 µl of Array Buffer 6. Reconstituted Detection Antibody Cocktail (15 µl) was then added and samples were mixed and incubated at room temperature for 1 h. After membrane blocking, Array Buffer 6 was aspirated and the prepared sample/antibody mixtures were added to the membranes and incubated at 4°C on a rocking platform shaker overnight. The following day, membranes were washed 3x with 20 ml 1x Wash Buffer for 10 min. Streptavidin-HRP diluted (1:2000) in 2 ml Array Buffer 6 was then added to the membranes and incubated for 30 min on a rocking platform shaker. After which, membranes were washed 3x with 20 ml 1x Wash Buffer for 10 min and placed onto acetate sheets. Chemi Reagent Mix (1 ml) was pipetted onto the membrane and chemiluminescence was visualised using the VisionWorks LS Biospectrum™ 500 Imaging system (UVP). Relative protein quantification was performed using the UVP densitometry tool.

2.11. Protein alkylation by dansylated-ajoene

In order to determine whether garlic OSCs undergo a thiol-disulfide exchange reaction with the transcription factor STAT3, *E/Z*-ajoene labelled with a dansyl functional group (synthesised by Jonathon Cotton, Department of Chemistry, UCT) (Figure 2.4) was incubated with recombinant STAT3 protein and run on an SDS-PAGE gel either under non-reducing or reducing conditions (100 mM DTT).

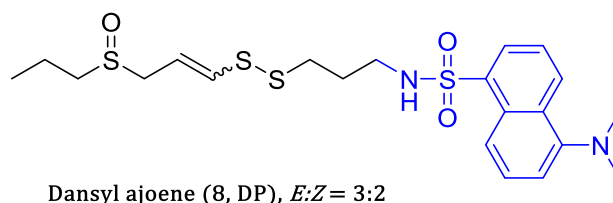


Figure 2.4: Chemical structure of the dansylated-*E/Z*-ajoene. The dansyl functional group is highlighted in blue.

Briefly, 25 µM of dansyl-labelled *E/Z*-ajoene was incubated with 0.5 µM of recombinant human STAT3 protein (Cat. No. SRP2062, Sigma-Aldrich), made up to 5 µl in PBS, for 2 min at room temperature.

Either 1 µl of 5x Non-Reducing Lane Marker (Thermo Scientific) or 1 µl of 5x Reducing Lane Marker (5x Non-Reducing Lane Marker, containing 100 mM DTT), was added to the sample and samples were incubated at 95°C for 5 min. Samples were loaded and run on an SDS-PAGE gel (Section 2.9.2.2) and then transferred to a nitrocellulose membrane (Section 2.9.2.2). Nitrocellulose membranes were probed with the dansyl antibody, and reprobed with the STAT3 antibody (see Table 2.6). Co-localization of the STAT3 and dansyl residue under non-reducing conditions indicates that a thiol-disulfide reaction took place between the dansyl-labelled *E/Z*-ajoene and STAT3.

2.12. Statistical analysis

One-way analysis of variance (ANOVA) significance testing along with Tukey's Hypothesis testing was performed to compare differences in gene and protein expression of the 4 treatment groups namely; untreated, LPS-treated, garlic treated and garlic treatment in conjunction with LPS-stimulation. Prior to one-way ANOVA testing, the D'Agostino & Pearson omnibus normality test and Levene's test were performed to determine whether the data violated the normality and homogeneity of variance assumptions, respectively. A violation of homogeneity of variance can, however, be ignored if the sample sizes in each group are equal¹⁷⁴. Further, as many cytokines are only expressed by macrophages upon exposure to an inflammatory stimulus such as LPS, the untreated group and the garlic OSC -treated group often displayed very small variance (the expression was often zero or close to zero). Therefore the homogeneity of variance assumption was sometimes violated due to more variance in the LPS-treated groups compared to the control groups. For this reason, if the groups were normally distributed, the data were considered to be parametric and one-way ANOVA significance testing was performed.

Chapter 3 Results

3.1. MTT colorimetric cell viability assays

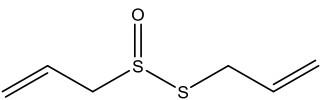
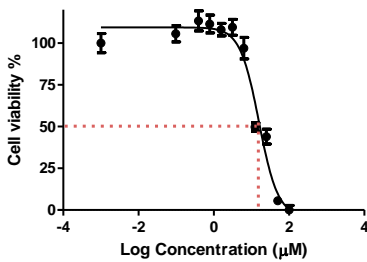
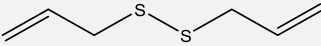
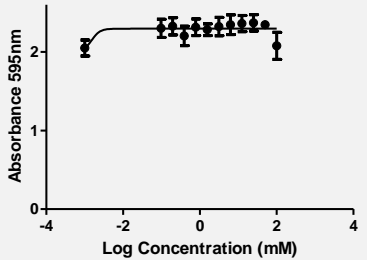
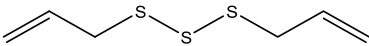
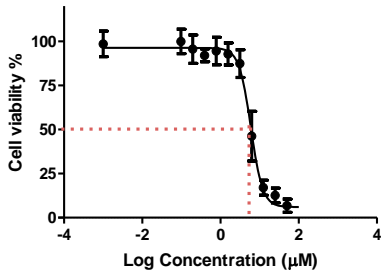
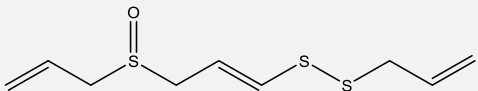
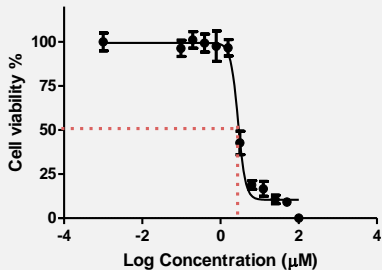
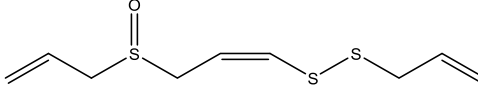
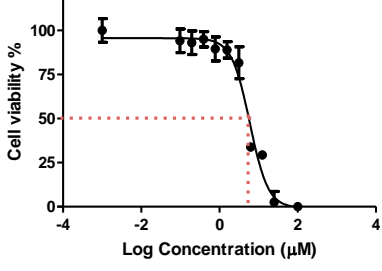
In order to determine the concentration at which the selected garlic OSCs show sub-toxic effects on the murine macrophage cell line RAW264.7, thiazolyl blue tetrazolium bromide (MTT) colorimetric viability assays were performed. This assay is based on the reduction of yellow tetrazolium salt (MTT) to purple formazan crystals by metabolically active cells. We determined percentage cell viability by measuring relative absorbance at 595 nm and this was plotted against the log concentration of the garlic OSC to generate a dose-response curve (Table 3.1) using GraphPad Prism 5.00 (GraphPad Software, <http://www.graphpad.com>) dose-response curve fitting to a non-linear response. The IC₅₀ value is defined as the concentration of the compound found to inhibit cell viability by 50% after a 24 h incubation period. Since we wanted to study the effects of the garlic OSCs on immune modulation, we wanted to select a dose that did not elicit any cytotoxic effects to the macrophages. We therefore selected half the IC₅₀ value (a value in the sub-toxic concentration range of the compound determined to be ≥ 90 % cell viability) for the garlic OSCs, for all subsequent gene and protein expression experiments.

3.2. Establishing an *in vitro* inflammatory model

In order to determine the effects of the selected garlic OSCs on the inflammatory immune response, an *in vitro* inflammatory model was developed. The murine macrophage cell line RAW264.7 was chosen with the idea of ultimately determining the effects of garlic OSC gavage on induced gastrointestinal and colorectal inflammation in BALB/c mice (an *in vivo* inflammatory model). The experimental work from this thesis will serve as the basis for the *in vitro* proof-of-concept required for an ethics application for future *in vivo* experiments. It must be noted that although LPS-induced inflammation in macrophages is a common model for acute bacterial infection, cancer-friendly chronic inflammation cannot be studied at an *in vitro* level using cultured macrophages as these cells become unresponsive to inflammatory stimuli following prolonged exposure¹⁷⁵.

In this *in vitro* model, we stimulated an inflammatory response in murine RAW264.7 macrophages using lipopolysaccharide (LPS), before assessing the effects of garlic OSC treatment on said inflammatory response. To simulate regular dietary consumption of garlic, cells were given two $\frac{1}{2}$ IC₅₀-concentration doses of the individual garlic OSCs, 24 h apart. Twenty-four hours after the first dose of the garlic OSC was given, cells were treated with a second dose of the garlic OSC in conjunction with LPS. However, in order to establish this *in vitro* model, it was important for us to first optimise the conditions for LPS treatment.

Table 3.1 Chemical structures and representative IC₅₀ dose-response curves of selected garlic OSCs. Log concentration is plotted against percentage cell viability determined using MTT colorimetric assays for the RAW264.7 murine macrophage cell line. Average IC₅₀ values were calculated from 4 independent experiments and half IC₅₀ values were chosen as a sub-toxic concentration for all subsequent cell culture experiments.

| Compound | Chemical Structure | Sigmoidal Dose-Response Curve | Mean IC ₅₀ ± SD (μM) | ½ IC ₅₀ (μM) |
|---------------------------|---|--|---------------------------------|-------------------------|
| Allicin |  |  | 22.4 ± 5.77 | 11.2 |
| Diallyl disulfide (DADS) |  |  | IC ₅₀ > 100 mM* | |
| Diallyl trisulfide (DATS) |  |  | 4.59 ± 1.66 | 2.30 |
| E-ajoene |  |  | 2.71 ± 0.50 | 1.36 |
| Z-ajoene |  |  | 4.39 ± 1.31 | 2.20 |

*An IC₅₀ dose-response curve could not be determined for DADS even at millimolar (mM) concentrations. The DADS graph is therefore depicted as the absorbance at 595nm plotted against log concentration.

3.2.1. Optimizing LPS concentration and stimulation time

Cells of the innate immune system recognise pathogen-associated molecular patterns (PAMPs) from foreign microorganisms to which they mount an immune response¹⁷⁶. The bacterial endotoxin LPS is a PAMP found in the outer membrane of gram-negative bacteria¹⁷⁶. While LPS stimulation of cultured macrophages is a common *in vitro* assay used to study the inflammatory response, the concentration used for a particular experiment can vary from 1 ng/ml up to 10 µg/ml^{146,177–179}. The chosen dosage depends on the biological origin of the LPS, the cell line used, the stimulation time and the desired level of inflammatory response. In this study we used LPS from *E. coli* serotype O55:B5 (Cat. No. L4005, Sigma-Aldrich) and initially determined the optimum concentration and stimulation time for the *in vitro* inflammatory model.

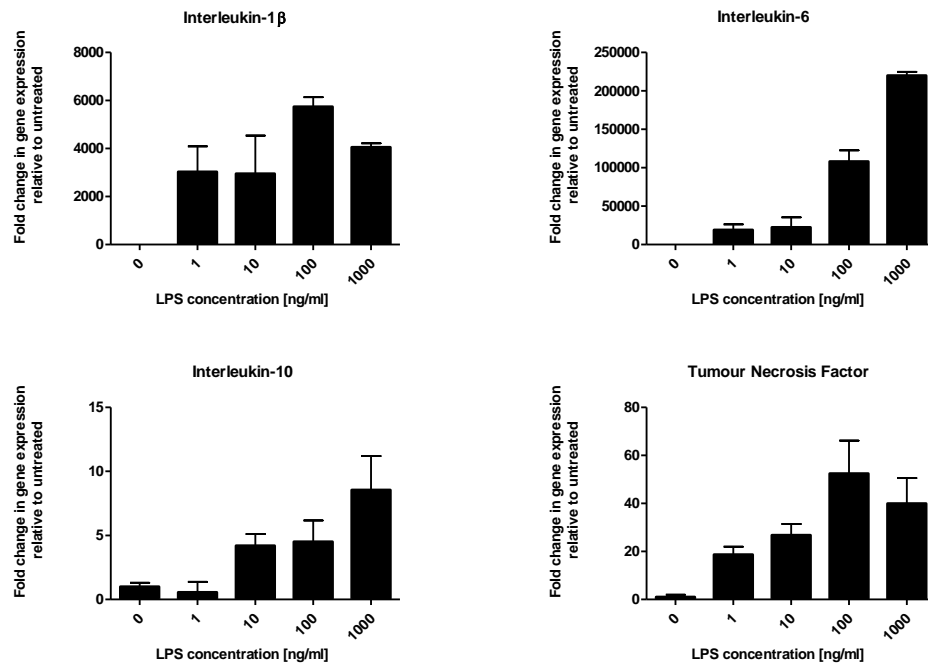
3.2.1.1. Determining the optimal concentration of LPS

Gene expression of the cytokines *Il1b*, *Il6*, *Il10* and *Tnf* was measured by qPCR analysis after a 4 h-stimulation period with either 0, 1, 10, 100 or 1000 ng/ml LPS (Figure 3.1 A). A review of the literature suggested that a 4 h LPS-stimulation time was most appropriate for the analysis of the gene expression of multiple cytokines and chemokines^{177,180,181}. After 4 h, 1000 ng/ml LPS induced the highest gene expression of *Il6* and *Il10*, while LPS-induced expression of *Il1b* and *Tnf* peaked at 100 ng/ml (Figure 3.1A). Furthermore, while 1 ng/ml LPS was sufficient to induce increased gene expression for *Il1b*, *Il6* and *Tnf* after 4 h, this concentration did not induce *Il10* gene expression at the same timepoint. As we wanted an LPS concentration high enough to detect inflammatory gene and protein expression, but low enough to determine whether treatment with garlic OSCs modulated the inflammatory response, a concentration of 10 ng/ml LPS was chosen for all further experiments.

3.2.1.2. Determining optimal timepoints for gene and protein expression analysis

Cytokines, chemokines and inflammatory mediators are expressed at different times during the inflammatory response^{182,183}. We performed preliminary experiments to determine the best timepoints at which to harvest RNA and cell culture supernatants for gene and protein expression analysis of selected cytokines, respectively. Murine RAW264.7 macrophages were treated with 10 ng/ml LPS and RNA and cell culture supernatants were collected 0, 2, 4, 6, 8, 12 and 24 h after addition of LPS. Figure 3.1B shows the gene and protein expression profiles for the aforementioned cytokines at these timepoints. Gene expression peaked between 2 and 8 h for all cytokines tested, while protein expression generally peaked between 6 and 12 h.

A



B

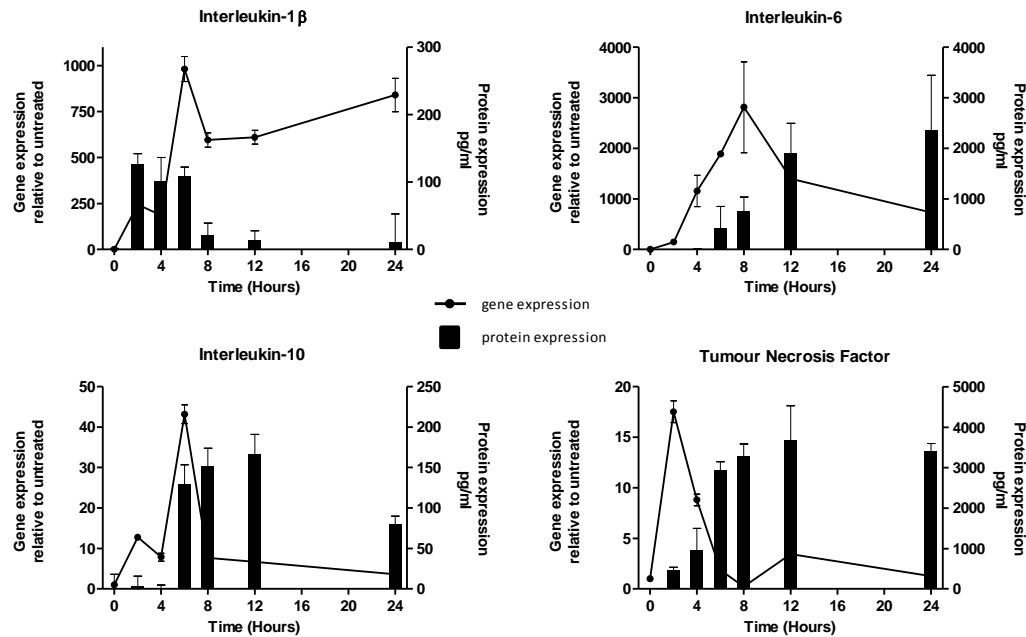


Figure 3.1: Dose- and time-dependent gene and protein expression of interleukin-1 β , interleukin-6, interleukin-10 and tumour necrosis factor in response to LPS. A. LPS-induced gene expression of selected cytokines was measured by qPCR after 4 h incubation with 0, 1, 10, 100 and 1000 ng/ml LPS. Mean fold change in gene expression (\pm SEM) compared to the untreated control samples was determined for 3 samples per condition. **B.** Temporal gene- and protein-expression profiles of selected LPS-induced cytokines. Samples harvested 0, 2, 4, 6, 8, 12 and 24 h after LPS addition were analysed by qPCR and sandwich ELISA, respectively. While mean gene expression (lines) is presented relative to untreated controls, due to detectable background transcription, protein expression (bars) is presented as pg/ml as some cytokines are not expressed in the absence of an inflammatory stimulus.

It must be noted that in Figure 3.1B, the peak in IL1B protein expression (between 2 and 6 h) precedes the peak in gene expression (at 6 h). This may be explained by cleavage, activation and secretion of the inactive cytosolic pro-IL1B into mature IL1B which occurs in response to PAMP stimulation¹⁸⁴. As we wanted to assess the effects of garlic OSC treatment on the LPS-induced expression of multiple cytokines, chemokines and inflammatory mediators, time points for sampling gene and protein expression levels were chosen to best represent the peaks in expression of the cytokines seen in the preliminary experiments (Figure 3.1A). Therefore, the timepoints 4 h and 8 h were chosen for all subsequent gene expression analyses while 8 h and 24 h were chosen for subsequent protein expression analyses. Figure 3.2 shows a workflow diagram summarising the methods used to obtain RNA and cell culture supernatant or cell lysate samples for all subsequent gene and protein expression analysis experiments.

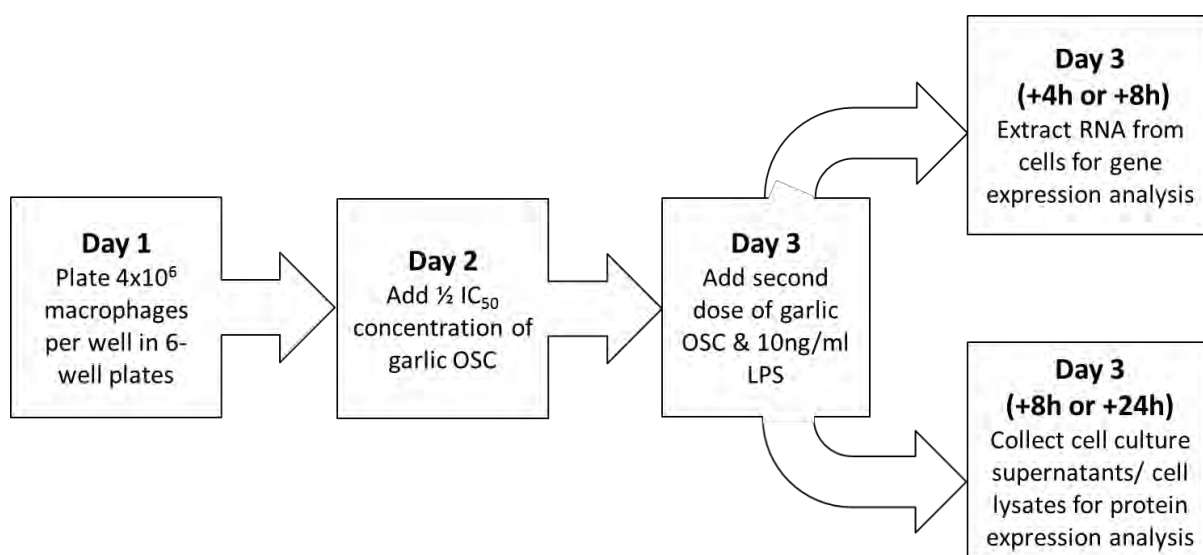


Figure 3.2: Workflow diagram for the *in vitro* inflammatory model in murine RAW264.7 macrophages.

3.2.1.3. Selection of garlic organosulfur compounds

The effects of the garlic OSCs allicin, DATS, *E*-ajoene, and *Z*-ajoene on LPS-induced gene expression of *Il1b*, *Il6*, *Il10* and *Tnf* were determined in order to select the representative garlic OSCs for subsequent experiments. We excluded DADS because we could not obtain an IC₅₀ value even at 100mM concentrations (Table 3.1). The MTT assay was working as the cells were able to reduce MTT reagent into formazan crystals and DADS compound purity was assessed by ¹H NMR and TLC. Preliminary experiments showed that *E*-ajoene, *Z*-ajoene and DATS did not appear to affect the LPS-induced expression of *Il6* (Figure 3.3B), *Il10* (Figure 3.3C) and *Tnf* (Figure 3.3D) after 4 h. However, DATS and *E*-ajoene treatment showed a downregulating trend on the LPS-induced expression of *Il1b*, while *Z*-

ajoene treatment resulted in the largest decrease in LPS-induced *Il1b* expression (Figure 3.3A). Allicin treatment, on the other hand, upregulated the LPS-induced expression of all four cytokines tested (Figure 3.3). Therefore allicin (a major component of raw garlic) and DATS, *E*-ajoene, and *Z*-ajoene (major components of cooked garlic) appeared to elicit contrasting immune responses. Allicin is a highly unstable compound which is present in high concentrations in freshly crushed garlic preparations, while *Z*-ajoene is present in aged garlic preparations or cooked garlic preparations and is more representative of dietary garlic¹⁸⁵. To best simulate the effect of dietary garlic on LPS-induced inflammation, we wanted to choose two compounds that represent raw and cooked garlic. As allicin is the major garlic OSC in raw garlic it was chosen for further experimentation. In addition, *Z*-ajoene was chosen to represent cooked garlic as it had the strongest effect on LPS-induced *Il1b* expression and we had a dansyl-tagged *E/Z*-ajoene which would be used for protein interaction studies

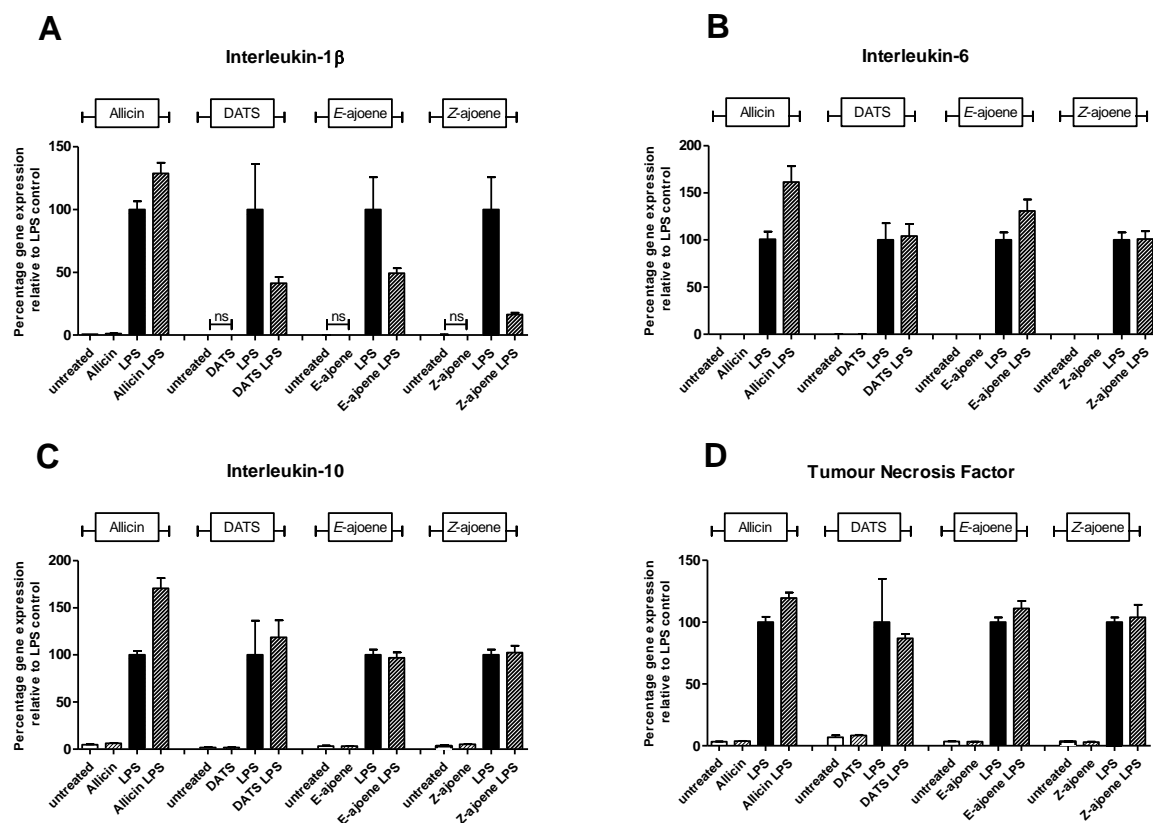


Figure 3.3: The effect of garlic OSC treatment on LPS-induced gene expression of selected cytokines in murine RAW264.7 macrophages. qPCR gene expression analysis was performed on RNA extracted from cells pre-treated with $\frac{1}{2}$ IC₅₀ concentrations of either allicin, DATS, *E*-ajoene or *Z*-ajoene. After 24 h cells were stimulated with a second dose of the garlic OSC and stimulated with 10 ng/ml LPS for 4 h. Mean percentage gene expression of **A.** interleukin-1 β , **B.** interleukin-6, **C.** interleukin-10 and **D.** tumour necrosis factor is shown relative to the LPS control (set to 100% expression). All data are presented as mean \pm SEM of three samples per condition for a single experiment.

3.3. Gene and protein expression of selected cytokines and inflammatory mediators

In order to determine whether the garlic OSCs allicin and Z-ajoene affect LPS-induced inflammation, gene and protein expression analysis on selected cytokines and inflammatory mediators was performed. Experiments were performed as described in the Figure 3.2. Briefly, cells were stimulated with $\frac{1}{2}$ IC₅₀ concentrations of allicin or Z-ajoene; after 24 h a second dose was administered in conjunction with 10 ng/ml LPS.

Total RNA was extracted 4 h and 8 h after addition of LPS (in conjunction with the second dose of the selected garlic OSC) and analysed by qPCR. Gene expression analysis was performed on the inflammatory cytokines *Il1b*, *Il6*, *Il10*, *Il12b* and *Tnf*; inflammatory enzymes *Nos2* and *Cox2/Ptgs2*; and the pro-apoptotic ligand *Trail/Tnfsf10*.

Protein expression of IL1B, IL6, IL10, IL12B, TNF and TRAIL/TNFSF10 was analysed by sandwich ELISA using cell culture supernatants collected 8 h and 24 h after addition of LPS (in conjunction with the second dose of the selected garlic OSC). COX2 protein expression was analysed by Western blotting using whole cell lysates.

As many of the genes and proteins are only expressed upon exposure to an inflammatory stimulus, all figures show percentage gene or protein expression relative to the LPS-treated (positive control) samples (set to 100% expression).

In general, the mRNA gene expression data are supported at the protein level (Figure 3.4-3.11) and LPS treatment either significantly upregulated or showed a strong increasing trend in the expression of the selected cytokines and inflammatory mediators. Treatment with the garlic OSCs alone did not significantly affect the gene or protein expression of any of the analysed cytokines or inflammatory mediators (Figures 3.4 - 3.11). Treatment with allicin or Z-ajoene, however, did affect LPS-induced expression and these effects were, in general, similar for both allicin and Z-ajoene (Figure 3.4-3.11 & summarised in Table 3.2). However, allicin mostly had a more potent immunomodulatory effect (Table 3.2).

Gene and/or protein expression of *Il1b*/IL1B, *Il6*/IL6 and *Il12b*/IL12B (Figure 3.4 - 3.6) were downregulated, while *Il10*/IL10, *Cox2*/COX2 and *Trail/Tnfsf10* (Figure 3.7, Figure 3.9 & Figure 3.10) were upregulated by garlic OSC treatment. LPS-induced expression of *Tnf*/TNF and *Nos2* was differentially affected by allicin and Z-ajoene (Figure 3.8).

Interleukin-1 β

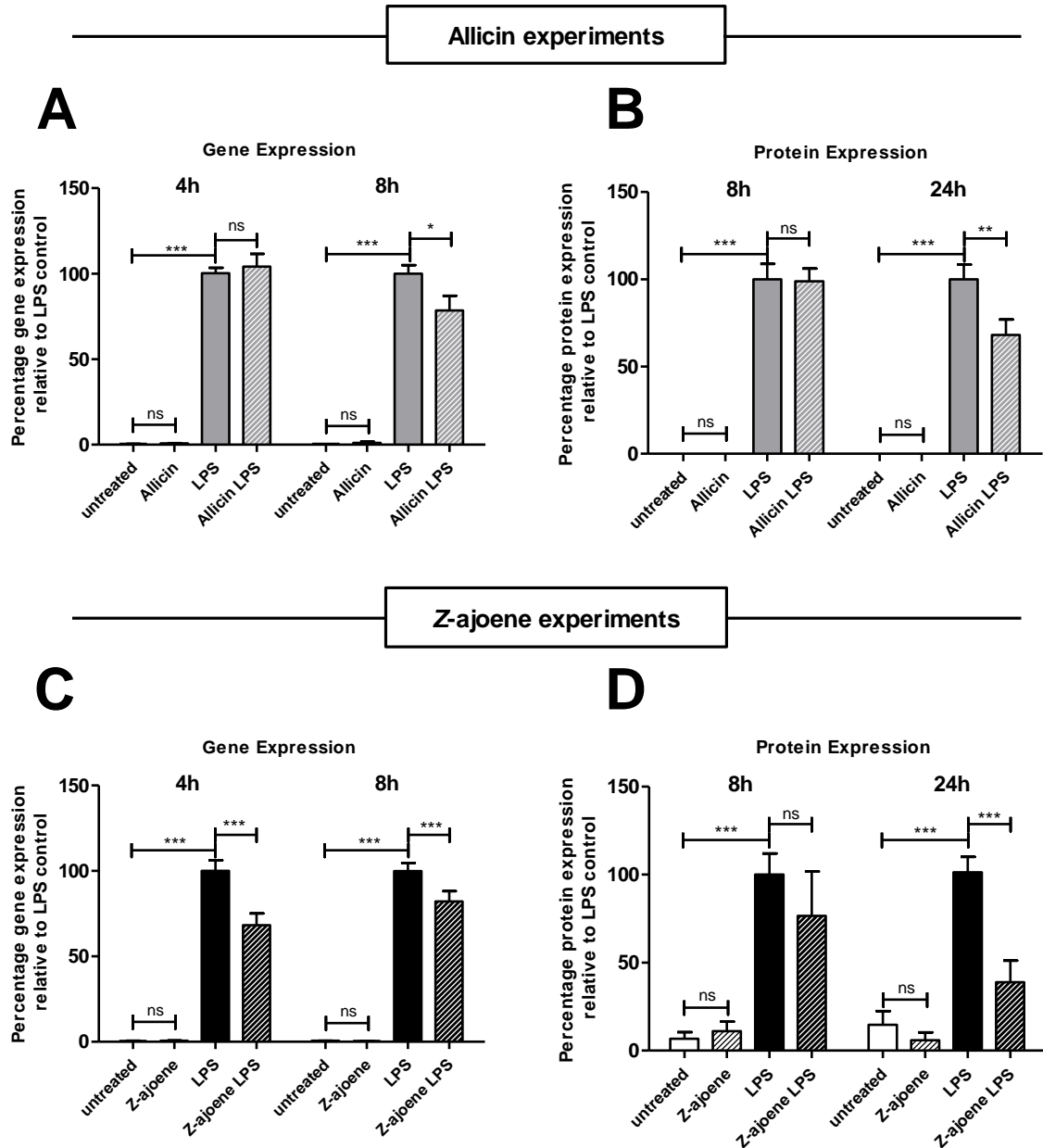
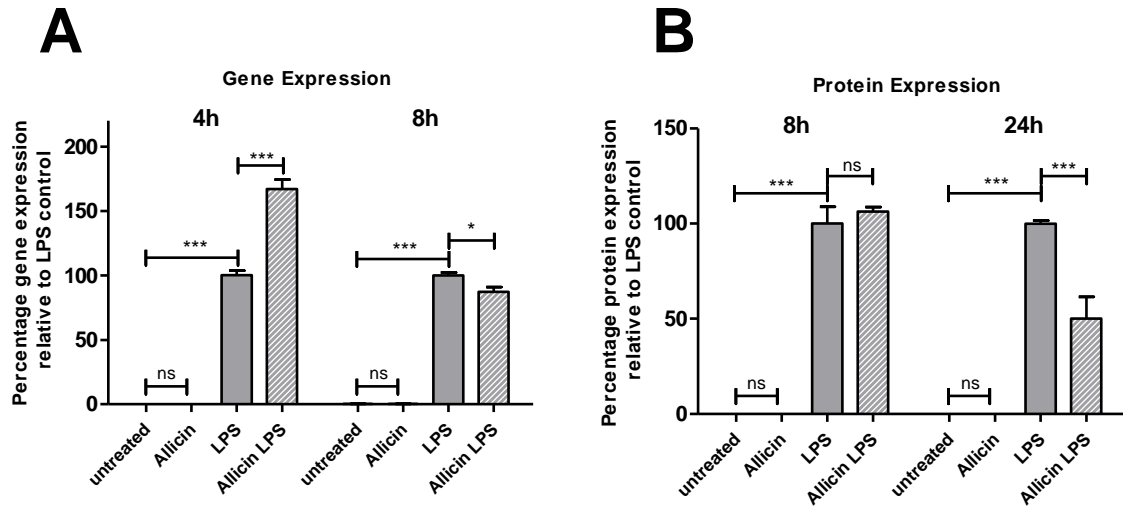


Figure 3.4: The effect of selected garlic OSCs on LPS-induced interleukin-1 β gene and protein expression in murine RAW264.7 macrophages. Cells were pre-treated with $\frac{1}{2}$ IC₅₀ concentrations of allicin or Z-ajoene, followed by a second dose after 24 h in conjunction with 10 ng/ml LPS. Total RNA for qPCR gene expression analysis was extracted 4 h or 8 h after LPS stimulation, while cell culture supernatants for sandwich ELISA protein expression analysis were collected 8 h or 24 h after LPS stimulation. **A, B.** Allicin experiment. **C, D.** Z-ajoene experiment. Percentage mean expression (\pm SEM), determined from three independent experiments, is shown relative to the LPS-control (set to 100% expression). One-way ANOVA significance testing followed by Tukey's HSD test (* $p < 0.05$; ** $p < 0.01$; *** $p < 0.001$; ns, not significant) was performed to assess statistical relevance. Note that the differences in IL1 β protein production in the untreated samples (panel B versus panel D) might be caused by interassay variability due to different batches of the ELISA kit used.

Interleukin-6

Allicin experiments



Z-ajoene experiments

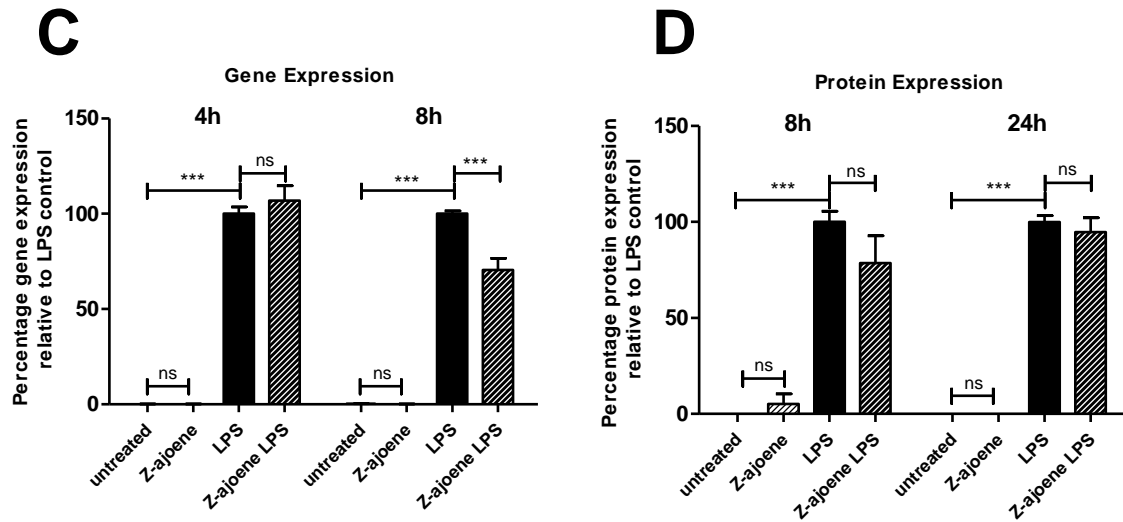


Figure 3.5: The effect of selected garlic OSCs on LPS-induced interleukin-6 gene and protein expression in murine RAW264.7 macrophages. Cells were pre-treated with $\frac{1}{2}$ IC₅₀ concentrations of allicin or Z-ajoene, followed by a second dose after 24 h in conjunction with 10 ng/ml LPS. Total RNA for qPCR gene expression analysis was extracted 4 h or 8 h after LPS stimulation, while cell culture supernatants for sandwich ELISA protein expression analysis were collected 8 h or 24 h after LPS stimulation. **A, B.** Allicin experiment. **C, D.** Z-ajoene experiment. Percentage mean expression (\pm SEM), determined from three independent experiments, is shown relative to the LPS-control (set to 100% expression). One-way ANOVA significance testing followed by Tukey's HSD test (* $p < 0.05$; ** $p < 0.01$; *** $p < 0.001$; ns, not significant) was performed to assess statistical relevance.

Interleukin-12 subunit- β

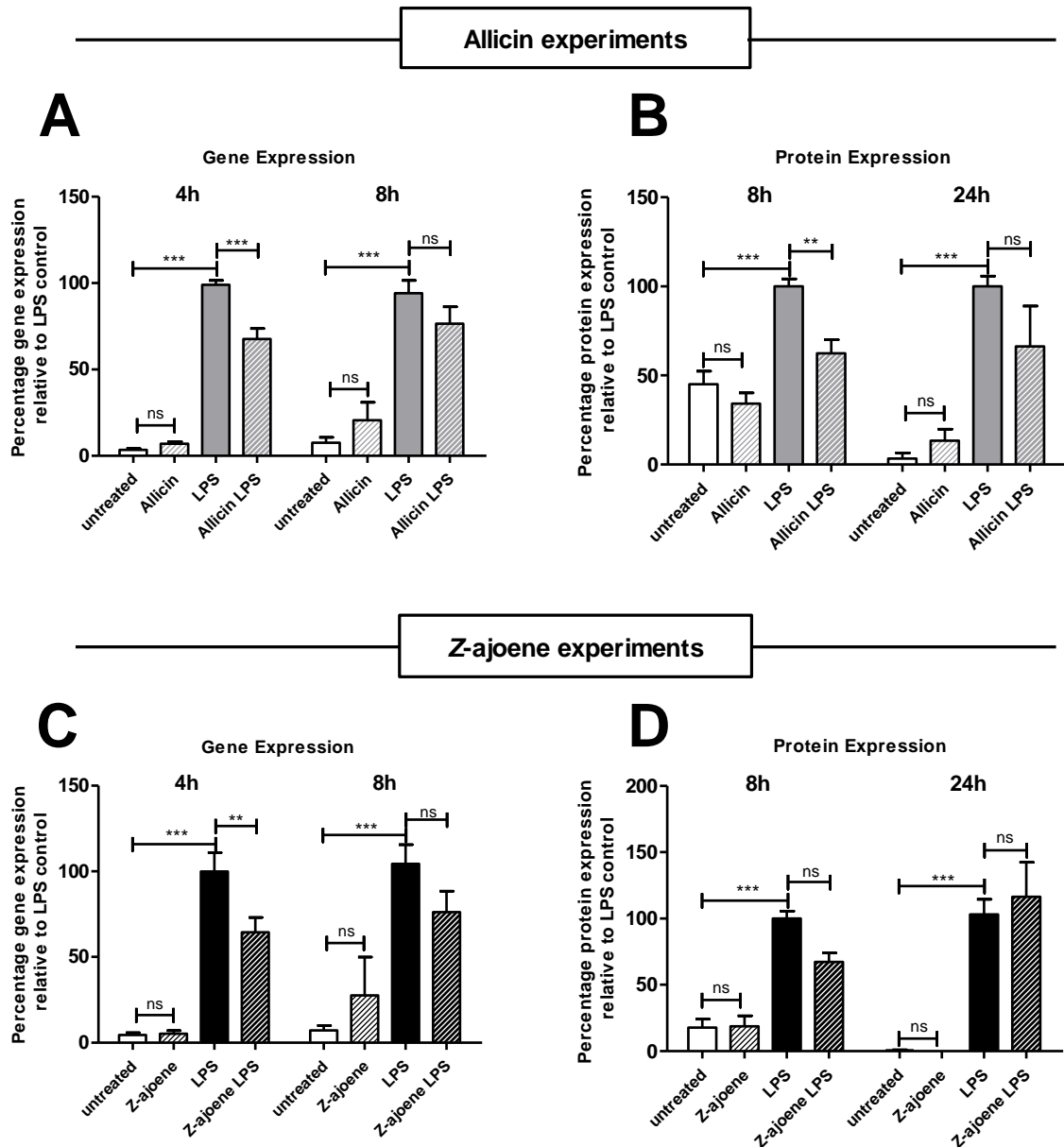
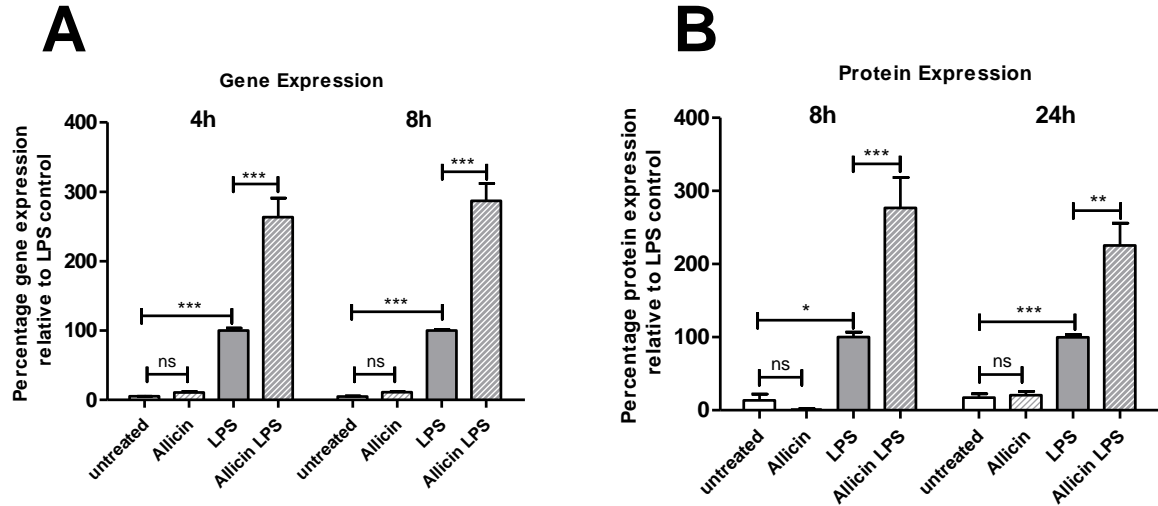


Figure 3.6: The effect of selected garlic OSCs on LPS-induced interleukin-12 subunit- β gene and protein expression in murine RAW264.7 macrophages. Interleukin-12 subunit- β is a subunit of the interleukin-12 and interleukin-23 cytokines. Cells were pre-treated with $\frac{1}{2}$ IC_{50} concentrations of allicin or Z-ajoene, followed by a second dose after 24 h in conjunction with 10 ng/ml LPS. Total RNA for qPCR gene expression analysis was extracted 4 h or 8 h after LPS stimulation, while cell culture supernatants for sandwich ELISA protein expression analysis were collected 8 h or 24 h after LPS stimulation. **A, B.** Allicin experiment. **C, D.** Z-ajoene experiment. Percentage mean expression (\pm SEM), determined from three independent experiments, is shown relative to the LPS-control (set to 100% expression). One-way ANOVA significance testing followed by Tukey's HSD test (* $p < 0.05$; ** $p < 0.01$; *** $p < 0.001$; ns, not significant) was performed to assess statistical relevance.

Interleukin-10

Allicin experiments



Z-ajoene experiments

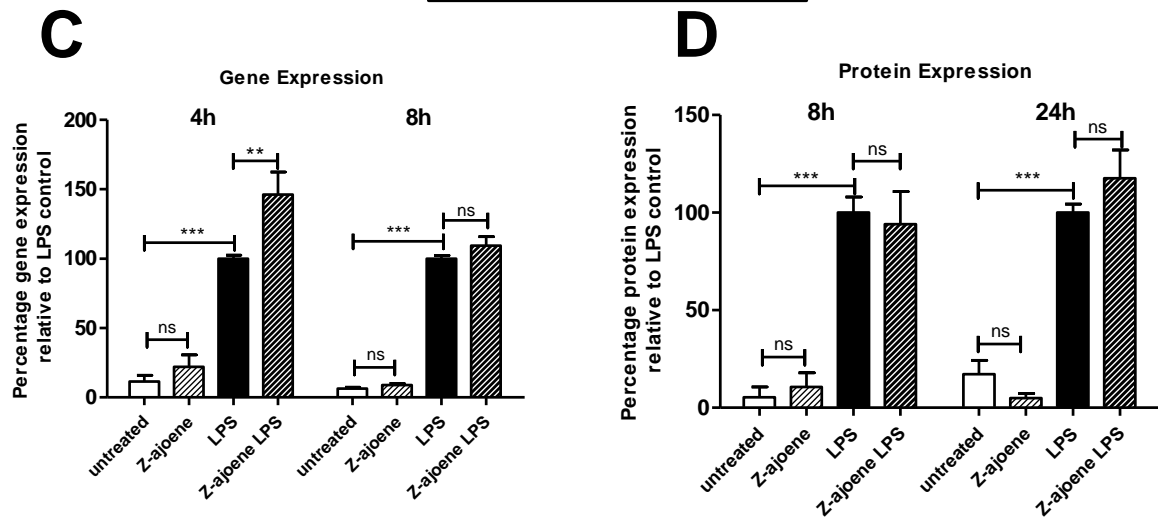


Figure 3.7: The effect of selected garlic OSCs on LPS-induced interleukin-10 gene and protein expression in murine RAW264.7 macrophages. Cells were pre-treated with $\frac{1}{2}$ IC₅₀ concentrations of allicin or Z-ajoene, followed by a second dose after 24 h in conjunction with 10 ng/ml LPS. Total RNA for qPCR gene expression analysis was extracted 4 h or 8 h after LPS stimulation, while cell culture supernatants for sandwich ELISA protein expression analysis were collected 8 h or 24 h after LPS stimulation. **A, B.** Allicin experiment. **C, D.** Z-ajoene experiment. Percentage mean expression (\pm SEM), determined from three independent experiments, is shown relative to the LPS-control (set to 100% expression). One-way ANOVA significance testing followed by Tukey's HSD test (* $p < 0.05$; **, $p < 0.01$; ***, $p < 0.001$; ns, not significant) was performed to assess statistical relevance.

Tumour Necrosis Factor

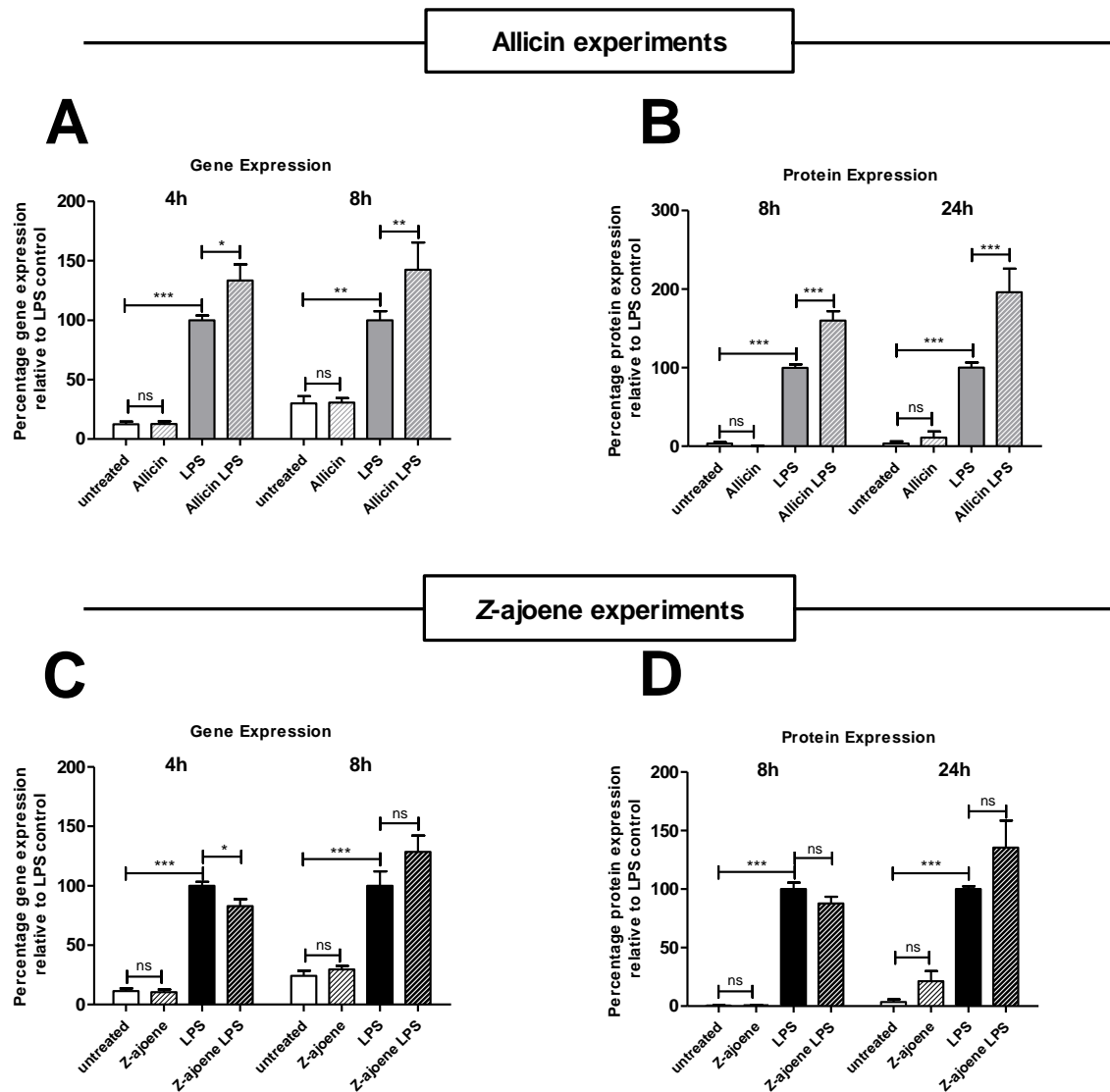


Figure 3.8: The effect of selected garlic OSCs on LPS-induced tumour necrosis factor gene and protein expression in murine RAW264.7 macrophages. Cells were pre-treated with $\frac{1}{2}$ IC₅₀ concentrations of allicin or Z-ajoene, followed by a second dose after 24 h in conjunction with 10 ng/ml LPS. Total RNA for qPCR gene expression analysis was extracted 4 h or 8 h after LPS stimulation, while cell culture supernatants for sandwich ELISA protein expression analysis were collected 8 h or 24 h after LPS stimulation. **A, B.** Allicin experiment. **C, D.** Z-ajoene experiment. Percentage mean expression (\pm SEM), determined from three independent experiments, is shown relative to the LPS-control (set to 100% expression). One-way ANOVA significance testing followed by Tukey's HSD test (* $p < 0.05$; ** $p < 0.01$; *** $p < 0.001$; ns, not significant) was performed to assess statistical relevance.

Cyclooxygenase-2

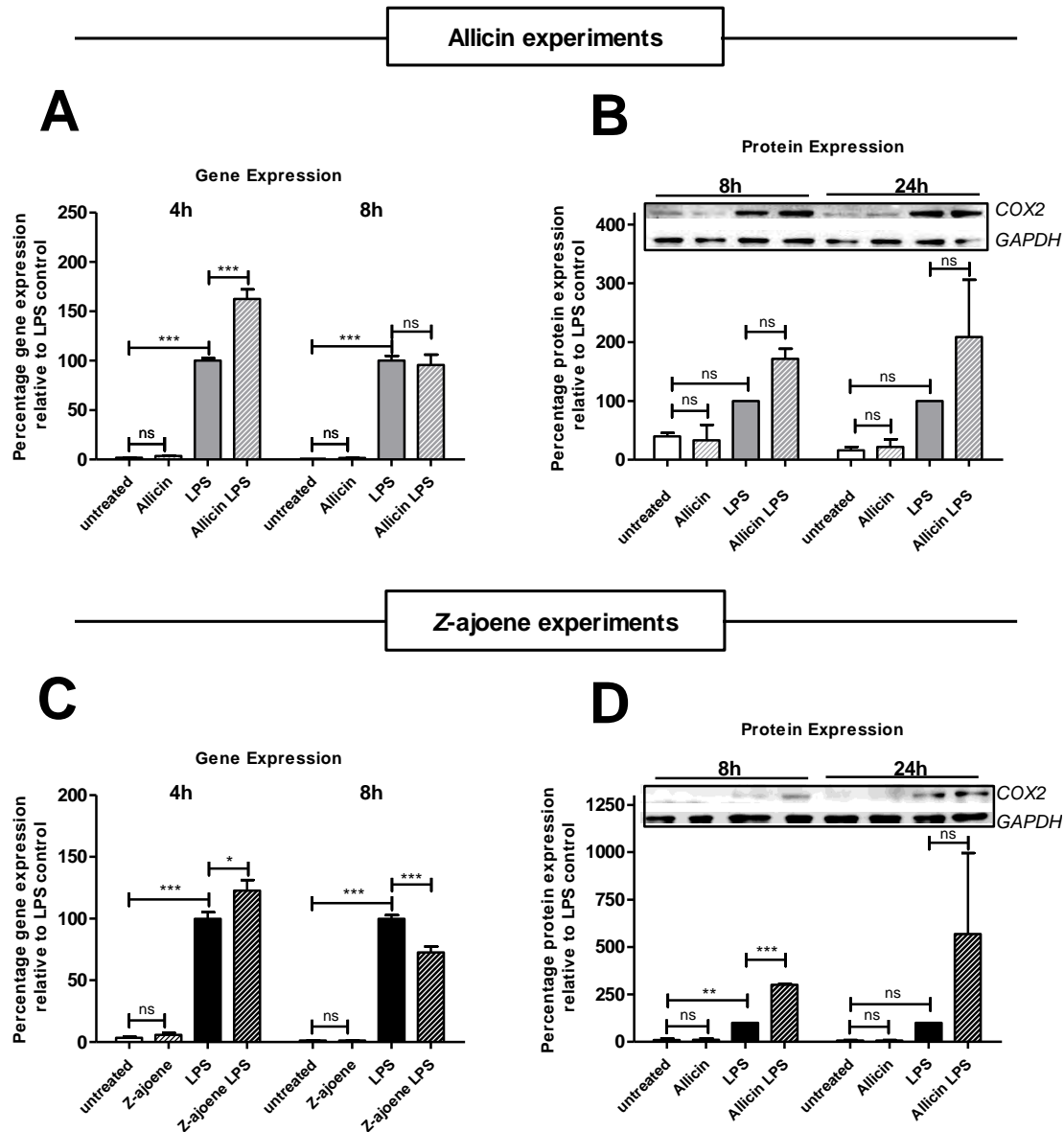


Figure 3.9: The effect of selected garlic OSCs on LPS-induced cyclooxygenase-2 gene and protein expression in murine RAW264.7 macrophages. Cells were pre-treated with $\frac{1}{2}$ IC_{50} concentrations of allicin or Z-ajoene, followed by a second dose after 24 h in conjunction with 10 ng/ml LPS. Total RNA for qPCR gene expression analysis was extracted 4 h or 8 h after LPS stimulation, while whole cell lysates for western blot analysis were collected 8 h or 24 h after LPS stimulation. **A, B.** Allicin experiment. **C, D.** Z-ajoene experiment. Percentage mean gene expression (\pm SEM), determined from three independent gene expression experiments and two independent protein expression experiments, is shown relative to the LPS-control (set to 100% expression). Protein expression was determined by densitometric analysis normalised to *GAPDH* expression. One-way ANOVA significance testing followed by Tukey's HSD test (*, $p < 0.05$; **, $p < 0.01$; ***, $p < 0.001$) was performed to assess statistical relevance.

TNF-Related Apoptosis-Inducing Ligand

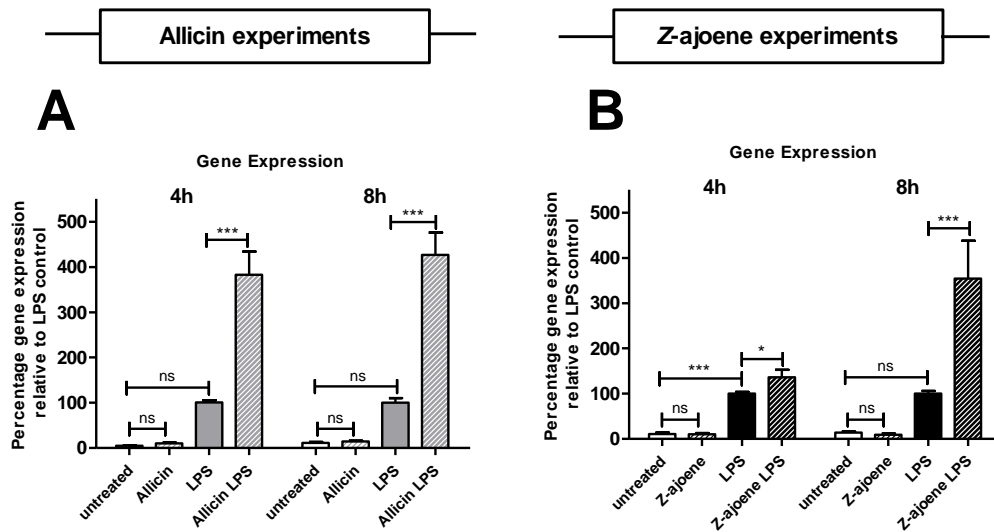


Figure 3.10: The effect of selected garlic OSCs on LPS-induced TNF-related apoptosis-inducing ligand gene expression in murine RAW264.7 macrophages. Cells were pre-treated with $\frac{1}{2}$ IC₅₀ concentrations of allicin or Z-ajoene, followed by a second dose after 24 h in conjunction with 10 ng/ml LPS. Total RNA for qPCR gene expression analysis was extracted 4 h or 8 h after LPS stimulation. **A.** Allicin experiment. **B.** Z-ajoene experiment. Percentage mean expression (\pm SEM), determined from three independent experiments, is shown relative to the LPS-control (set to 100% expression). One-way ANOVA significance testing followed by Tukey's HSD test (* $p < 0.05$; **, $p < 0.01$; ***, $p < 0.001$; ns, not significant) was performed to assess statistical relevance.

Nitric Oxide Synthase-2

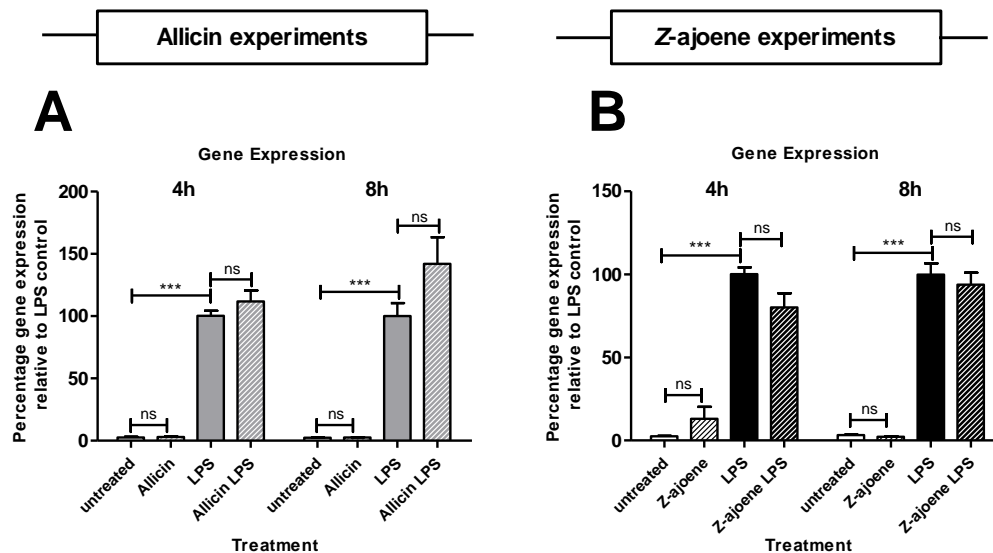


Figure 3.11: The effect of selected garlic OSCs on LPS-induced nitric oxide synthase-2 gene expression in murine RAW264.7 macrophages. Cells were pre-treated with $\frac{1}{2}$ IC₅₀ concentrations of allicin or Z-ajoene, followed by a second dose after 24 h in conjunction with 10 ng/ml LPS. Total RNA for qPCR gene expression analysis was extracted 4 h or 8 h after LPS stimulation. **A.** Allicin experiment. **B.** Z-ajoene experiment. Percentage mean expression (\pm SEM), determined from three independent experiments, is shown relative to the LPS-control (set to 100% expression). One-way ANOVA significance testing followed by Tukey's HSD test (* $p < 0.05$; **, $p < 0.01$; ***, $p < 0.001$; ns, not significant) was performed to assess statistical relevance.

Table 3.2: Summary of the effect of allicin and Z-ajoene treatment on LPS-induced gene and protein expression of selected cytokines and inflammatory mediators. Mean percentage gene or protein expression (\pm SEM) is shown relative to the LPS control. Significant changes in expression are shown in green for downregulation and red for upregulation. Values are reported to one decimal place.

| Cytokine/ Inflammatory mediator | Protein Symbol | Allicin experiments | | | | Z-ajoene experiments | | | |
|--|-------------------|--|---------------------|---|---------------------|--|----------------------|---|----------------------|
| | | Mean % Gene Expression \pm SEM | | Mean % Protein Expression \pm SEM | | Mean % Gene Expression \pm SEM | | Mean % Protein Expression \pm SEM | |
| | | 4 h | 8 h | 8 h | 24 h | 4 h | 8 h | 8 h | 24 h |
| Interleukin-1 β | IL1B | 104.2 \pm 7.4 | 78.6 \pm 8.6 | 98.8 \pm 7.4 | 68.2 \pm 8.8 | 72.2 \pm 6.5 | 77.6 \pm 6 | 76.5 \pm 25.1 | 39.0 \pm 12.1 |
| Interleukin-6 | IL6 | 167.1 \pm 7.3 | 87.3 \pm 7.8 | 106.4 \pm 2.3 | 50.0 \pm 11.5 | 107.0 \pm 7.7 | 70.6 \pm 6.1 | 78.6 \pm 14.9 | 94.7 \pm 7.4 |
| Interleukin-12 subunit β | IL12B | 67.7 \pm 6 | 76.5 \pm 9.7 | 62.5 \pm 7.7 | 66.4 \pm 22.5 | 64.4 \pm 8.7 | 76.2 \pm 12.2 | 67.2 \pm 7.0 | 116.4 \pm 26.0 |
| Interleukin-10 | IL10 | 263.6 \pm 27.1 | 287.3 \pm 24.9 | 276.8 \pm 41.6 | 225.5 \pm 30.3 | 146.3 \pm 16.3 | 109.5 \pm 6.4 | 94.1 \pm 6.7 | 117.5 \pm 14.5 |
| Tumour Necrosis Factor | TNF | 133.6 \pm 13.6 | 142.5 \pm 22.9 | 159.9 \pm 11.9 | 196.0 \pm 29.9 | 83.0 \pm 5.8 | 128.6 \pm 13.58 | 87.8 \pm 5.6 | 135.3 \pm 23.3 |
| Cyclooxygenase-2 | COX2/ PTGS2 | 162.6 \pm 9.6 | 95.8 \pm 10.3 | 171.8 \pm 17.0 | 208.9 \pm 97.2 | 122.7 \pm 8.5 | 72.6 \pm 4.9 | 300.3 \pm 6.3 | 568.5 \pm 427.9 |
| TNF-Related Apoptosis Inducing Ligand | TRAIL/ TNFSF10 | 382.8 \pm 51.4 | 426.9 \pm 49.0 | None detected* | | 136.2 \pm 16.1 | 352.9 \pm 84.0 | None detected* | |
| Nitric Oxide Synthase 2 | NOS2 | 111.9 \pm 8.7 | 142.0 \pm 21.4 | Not analysed** | | 80.0 \pm 8.6 | 93.8 \pm 7.3 | Not analysed** | |

* Cell culture supernatants were analysed for TRAIL/TNFSF10, but no expression was detected. **Protein expression levels of NOS2 were not measured.

3.3.1. Cytokines downregulated by garlic OSC treatment

Interestingly, while allicin generally had a more potent effect on LPS-induced gene regulation (Table 3.2), the effect on *Il1b*/IL1B downregulation was stronger for Z-ajoene treatment. Z-ajoene decreased LPS-induced IL1B protein to 39.0% expression after 24 h as opposed to 68.2% for allicin. This finding is supported by the preliminary gene expression data looking at the effect of garlic OSCs (allicin, DATS, E-ajoene and Z-ajoene) where Z-ajoene was found to have the strongest downregulating effect after 4 h (Figure 3.3A). In contrast, the preliminary gene expression experiment (Figure 3.3A) shows a significant increase in LPS-induced *Il1b* following allicin treatment, while no change in expression was seen in Figure 3.4A. While these data are inconsistent, the gene expression analysis shown in Figure 3.4A is more reliable as it is an average of three independent experiments, while the data from Figure 3.3A is a single preliminary experiment.

Of particular interest is the effect of allicin on *Il6* gene expression. While both garlic OSCs had an overall-downregulating effect on *Il6*/IL6 expression, *Il6* gene expression was shown to be significantly upregulated by allicin treatment to 167.1% after 4 h (Figure 3.5A, Table 3.2., see also Figure 3.3B). At 8 h, however, allicin treatment significantly downregulated *Il6* gene expression to 87.3%. Protein expression data show that after 8 h, allicin treatment results in no significant difference in expression levels of IL6, but after 24 h IL6 expression is halved relative to LPS alone (Table 3.2). Based on the preliminary temporal expression profile (Figure 3.1B), *Il6* gene expression peaks at 8 h, while protein

expression peaks between 12 and 24 h. Allicin treatment, therefore, appears to cause a shift in the temporal LPS-induced *IL6/IL6* expression profile towards earlier peaks in gene and protein expression.

IL12B (MW: 40 kDa) is a subunit of the pro-inflammatory IL12 and IL23 cytokines¹⁸⁶. Allicin and Z-ajoene significantly decreased LPS-induced *IL12b* gene expression to approximately 65% after 4 h (Table 3.2). In addition, allicin treatment resulted in a significant decrease in IL12B protein expression after 8 h. Further *IL12b/IL12B* gene and protein expression at other timepoints, while not statistically significant, showed a decreasing trend in expression following garlic OSC treatment.

3.3.2. Cytokines and inflammatory mediators upregulated by garlic OSC treatment

LPS-induced *IL10/IL10* gene and protein expression is greatly upregulated (>225.5% in expression compared to LPS treated cells) by allicin treatment at all timepoints (Figure 3.5A & B & Table 3.2). Z-ajoene while significantly upregulating *IL10* gene expression after 4 h (146.3%) only shows a weak-increasing trend in protein expression after 24 h (Figure 3.5C & D & Table 3.2). It should be noted, however, that this significant increase in gene expression of *IL10* seen for Z-ajoene treatment after 4 h (Figure 3.5C) is not consistent with Figure 3.3C which shows no change in expression. Figure 3.3C, however, shows the results from a single experiment, whereas Figure 3.5C is an average of three independent experiments, and is thus more reliable.

LPS-induced expression of the *Cox2/COX2* enzyme was generally upregulated by garlic OSC treatment (Figure 3.9 & Table 3.2). Both allicin and Z-ajoene significantly upregulated LPS-induced *Cox2* expression after 4 h, but allicin had no effect and Z-ajoene significantly decreased *Cox2* gene expression after 8 h. Western blot densitometry data showed an increasing trend in COX2 protein expression for both allicin and Z-ajoene treatment. While two independent experiments showed increases in LPS-induced COX2 protein expression when treated with allicin or Z-ajoene, when percentage expression values from these experiments were averaged, inter-experimental variability resulted in large SEM values. Statistically significant differences in COX2 protein expression could not be reached due to this inter-experiment variability, however, it does appear that both allicin and Z-ajoene induce increased COX2 protein expression in LPS-treated macrophages.

Both allicin and Z-ajoene treatment greatly increased (generally more than 300% expression) the LPS-induced gene expression of *Trail/Tnfsf10* (Figure 3.10 & Table 3.2). Cell culture supernatants were tested by sandwich ELISA for TRAIL/TNFSF10 protein expression, but as no protein was detected in any of these samples, no protein expression data is shown for TRAIL (TNFSF10).

3.3.3. Cytokines and inflammatory mediators affected differently by garlic

OSCs

Tnf/TNF gene and protein expression was significantly upregulated by allicin treatment for all timepoints measured (Figure 3.8A & B & Table 3.2., see also Figure 3.3D). Z-ajoene, on the other hand, downregulated LPS-induced TNF expression after 4 h for gene expression, but this was not seen after 8 h or at the protein level after 8 h and 24 h (Figure 3.8C & D & Table 3.2). Further, Z-ajoene mediated downregulation of LPS-induced *Tnf* gene expression after 4 h of treatment was not seen in Figure 3.3D, which showed no change in expression. Z-ajoene treatment, however, showed upregulating trends on LPS-induced TNF gene- and protein expression after 8 h and 24 h respectively. Due to large SEM values (Table 3.2), however, it is likely that Z-ajoene has no effect on TNF expression at these timepoints.

While allicin treatment slightly increased LPS-induced *Nos2* gene expression, Z-ajoene showed a modest downregulation of LPS-induced *Nos2* expression. These trends, however, were not statistically significant. Due to time constraints, NOS2 protein expression was not investigated.

3.3.4. Selecting optimal timepoints for gene and protein array experiments

As suggested by the preliminary experiments shown in Figure 3.1B, it is important to consider that cytokines and inflammatory mediators have different temporal expression profiles. The findings presented in Figures 3.4-3.11 show that allicin and Z-ajoene clearly modulate the expression of the selected cytokines and inflammatory mediators. We therefore decided to conduct gene and protein expression arrays which will provide a broader indication of the effects of allicin and Z-ajoene on LPS-induced gene and protein expression. These arrays are, however, limited in that only a few samples can be analysed. We therefore had to choose the most appropriate timepoints at which to measure gene- and protein expression. In Table 3.2 it is apparent that both allicin and Z-ajoene generally elicited stronger effects on LPS-induced gene expression of the selected cytokines and inflammatory mediators after a 4 h treatment period as compared to 8 h. We therefore chose the 4 h timepoint for gene expression arrays.

Similarly, the 24 h treatment period resulted in a greater number of significant differences in LPS-induced protein expression for allicin-treated cells (Table 3.2). In contrast, Z-ajoene treatment only resulted in the significant increase of LPS-induced COX2 protein levels after 8 h and a significant decrease in LPS-induced IL1B protein levels after 24 h of treatment. As allicin treatment showed the strongest effect on LPS-induced expression of the selected cytokines and inflammatory mediators after 24 h of treatment, along with the fact that Z-ajoene treatment shows a similar upregulating trend

on LPS-induced COX2 protein expression after 24 h, the 24 h timepoint was chosen for subsequent protein array analyses.

3.4. RT² Profiler PCR Array for Inflammatory Response and Autoimmunity

Once the conditions, as described in Figure 3.2, and the optimal treatment timepoint (4 h for the gene expression analysis experiments) were established (Section 3.3.4), the effect of allicin and Z-ajoene-treatment on LPS-induced inflammatory gene expression using RNA samples isolated 4 h after stimulation with 10 ng/ml LPS was analysed on the commercially available RT² Profiler™ PCR Array (Qiagen®). This array analyzed the expression of 84 genes known to be involved in the inflammatory response and autoimmune pathways.

While this array provides a broad indication of the effects of the selected garlic OSCs on LPS-induced inflammatory gene expression, it is important to note that the array does not allow for technical repeats. Therefore, a single sample, pooled from 3 biological samples, was used per treatment condition.

Results of allicin and Z-ajoene treatment on the expression of 84 genes with and without LPS-stimulation are summarised in Figure 3.12 and Figure 3.14, respectively. The selection criterion for gene-responsiveness to a given treatment was a fold change ≥ 2 upon treatment with LPS and/or garlic OSCs. LPS-treated cells, garlic OSC-treated cells and garlic OSC- and LPS-treated cells were compared to untreated cells, while garlic OSC-LPS-treated cells were also compared to LPS treatment alone. Genes were excluded from the analysis if the average quantification cycle (Cq) was above the defined Cq cut-off of 35, which indicates that gene expression was very low and therefore unreliable.

Changes in gene expression in Table 3.3 and Table 3.4 are displayed as fold up- or downregulation compared to untreated cells or LPS-treated cells. We chose to show fold regulation as opposed to fold change as the latter method can result in data which is skewed in favour of upregulation in expression. This is because a decrease in expression is represented by a number between 0 and 1, while an increase in expression is represented as a value greater than 1. Fold up or downregulation uses the reciprocal of the fold change values showing downregulation (i.e. between 0 and 1) in order to apply equal weight to increases and decreases in expression. A fold change of 0.75, for example, can be converted to fold down-regulation by taking the reciprocal of the fold change: $\frac{1}{0.75}$ equals a fold down-regulation of 1.33 (shown as -1.33). One drawback, however, is that large fold down-regulation values are seen when the gene expression is zero or very close to zero expression (Table 3.3 and Table 3.4). Similarly very large fold upregulation values can indicate that the reference sample had little or no

expression of the gene of interest. Those data must be treated with caution as the fold up- or downregulation values, while indicating that there is a large difference in expression between the sample of interest and the reference sample, may not be biologically relevant.

3.4.1. Allicin treatment

Of the 84 genes analysed, ten were excluded for technical reasons, and 16 did not respond to any of the treatment conditions (Figure 3.12). As this thesis focuses on the immunomodulatory effects of garlic OSCs, the 20 genes responsive to both LPS treatment and allicin-LPS treatment (numbers shown in red, Figure 3.12) were selected for further analysis. Responsive genes were those that had a positive or negative fold change ≥ 2 compared to untreated cells for allicin-responsive and LPS-responsive genes, and LPS-treated cells for allicin-LPS-responsive genes.

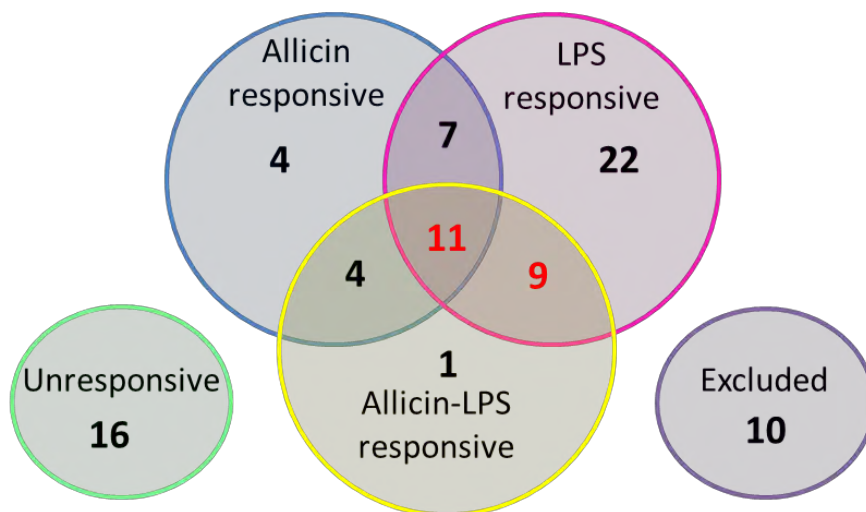


Figure 3.12: A Venn diagram summarising the results of the Inflammatory Response and Autoimmunity RT² Profiler PCR Array (Qiagen®) following treatment with LPS and/or allicin treatment of murine RAW264.7 macrophages. The number of genes responsive to allicin treatment, LPS treatment and allicin-LPS treatment is shown. Responsive genes were those that had a positive or negative fold change ≥ 2 compared to untreated cells for allicin-responsive and LPS-responsive genes, and LPS-treated cells for allicin-LPS-responsive genes. Genes with an average quantification cycle (Cq) of ≥ 35 were excluded. Genes responsive to both LPS and allicin-LPS treatment (red numbers) were chosen for further analysis.

These genes were divided into 5 functional categories, namely chemokines, interleukins, receptors, TNF Ligand Superfamily and other genes (Figure 3.13) and are listed in detail in Table 3.3.

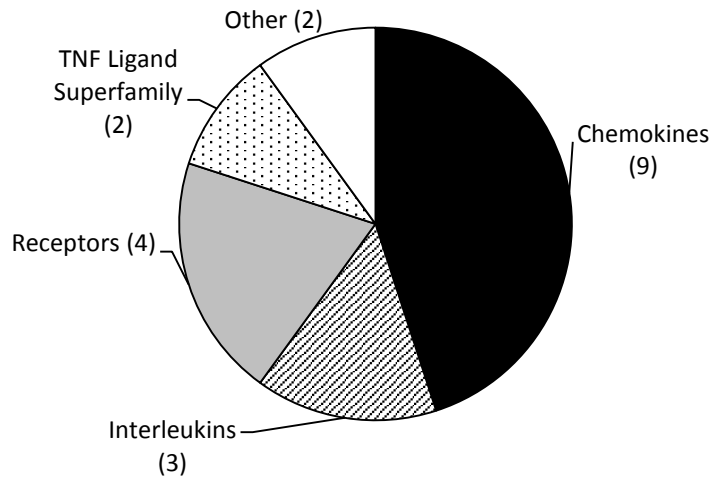


Figure 3.13: Gene groupings of the inflammatory genes responsive to both LPS treatment and allicin-LPS treatment in murine RAW264.7 macrophages. Genes identified from the RT² Profiler PCR Array to have a ≥ 2 fold up- or downregulation in expression for both LPS-treated cells and allicin-LPS-treated cells were selected for further analysis and categorised as either chemokines, interleukins, receptors, TNF ligand superfamily or other.

3.4.1.1. Chemokines

In Figure 3.13 and Table 3.3, the largest group of genes is the chemokines consisting of 4 C-C motif- and 5 C-X-C motif ligand chemokines. Interestingly, all C-X-C motif ligand family chemokines analysed in this array were affected by both LPS treatment as well as allicin-LPS treatment, with the exception of *Cxcl1* and *Cxcl5* which were excluded. Of the nine chemokines analyzed, LPS-induced *Ccl8* and *Ccl20* gene expression was downregulated by allicin treatment, while LPS-induced *Ccl5* (also known as regulated on activation, normal T cell expressed and secreted (*Rantes*)), *Ccl11*, *Cxcl2*, *Cxcl3*, *Cxcl9*, *Cxcl10* and *Cxcl11* expression was upregulated by allicin treatment (Table 3.3). In general it appears that allicin treatment enhances LPS-induced gene expression of chemokines after 4 h.

3.4.1.2. Interleukins

Of the interleukins, LPS-induced *Il6* and *Il10* gene expression was upregulated by allicin treatment, consistent with the 4 h treatment qPCR gene expression data from Figure 3.5A and Figure 3.7A, respectively. The expression of *Il22*, a member of the IL10 superfamily of interleukin cytokines, was downregulated by all treatment conditions (Table 3.3). LPS treatment resulted in a 2.8-fold decrease in *Il22* expression, which was further decreased upon allicin treatment trending towards zero expression compared to untreated cells.

Table 3.3: Fold regulation of selected inflammatory genes responsive to both LPS treatment and allicin-LPS treatment. Fold up- (red) or downregulation (green) is shown relative to untreated cells. Fold-up or downregulation is also shown for allicin-LPS-treated cells compared to LPS-only treated cells (numbers in bold). Genes are grouped according to functional family as chemokines, interleukins, receptors, TNF ligand superfamily members and other.

| Gene name | Gene Symbol | Fold Up- or Downregulation | | | |
|---------------------------------------|-----------------------------------|----------------------------|-------------------|---------------------------|---------------------|
| | | Allicin vs. untreated | LPS vs. untreated | Allicin-LPS vs. untreated | Allicin-LPS vs. LPS |
| Chemokines | | | | | |
| Chemokine C-C motif Ligand 5 | <i>Ccl5</i> (also <i>Rantes</i>) | 3.7 | 802.6 | 1685.4 | 2.1 |
| Chemokine C-C motif Ligand 8 | <i>Ccl8</i> | -115.1 | 2.6 | -141.5 | -370.6 |
| Chemokine C-C motif Ligand 11 | <i>Ccl11</i> | 2.7 | -7.1 | 1.8 | 12.6 |
| Chemokine C-C motif Ligand 20 | <i>Ccl20</i> | 25.7 | 457.8 | 184.2 | -2.5 |
| Chemokine C-X-C motif Ligand 2 | <i>Cxcl2</i> | 1.4 | 356.7 | 713.4 | 2.0 |
| Chemokine C-X-C motif Ligand 3 | <i>Cxcl3</i> | -1.1 | 139.0 | 275.4 | 2.0 |
| Chemokine C-X-C motif Ligand 9 | <i>Cxcl9</i> | -29.8 | -8.3 | 24075.6 | 199602.1 |
| Chemokine C-X-C motif Ligand 10 | <i>Cxcl10</i> | -1.1 | 203.4 | 426.2 | 2.1 |
| Chemokine C-X-C motif Ligand 11 | <i>Cxcl11</i> | -1.1 | 830.9 | 2988.9 | 3.6 |
| Interleukins | | | | | |
| Interleukin-6 | <i>Il6</i> | 17.1 | 68728.2 | 158639.1 | 2.3 |
| Interleukin-10 | <i>Il10</i> | -1.8 | 10.1 | 25.6 | 2.5 |
| Interleukin-22 | <i>Il22</i> | -11639.6 | -2.8 | -14313.0 | -5090.3 |
| Receptors | | | | | |
| Chemokine C-X-C motif receptor type 4 | <i>Cxcr4</i> | 1.8 | -16.5 | -3.8 | 4.3 |
| Interleukin 10 receptor, subunit-β | <i>Il10rb</i> | 1.2 | -2.0 | 1.0 | 2.0 |
| Interleukin-23 receptor | <i>Il23r</i> | -9132.3 | -172.6 | 29.1 | 5031.5 |
| Toll-like receptor 3 | <i>Tlr3</i> | 2.5 | 2.7 | 6.3 | 2.3 |
| TNF Ligand Superfamily | | | | | |
| Fas Ligand | <i>Fasl</i> (also <i>Tnfsf6</i>) | -4115.9 | -6086.9 | -2426.6 | 2.5 |
| TNF ligand superfamily member 14 | <i>Tnfsf14</i> | 3.7 | -4.4 | -1.7 | 2.6 |
| Other | | | | | |
| Cyclooxygenase-2 | <i>Cox2</i> (also <i>Ptgs2</i>) | 1.8 | 45.8 | 92.1 | 2.0 |
| E-selectin | <i>Sele</i> | 22.8 | 28.6 | 110.3 | 3.9 |

3.4.1.3. Receptors

Table 3.3 shows that LPS treatment and allicin-LPS treatment affected the expression of four receptors including chemokine C-X-C motif receptor-4 (*Cxcr4*), IL10 receptor subunit- β (*Il10rb*), IL23 receptor (*Il23r*) and Toll-like receptor 3 (*Tlr3*) (Table 3.3). LPS treatment caused the downregulation of *Cxcr4*, *Il10rb* and *Il23r* expression while increasing *Tlr3* expression (Table 3.3). LPS treatment resulted in a 16.5-fold decrease in *Cxcr4* expression compared to untreated cells. Allicin treatment was able to buffer the LPS-induced downregulation of *Cxcr4* to only a 3.8-fold decrease compared to untreated cells. *Il10rb* expression was downregulated 2-fold by LPS treatment, and allicin treatment was able to

completely abrogate this downregulation. *Il23r* was downregulated by both LPS-only treatment and allicin-only treatment, but LPS-induced downregulation was reversed by allicin-treatment in conjunction with LPS-treatment, resulting in a 29.1-fold increase in expression compared to untreated cells (a 5031.5-fold increase compared to LPS-treated cells). LPS and allicin treatment on their own therefore downregulated the expression of the *Il23r*, but the synergistic effect of both treatments resulted in a sizeable upregulation of expression. *Tlr3* gene expression was increased in response to allicin treatment (2.5-fold) and LPS treatment (2.7-fold). Allicin treatment further increased the LPS-induced upregulation of *Tlr3*, 2.3-fold compared to LPS-treated cells.

3.4.1.4. TNF ligand superfamily

LPS treatment reduced the expression of TNF ligand superfamily member 14 (*Tnfsf14*) and Fas ligand (*Fasl/Tnfsf6*), both members of the TNF ligand superfamily (Table 3.3). The downregulating effect of LPS on the expression of these pro-apoptotic ligands was lessened when cells were treated with allicin. Allicin-LPS treatment resulted in an approximately 2.5-fold increase in expression of both pro-apoptotic ligands when compared to LPS-treated cells but did not reach the expression level of the untreated cells. Further, while allicin treatment alone greatly reduced *Fasl/Tnfsf6* expression (tending towards zero expression), it resulted in a 3.7-fold increase in expression of *Tnfsf14* as compared to untreated cells.

3.4.1.5. Other

Cyclooxygenase-2 (COX2), also known as prostaglandin-endoperoxide synthase 2 (PTGS2), is an enzyme involved in the production of prostaglandins. LPS-treatment resulted in a 46-fold increase in *Cox2* expression and allicin treatment doubled this LPS-induced *Cox2* expression (Table 3.3). These data are consistent with Figure 3.9A which shows that allicin treatment significantly increases the gene expression of LPS-induced *Cox2* ($p < 0.001$) after 4 h.

The expression of E-selectin (*Sele*), an adhesion molecule involved in immune cell recruitment, was increased 22.8-fold by allicin treatment alone and 28.6-fold by LPS treatment as compared to untreated cells. Allicin treatment further increased the LPS-induced expression of *Sele* 3.9-fold.

3.4.2. Z-ajoene treatment

Of the 84 genes analysed, 18 were excluded and 22 did not respond to any of the treatment conditions (Figure 3.14). In general, Z-ajoene had a less pronounced effect on LPS-induced expression of the genes analysed, compared to allicin treatment (Figure 3.12). This is in agreement with the qPCR and ELISA data from Section 3.3, which also showed that allicin treatment had a more pronounced immunomodulatory effect than Z-ajoene.

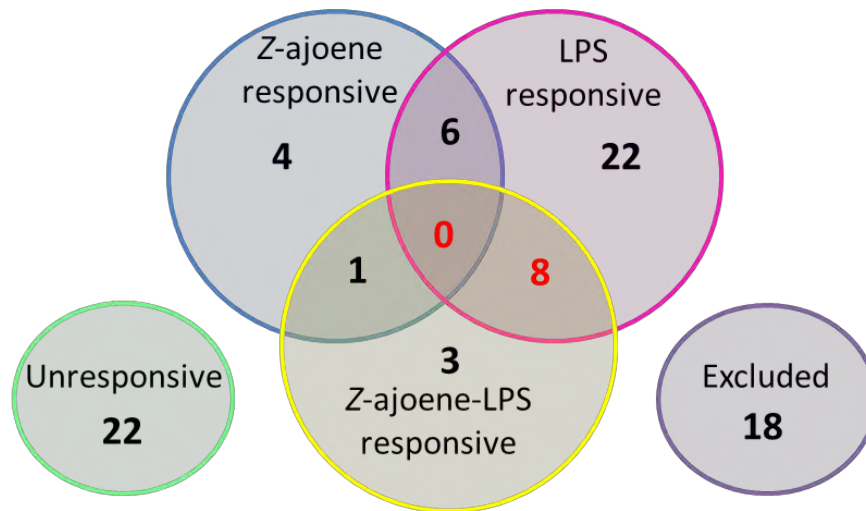


Figure 3.14: A Venn diagram summarising the results of the Inflammatory Response and Autoimmunity RT² Profiler PCR Array following treatment with LPS and/or Z-ajoene treatment of murine RAW264.7 macrophages. The number of genes responsive to Z-ajoene treatment, LPS treatment and Z-ajoene-LPS treatment is shown. Responsive genes were those that had a positive or negative fold change ≥ 2 compared to untreated cells for Z-ajoene-responsive and LPS-responsive genes, and LPS-treated cells for Z-ajoene-LPS-responsive genes. Genes with an average quantification cycle (Cq) of ≥ 35 were excluded. -Genes responsive to both LPS and Z-ajoene-LPS treatment (red numbers) were chosen for further analysis.

Further, no genes were found to be responsive to all three treatments according to the 2-fold up- or downregulation cut-off (Figure 3.14). Of the eight genes regulated by both LPS treatment and Z-ajoene-LPS treatment (red numbers in Figure 3.14), four chemokines, two receptors and two members of the TNF ligand superfamily were identified (summarised in Figure 3.15).

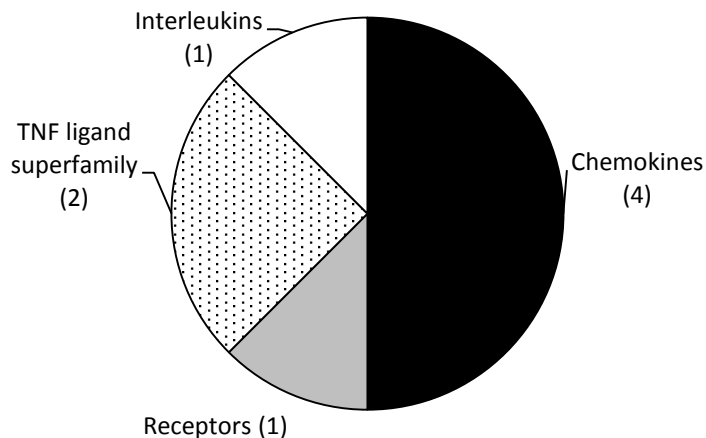


Figure 3.15 Gene groupings of the inflammatory genes responsive to both LPS treatment and Z-ajoene-LPS treatment in murine RAW264.7 macrophages. Genes identified from the RT² Profiler PCR Array to have a ≥ 2 fold up- or downregulation in expression for both LPS-treated cells and Z-ajoene-LPS-treated cells were selected for further analysis and categorised as either chemokines, interleukins, receptors or TNF ligand superfamily members.

3.4.2.1. Chemokines

LPS treatment upregulated all chemokines that met the inclusion criterion (Table 3.4). Z-ajoene treatment resulted in a 2.1-fold reduction of LPS-induced expression of *Ccl7* and *Ccl20* and a 3.1-fold reduction in *Cxcl3* expression. LPS-induced *Cxcl11* expression, however, was upregulated 2.7-fold by Z-ajoene treatment. In general, Z-ajoene appears to downregulate the gene expression of chemokines (Table 3.3), in contrast to allicin treatment where greater upregulation of inflammatory mediators was observed (Table 3.4).

3.4.2.2. Interleukins

LPS-induced a 15.8-fold increase in interleukin-1 receptor antagonist (*Il1rn*) expression, while Z-ajoene downregulated its LPS-induced expression 4.4-fold (Table 3.3). While *Il1b* expression was not affected by Z-ajoene-LPS treatment (determined by the cut off of a 2-fold change in expression compared to LPS treated cells), we looked at *Il1b* expression as qPCR and ELISA experiments showed significant downregulation of LPS-induced expression by Z-ajoene treatment (Figure 3.4C and D). Consistent with this data, Z-ajoene treatment reduced LPS-induced expression of *Il1b* 1.5-fold in the RT² Profiler PCR array experiment (data not shown).

Table 3.4: Fold regulation of selected inflammatory genes responsive to both LPS treatment and Z-ajoene-LPS treatment. Fold up- (red) or downregulation (green) is shown relative to untreated cells. Fold-up or downregulation is also shown for Z-ajoene-LPS-treated cells compared to LPS-treated cells (numbers in bold). Genes are grouped according to functional family as chemokines, interleukins, receptors and TNF ligand superfamily members.

| Gene name | Gene Symbol | Fold Up Or Downregulation | | | |
|---------------------------------------|---------------------|---------------------------|-------------------|----------------------------|----------------------|
| | | Z-ajoene vs. untreated | LPS vs. untreated | Z-ajoene-LPS vs. untreated | Z-ajoene-LPS vs. LPS |
| Chemokines | | | | | |
| Chemokine C-C motif ligand 7 | Ccl7 | 1.0 | 6.6 | 3.1 | -2.1 |
| Chemokine C-C motif ligand 20 | Ccl20 | 1.0 | 64.0 | 31.1 | -2.1 |
| Chemokine C-X-C motif ligand 3 | Cxcl3 | 1.0 | 4.1 | 1.3 | -3.1 |
| Chemokine C-X-C motif ligand 11 | Cxcl11 | 1.0 | 2.0 | 5.3 | 2.7 |
| Interleukins | | | | | |
| Interleukin receptor antagonist | Ilrn | 1.0 | 15.8 | 3.6 | -4.4 |
| Receptors | | | | | |
| Chemokine C-X-C motif receptor type 4 | Cxcr4 | 1.2 | -8.2 | -22.9 | -2.8 |
| TNF Ligand Superfamily | | | | | |
| Lymphotoxin-β | Ltb (also Tnfsf3) | 1.0 | 3.1 | 1.2 | -2.6 |
| CD40 ligand | Cd40l (also Tnfsf5) | 1.0 | 2.4 | -1.1 | -2.5 |

3.4.2.3. Receptors

Cxcr4 was the only receptor whose gene expression was affected by both LPS and Z-ajoene-LPS treatment. Interestingly, this receptor was also affected by allicin-LPS treatment (Table 3.3). LPS treatment resulted in an 8.2-fold downregulation of *Cxcr4*, and this downregulation was further decreased by Z-ajoene-LPS (Table 3.4).

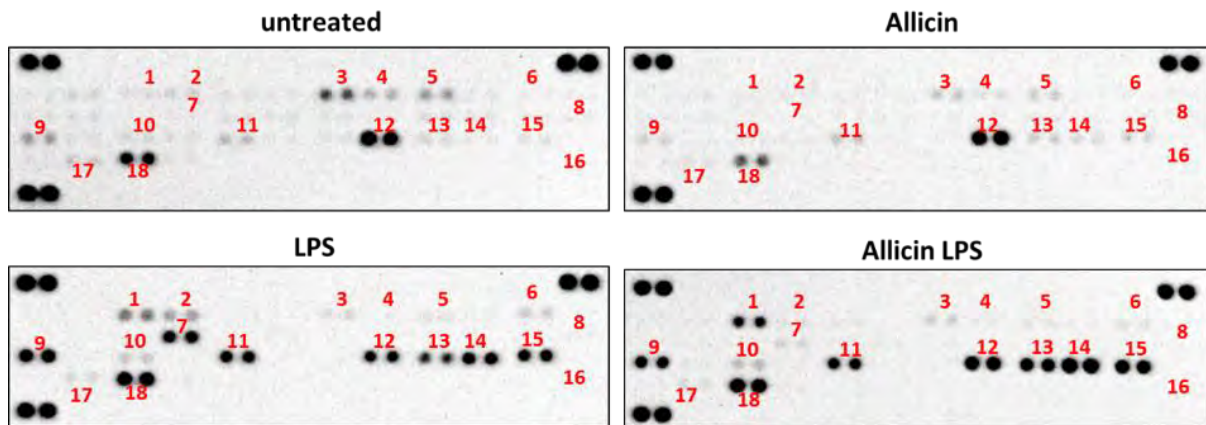
3.4.2.4. TNF ligand superfamily

Lymphotoxin- β (LTB/TNFSF3) and the Cd40 ligand (CD40L/TNFSF5) are members of the TNF ligand superfamily. LPS treatment induced a 3.1-fold and 2.4-fold increase in *Ltb/Tnfsf3* and *Cd40l* gene expression, respectively. Z-ajoene treatment, however, resulted in an approximately 2.5-fold downregulation of the LPS-induced expression of both ligands. Z-ajoene treatment therefore essentially negates LPS-induced upregulation of *Ltb/Tnfsf3* and *Cd40l/Tnfsf5*.

3.5. Proteome Profiler Mouse Cytokine Array

While studying mRNA expression is a useful way to detect rapid changes in gene expression, investigating protein expression provides a clearer and more detailed view of cellular activity in response to a stimulus¹⁸⁷. We therefore performed a Proteome Profiler™ Mouse Cytokine Array (Cat. No. ARY006, R&D Systems) to obtain a more comprehensive indication of the effects of selected garlic OSCs on LPS-induced cytokine and chemokine expression. Murine RAW264.7 macrophages were pre-treated with $\frac{1}{2}$ IC₅₀ concentrations of either allicin or Z-ajoene, followed by a second dose of the garlic OSC 24 h later plus 10 ng/ml LPS (Figure 3.2). Cell culture supernatants were then harvested 24 h after addition of the LPS and the garlic OSC. Cell culture supernatants for each treatment condition were incubated with nitrocellulose membranes pre-spotted with antibodies for 40 mouse cytokines and chemokines. Experiments were performed in duplicate. Detection of the cytokines and chemokines was determined using secondary antibodies conjugated to streptavidin-HRP and developed using a chemiluminescent substrate. Proteins were selected for further analysis if there was a strong antibody signal in one or more of the treatment conditions. Densitometric analysis was performed and the mean density (\pm SEM) of duplicate spots from two independent experiments (\pm SEM) was plotted (Figure 3.17). Representative allicin and Z-ajoene experiments are displayed in Figure 3.16.

A



B

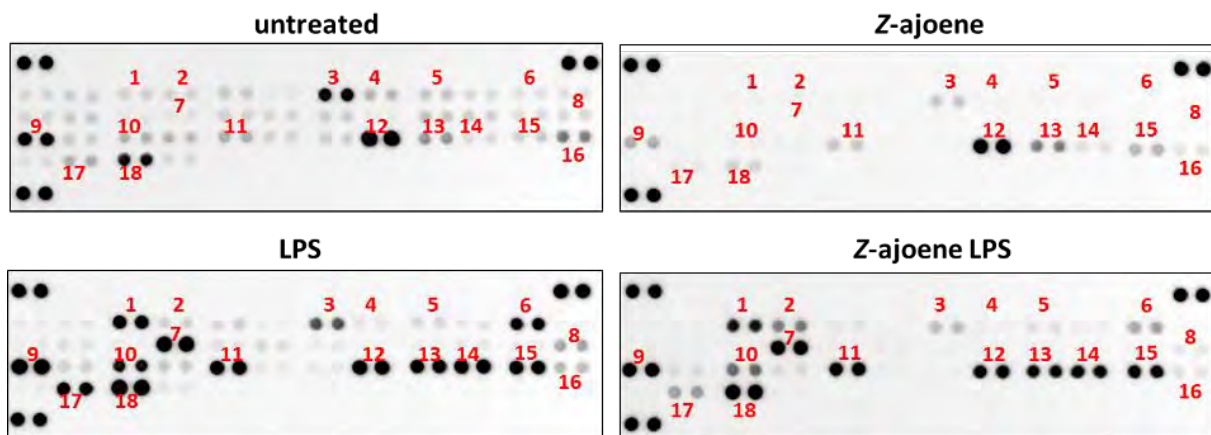
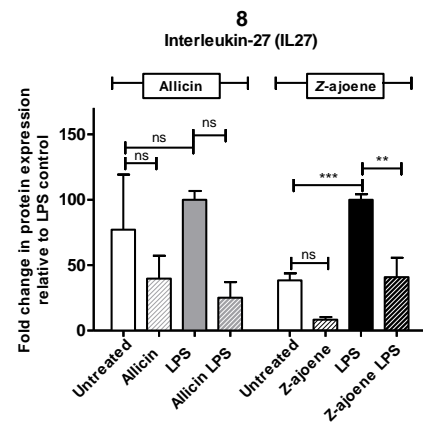
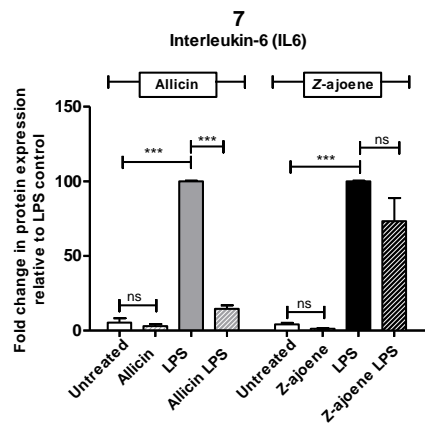
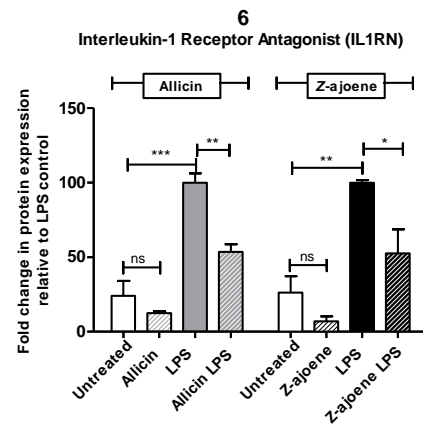
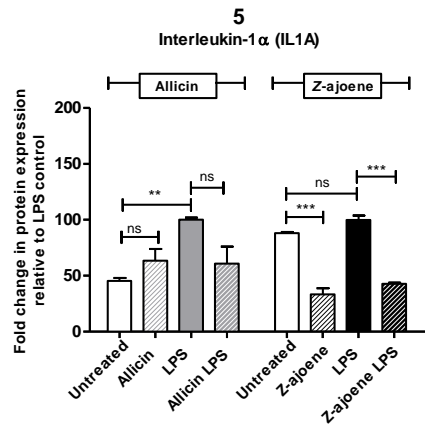
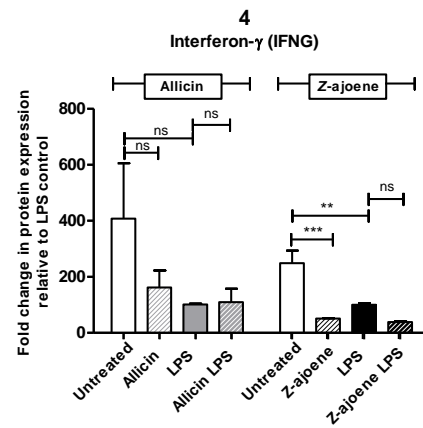
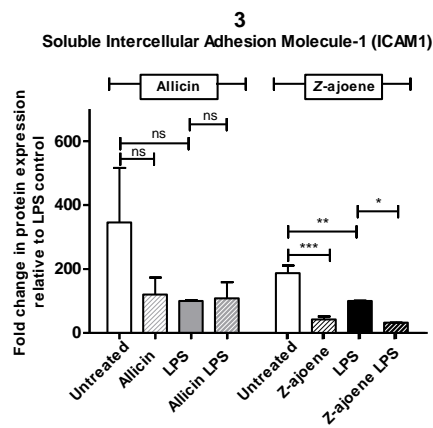
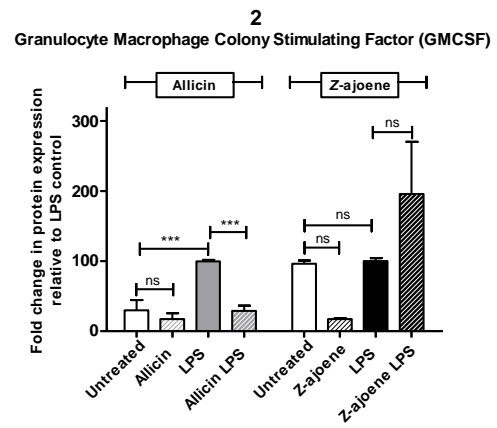
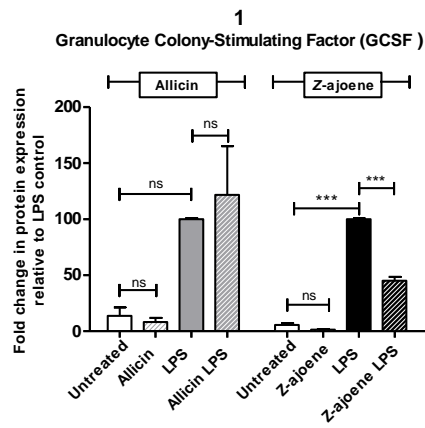
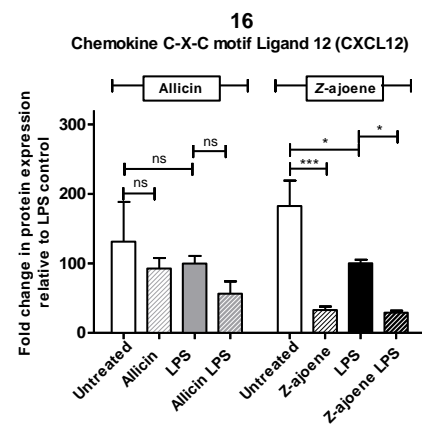
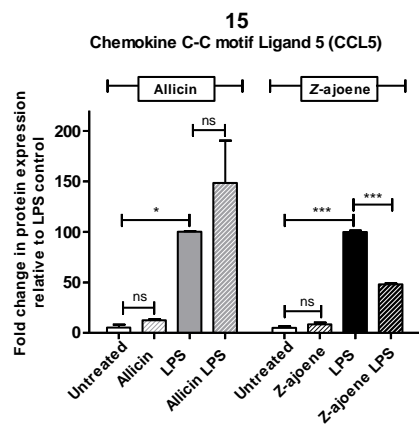
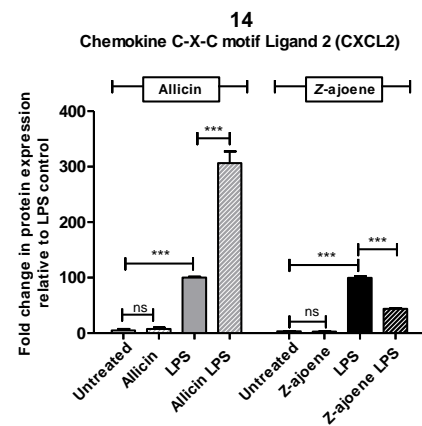
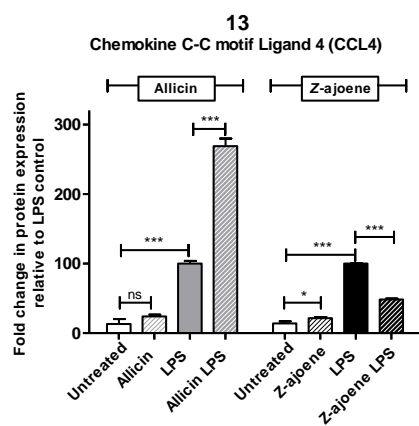
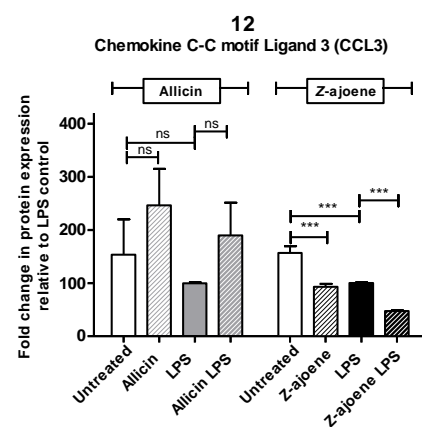
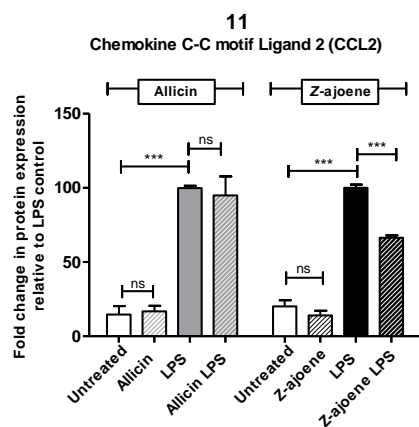
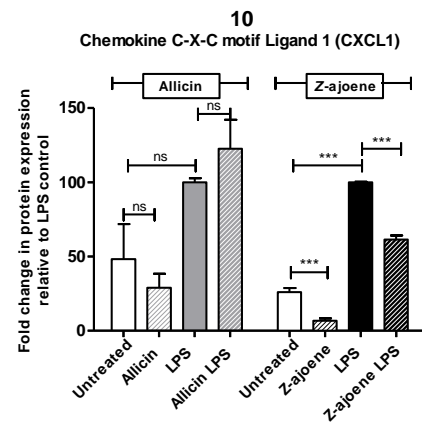
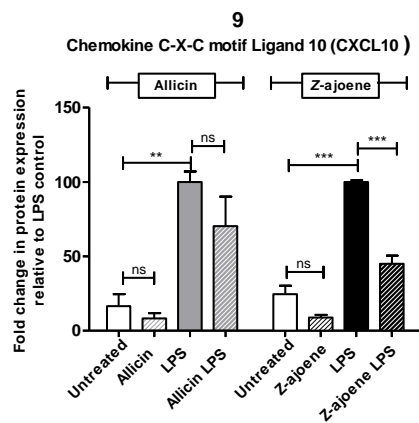


Figure 3.16: Representative Proteome Profiler™ Mouse Cytokine Arrays performed on cell culture supernatants harvested from murine RAW264.7 macrophages treated with LPS and/or a garlic OSC. A representative nitrocellulose blot is shown for the untreated, garlic OSC-treated, LPS-treated, and garlic OSC- LPS-treated conditions. A. allicin experiment B. Z-ajoene experiment. Numbers in red indicate duplicate spots for proteins chosen for densitometric analysis based on a strong antibody signal in one or more of the treatment conditions from either allicin or Z-ajoene experiments.

For easy referencing purposes, the number corresponding to the protein spots seen in Figure 3.16 and above each bar chart in Figure 3.17 is included in square brackets after the mention of each protein in the subsequent text.





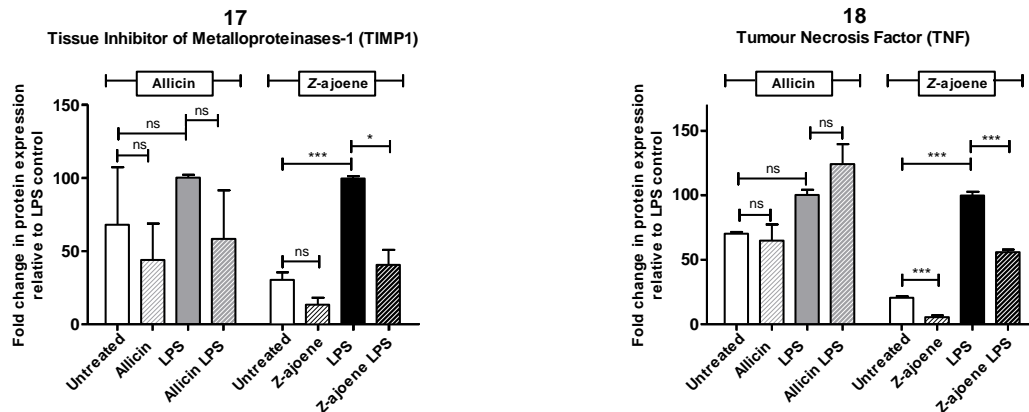


Figure 3.17: The effect of selected garlic OSCs on the LPS-induced expression of 18 selected cytokines and chemokines in murine RAW264.7 macrophages and identified using the Proteome Profiler™ Mouse Cytokine Array. Cells were pre-treated with $\frac{1}{2}$ IC₅₀ concentrations of allicin or Z-ajoene, followed by a second dose after 24 h in conjunction with 10 ng/ml LPS. Cell culture supernatants for protein expression analysis were harvested after 24 h of treatment with LPS and the garlic OSC. **A.** Allicin experiment, **B.** Z-ajoene experiment. Densitometric analysis was performed to obtain mean percentage expression (\pm SEM) for two independent experiments, shown relative to LPS-treated cells (set to 100%). One-way ANOVA significance testing followed by Tukey's HSD test (*, $p < 0.05$; **, $p < 0.01$; ***, $p < 0.001$; ns, not significant) was performed. Numbers above the charts correspond to the numbered spots in Figure 3.16.

Of the 18 cytokines and chemokines analysed, 14 were upregulated and four were downregulated by LPS treatment (Figure 3.17 and summarised in Table 3.5). The four proteins downregulated by LPS treatment were soluble intercellular adhesion molecule-1 (ICAM1) [3], interferon- γ (IFNG) [4], CCL3 [12] and CXCL12 [16]. Z-ajoene treatment further downregulated the expression of soluble ICAM1 ($p < 0.05$) [3], IFNG (decreasing trend) [4], CCL3 ($p < 0.001$) [12] and CXCL12 ($p < 0.05$) [16] (Figure 3.17 & Table 3.5).

Interestingly, Z-ajoene treatment alone was also able to significantly downregulate the expression of all four proteins ($p < 0.001$) compared to untreated cells. A decreasing trend in expression of soluble ICAM1 [3] and IFNG [4] was also seen upon allicin treatment alone and this response is comparable to the trend seen for the LPS-induced downregulation of expression for these proteins. Allicin treatment, unlike Z-ajoene treatment, did not have an additive effect on LPS-induced downregulation of expression of soluble ICAM1 [3] and IFNG [4], while there was a slight decreasing trend seen with allicin-treatment on LPS-induced downregulation of CXCL12 [16]. CCL3 [12] expression was elevated in allicin-treated cells and allicin treatment was able to buffer the downregulating effect of LPS-treatment. None of these effects on CCL3 [12] protein expression, however, were statistically significant.

Of the 14 cytokines and chemokines upregulated by LPS-treatment, Z-ajoene treatment significantly downregulated the LPS-induced expression of 12 proteins, showed a downward trend for two proteins and an upward trend for one protein (Table 3.5 and Figure 3.17). Granulocyte macrophage colony stimulating factor (GMCSF) [2] was the only protein where Z-ajoene treatment showed an increasing trend in expression compared to LPS-treated cells. This result is questionable, however, because there was no increase in expression upon LPS treatment, in contrast to the allicin experiments. Consistent with the RT² Profiler PCR Array, Z-ajoene significantly decreased the LPS-induced expression of IL1RN. Further, Z-ajoene treatment significantly decreased the expression of all eight chemokines selected for further analysis.

Table 3.5: Summary of the effect of allicin or Z-ajoene treatment on percentage protein expression of selected LPS-induced cytokines and chemokines identified using the Proteome Profiler™ Mouse Cytokine Array. This table summarises the results from Figure 3.17 showing the effect of LPS treatment and garlic OSC plus LPS treatment on cytokine and chemokine protein expression. The effect of LPS treatment on cells is shown as a red upward arrow for upregulation and a green downward arrow for downregulation. Statistically significant changes in LPS-induced protein expression following treatment with allicin or Z-ajoene are shown in red for upregulation and green for downregulation.

| Number | Cytokine/Inflammatory mediator | Protein Symbol | Up-/downregulated by LPS | % Protein Expression relative to LPS control | |
|--------|--|--------------------|--------------------------|--|--------------|
| | | | | Allicin-LPS | Z-ajoene-LPS |
| 1 | Granulocyte Colony-Stimulating Factor | GCSF | ↑ | 121.7 ± 43.6 | 45 ± 3.3 |
| 2 | Granulocyte Macrophage Colony Stimulating Factor | GMCSF | ↑ | 28.9 ± 7.7 | 196.1 ± 74.5 |
| 3 | Soluble Intercellular Adhesion Molecule-1 | ICAM1 | ↓ | 108.0 ± 50.8 | 31.9 ± 0.7 |
| 4 | Interferon-γ | IFNG | ↓ | 109.0 ± 47.9 | 38.7 ± 3.5 |
| 5 | Interleukin-1α | IL1A | ↑ | 61.0 ± 15.0 | 43.0 ± 0.9 |
| 6 | Interleukin-1 Receptor Antagonist | IL1RN | ↑ | 53.6 ± 5.1 | 52.5 ± 16.2 |
| 7 | Interleukin-6 | IL6 | ↑ | 14.6 ± 2.4 | 73.37 ± 15.5 |
| 8 | Interleukin-27 | IL27 | ↑ | 25.1 ± 11.9 | 40.8 ± 14.8 |
| 9 | Chemokine C-X-C motif Ligand 10 | CXCL10 | ↑ | 70.5 ± 19.8 | 45.0 ± 5.5 |
| 10 | Chemokine C-X-C motif Ligand 1 | CXCL1 | ↑ | 122.5 ± 19.6 | 61.4 ± 2.8 |
| 11 | Chemokine C-C motif Ligand 2 | CCL2 | ↑ | 95.0 ± 12.9 | 66.5 ± 1.6 |
| 12 | Chemokine C-C motif Ligand 3 | CCL3 | ↓ | 190 ± 61.5 | 47.4 ± 1.4 |
| 13 | Chemokine C-C motif Ligand 4 | CCL4 | ↑ | 269.1 ± 10.7 | 48.3 ± 1.7 |
| 14 | Chemokine C-X-C motif Ligand 2 | CXCL2 | ↑ | 306.3 ± 21.2 | 43.8 ± 1.5 |
| 15 | Chemokine C-C motif Ligand 5 | CCL5 (also RANTES) | ↑ | 148.3 ± 42 | 48.1 ± 1.0 |
| 16 | Chemokine C-X-C motif Ligand 12 | CXCL12 | ↓ | 56.6 ± 17.6 | 28.8 ± 3.4 |
| 17 | Tissue Inhibitor of Metalloprotease-1 | TIMP1 | ↑ | 58.2 ± 33.3 | 40.6 ± 10.4 |
| 18 | Tumour Necrosis Factor | TNF | ↑ | 123.9 ± 15.4 | 56.1 ± 1.9 |

Unlike Z-ajoene treatment, allicin treatment had a more variable effect on the LPS-induced upregulation of cytokine and chemokine protein expression (Figure 3.17 & Table 3.5). Allicin treatment significantly upregulated the LPS-induced expression of CCL4 ($p < 0.001$) [13] and CXCL2 ($p < 0.001$) [14], and showed an increasing trend in the expression of LPS-induced GCSF [1], CXCL1 [10], CCL5/RANTES [15] and TNF [18]. Conversely, allicin treatment significantly downregulated the LPS-induced increase in expression of GM-CSF ($p < 0.003$) [2], IL1RN ($p < 0.01$) [6] and IL6 ($p < 0.001$) [7]. Note that the downregulation of LPS-induced IL6 expression by allicin treatment is consistent with the ELISA data from Figure 3.3B for supernatant samples collected 24 h after addition of LPS and allicin. In addition, allicin treatment showed a trend towards abrogation of the LPS-induced increase in interleukin-1 α (IL1A) [5], IL27 [8], CXCL10 [9] and tissue inhibitor of metalloproteinases-1 (TIMP1) [17].

It is interesting to note that allicin treatment alone did not significantly affect the expression levels of any of the 18 cytokines and chemokines analysed, when compared to untreated cells. However, Z-ajoene treatment alone resulted in the significant downregulation of expression of soluble ICAM1 [3], IFNG [4], IL1A [5], CXCL1 [10], CCL3 [12], CXCL12 [16] and TNF ($p < 0.01$) [18] and showed a decreasing trend in expression for five of the other proteins whose expression is induced by LPS treatment. In addition, Z-ajoene treatment alone resulted in a significant increase in CCL4 [13].

Figure 3.18 summarises the effect of allicin and Z-ajoene treatment on LPS-induced expression of the 18 cytokines and chemokines identified in the Proteome Profiler™ Mouse Cytokine Array. While allicin treatment was found to be mildly up- or downregulating, Z-ajoene generally displayed stronger downregulatory effects on the expression of the selected LPS-induced inflammatory cytokines and chemokines.

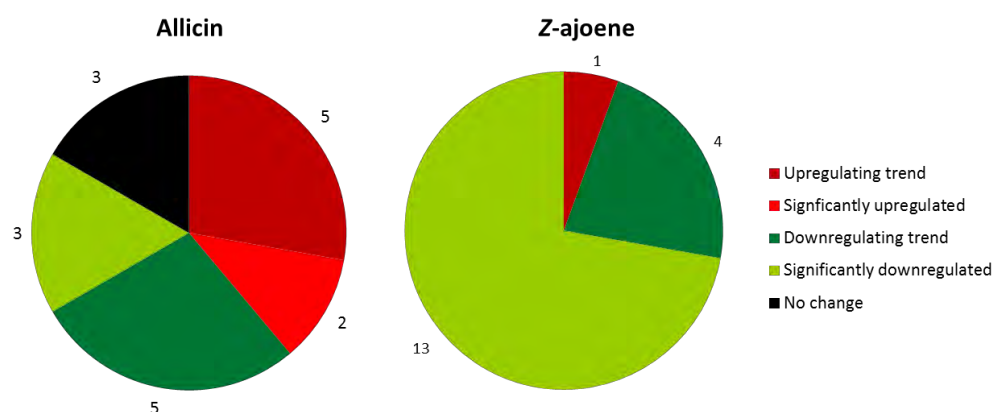


Figure 3.18: The effect of allicin and Z-ajoene treatment on the protein expression of 18 LPS-induced cytokines and chemokines selected for analysis from the Proteome Profiler™ Mouse Cytokine Array (R&D Systems). A. Allicin experiment, B. Z-ajoene experiment. Experiments were performed in duplicate.

3.6. The effect of selected garlic OSCs on LPS-induced STAT3 phosphorylation

The STAT3 transcription factor is an integral part of the inflammatory immune response, and has been shown to regulate the transcription of many genes which regulate said inflammatory response. Prior to STAT3 activation, cytokines and growth factors activate the Janus kinase/signal transducer and activator of transcription (JAK/STAT) signalling pathway resulting in the phosphorylation of STAT3 at Tyr705³¹. Phosphorylated-STAT3 (p-STAT3) can form homodimers and heterodimers (with STAT1) which facilitate its nuclear import. Once in the nucleus, p-STAT3 activates the transcription of many genes involved in inflammation, apoptosis and immune response signalling³¹. As treatment with allicin or Z-ajoene affects LPS-induced gene and protein expression of many STAT3 target genes including *IL10*/IL10 (Figure 3.7 & Table 3.3) and *IL6*/IL6 (Figure 3.5 & Table 3.3)(both activators of STAT3), we decided to investigate whether allicin or Z-ajoene treatment affected the phosphorylation of STAT3 at Tyr705. STAT3 target genes are discussed in more detail in Section 4.3.

A time course experiment was performed to determine the effect of allicin and Z-ajoene treatment on LPS-induced STAT3 phosphorylation. Preliminary experiments showed that STAT3 was not phosphorylated in response to LPS treatment in RAW264.7 macrophages between 0 and 2 h (data not shown) and hence a time course measuring STAT3 phosphorylation after 0, 2, 4, 6, 8 and 24 h was performed. Cell lysates harvested after these timepoints were analysed by Western blot using both p-STAT3 (Tyr705) and STAT3 antibodies, the latter served as a loading control (Figure 3.16). To control for the potential increase in protein expression of STAT3 upon LPS-treatment, GAPDH (Santa Cruz Biotechnology) was used as an additional loading control. Figure 3.17 shows the relative quantity of p-STAT3 after allicin and Z-ajoene treatment compared to the LPS-treated cells at the given timepoint.

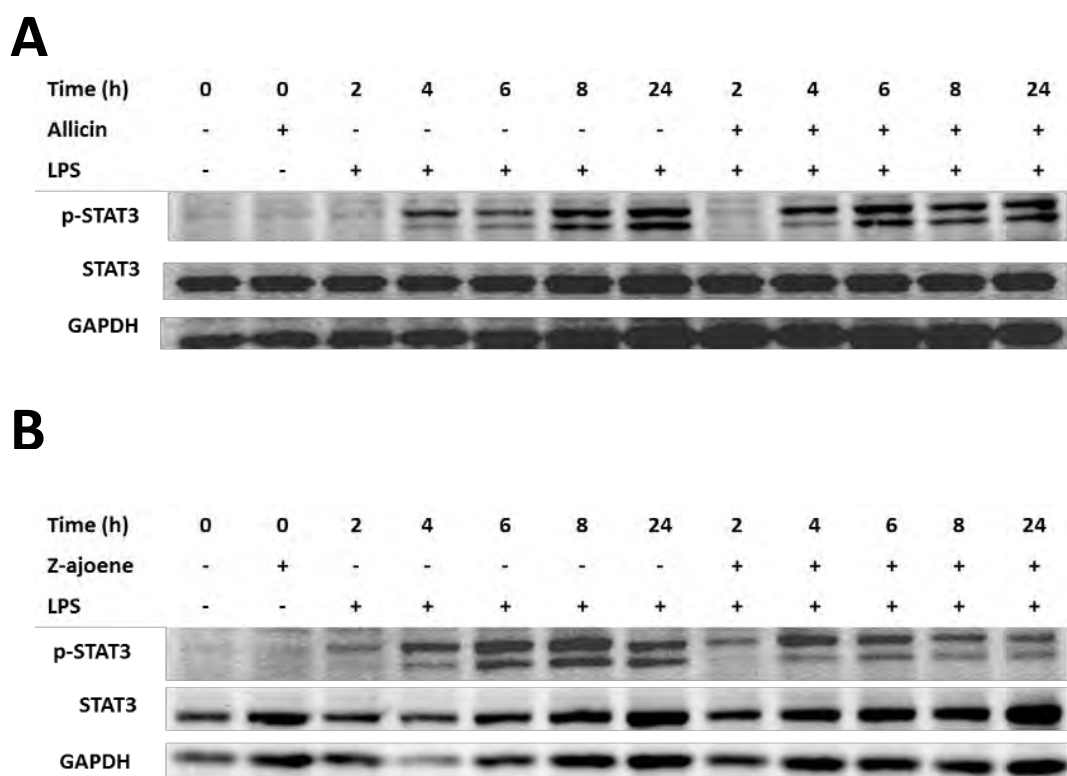


Figure 3.19: A representative Western blot showing a time course experiment performed to determine the effect of allicin and Z-ajoene treatment on LPS-induced phosphorylation of STAT3 in murine RAW264.7 macrophages. Cells were pre-treated with $\frac{1}{2}$ IC₅₀ concentrations of allicin or Z-ajoene, followed by a second dose after 24 h in conjunction with 10 ng/ml LPS. Whole cell lysates were harvested following the LPS/OSC treatment at timepoints 0, 2, 4, 6, 8 and 24 h and analysed by SDS-PAGE and Western blot. **A.** Allicin experiment, **B.** Z-ajoene experiment. Nitrocellulose membranes were probed with an anti-p-STAT3 (Tyr705), STAT3 and GAPDH antibodies where STAT3 and GAPDH served as loading controls.

Figure 3.19 shows that pre-treatment of cells with allicin or Z-ajoene does not result in any STAT3 phosphorylation (24 h after treatment with the selected garlic OSC and 0 h after addition of LPS and the second dose of the garlic OSC). When quantified by densitometric analysis (Figure 3.6) allicin treatment and Z-ajoene treatment differentially affect the LPS-induced phosphorylation of STAT3. Allicin treatment causes an early peak in p-STAT3 levels after 6 h, while between 8 and 24 h the p-STAT3 levels are very similar to that of the LPS-treated cells. Z-ajoene treatment, on the other hand, causes a 2.5-fold decrease in p-STAT3 levels between 6 and 24 h compared to the LPS treated cells. Allicin treatment was therefore found to induce a short, early peak in the LPS-induced phosphorylation of STAT3 after 6 h, while Z-ajoene was found to downregulate the levels of LPS-induced p-STAT3.

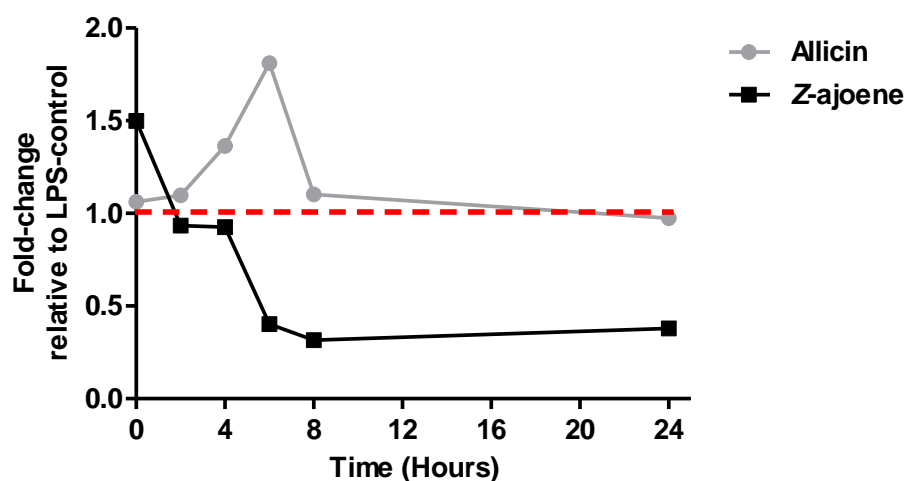


Figure 3.20: A line graph showing the fold change in LPS-induced phosphorylation of STAT3 after allicin or Z-ajoene treatment relative to the p-STAT3 levels in the LPS control. The dotted red line represents the LPS-treated sample at the given timepoints. Densitometric analysis on p-STAT3 bands (of representative experiment in Figure 3.19) was performed to quantify protein concentration and were normalised to STAT3 loading control. Relative phosphorylation was then normalised to the LPS-control.

3.7. STAT3 alkylation by *E/Z*-ajoene

In the previous section, we showed that the garlic OSCs allicin and Z-ajoene affect the phosphorylation of the transcription factor STAT3. A review of the literature indicates that STAT3 is susceptible to *S*-glutathionylation, a post-translational modification where glutathione (GSH) is reversibly added to a cysteine-thiol of a protein under oxidative conditions^{161,188}. Xie *et al.* (2009) showed that alkylation of STAT3 affects the phosphorylation, dimerization and transcriptional activity of STAT3¹⁶¹. Previous research in our laboratory led us to hypothesise that garlic OSCs may interact with proteins by undergoing thiol-disulfide exchange reactions with cysteine thiols of proteins (Figure 3.21). This thiol-disulfide exchange (alkylation) reaction is analogous to *S*-glutathionylation. We thus hypothesised that garlic OSCs may alkylate STAT3 affecting protein function.

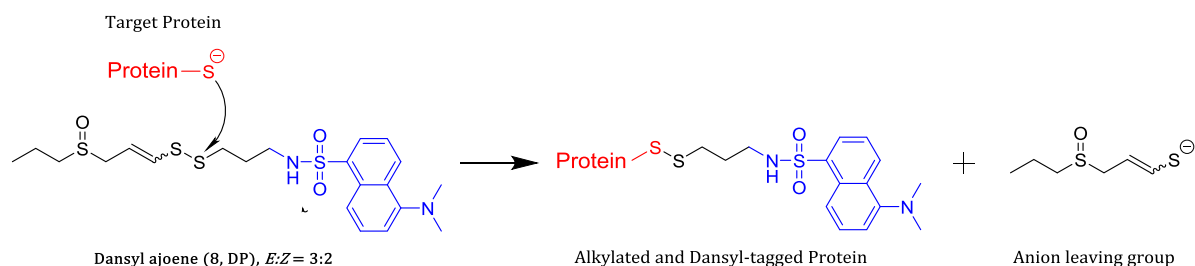


Figure 3.21: Schematic showing the reaction between dansylated-*E/Z*-ajoene and the cysteine nucleophile of a protein. The cysteine nucleophile reacts with the more electropositive sulfur of the *E/Z*-ajoene disulfide bond, resulting in the formation of a mixed disulfide product, consisting of the protein and the dansyl-tagged region of the *E/Z*-ajoene, and an anion leaving group.

In order to determine whether garlic OSCs undergo a thiol-disulfide exchange reaction with STAT3, *E/Z*-ajoene, labelled with a dansyl-residue (Department of Chemistry, UCT), was incubated with recombinant human STAT3 protein and run on an SDS-PAGE gel either under non-reducing or reducing conditions. Under non-reducing conditions, it is hypothesised that a mixed-disulfide may form between STAT3 and the ajoene analogue via a thiol-disulfide exchange reaction to form an alkylated STAT3 protein product. If this reaction indeed occurs, it is then hypothesised that incubation with a reducing agent, i.e. DTT, should cleave this disulfide bond to release the free STAT3 protein. By probing the nitrocellulose membrane with an anti-STAT3 antibody and an anti-dansyl antibody, it may be possible to determine whether a mixed disulfide reaction between STAT3 and ajoene occurs.

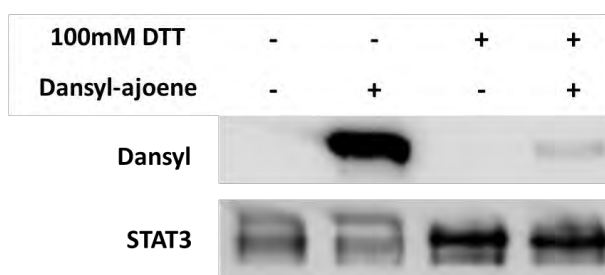


Figure 3.22: Western blot showing dansylation of recombinant human STAT3 via a thiol-disulfide exchange reaction with dansyl-tagged *E/Z*-ajoene. The nitrocellulose membrane was probed with an anti-dansyl antibody, stripped and re-probed with an anti-STAT3 antibody. The samples were run under reducing (100 mM DTT) or non-reducing (no DTT) conditions.

Figure 3.22 shows that STAT3 is indeed reversibly alkylated by *E/Z*-ajoene. Co-localisation of the dansyl-signal and the STAT3-signal indicates that the thiol-disulfide reaction has occurred. Incubating the STAT3 dansyl-tagged *E/Z*-ajoene mixture with a reducing agent resulted in a significant decrease in the intensity of the dansyl-signal. This indicates that STAT3 is indeed reversibly alkylated by *E/Z*-ajoene.

Chapter 4 Discussion

Inflammation is known to play a key role in the pathogenesis and maintenance of a number of diseases including autoimmune disorders, diabetes and cancer^{28,189,190}. Chronic inflammation has been described as an enabling characteristic of cancer as the pro-proliferative, pro-survival, pro-angiogenic mechanisms of wound healing are co-opted to facilitate tumourigenesis^{10,191–193}. Significantly, the long term use of NSAIDs has been shown to have protective effects against cancer via their anti-inflammatory activities⁷⁴. Due to the high risk of adverse side-effects associated with the long-term use of NSAIDs, these drugs have limited therapeutic application^{79–81}. A number of natural dietary anti-inflammatory compounds that have NSAID-like activity, have been proposed as healthy alternatives to NSAIDs for the prevention of cancer^{82,194}. The culinary plant, garlic has been shown to contain many natural bioactive compounds and is used to treat a variety of ailments. Historically, garlic was used as a prophylactic and therapeutic agent against infections, headaches, inflammation and tumours^{113,115}. Modern research has shown garlic to have cancer preventative and therapeutic applications^{96–99}. Significantly, a number of epidemiological studies suggests that regular dietary consumption of garlic (or related *Allium* vegetables) decreases the risk of gastric cancers^{104–106}. Of the many bioactive compounds found in garlic, garlic OSCs have been most widely studied for their role as anti-cancer agents¹¹³. This anti-cancer activity may be mediated through modulation of immune system-regulated inflammatory responses^{85,130–132}. While there are over 4000 published articles looking at the health benefits of garlic with respect to various diseases or conditions, differences in experimental design have made comparisons between studies challenging¹¹⁷. Many studies use garlic extracts or garlic oil with unspecified chemical composition and concentration. In addition, studies differ with respect to the cell type or experimental model used as well as the experimental time frame. There is therefore scope for experimental work focusing on the effect of individual pure garlic OSC treatment on stimulated inflammatory immune responses in a well-defined experimental system.

4.1. Establishment of a well-defined *in vitro* inflammatory model

In this study, we established an *in vitro* inflammatory model to determine the effects of selected garlic OSC treatment on the LPS-stimulated inflammatory response in RAW264.7 murine macrophages. This model was chosen with the idea of ultimately determining the effects of garlic OSC gavage on induced gastrointestinal- and colorectal inflammation in BALB/c mice. The experimental work from this thesis serves as the basis for the *in vitro* proof-of-concept required for an ethics application for future *in vivo* experiments.

In our model, we used pure synthesised garlic OSCs (verified by ^1H NMR spectroscopy) at sub-toxic ($\frac{1}{2}$ IC_{50}) concentrations determined by MTT cell viability assays. IC_{50} values were determined for allicin, DADS, DATS, *E*-ajoene, and *Z*-ajoene (Table 3.1) after 24 h treatment. Based on preliminary inflammatory gene expression experiments, the garlic OSCs allicin and *Z*-ajoene were chosen for subsequent experiments due to their different immunomodulating effects on the gene expression of LPS-stimulated cytokines (Figure 3.3). Further, we chose the comparatively low LPS concentration of 10 ng/ml for stimulation experiments as we expected garlic OSCs to have subtle immunomodulating effects (Figure 3.1A).

In line with the hypothesis that garlic OSCs, obtained from the regular dietary consumption of garlic, can aid in cancer prevention by counterbalancing the establishment of a chronic inflammatory microenvironment conducive to cancer, treatment conditions for RAW264.7 macrophages in the *in vitro* inflammatory model were chosen which best simulate regular dietary consumption. Cells were treated twice with $\frac{1}{2}$ IC_{50} concentrations of either allicin and *Z*-ajoene, 24 h apart. The second dose of the garlic OSC was given in conjunction with 10 ng/ml LPS, which was representative of an infection. Preliminary gene and protein expression experiments were conducted, and 4 h and 8 h (gene expression), and 8 h and 24 h (protein expression) were chosen as the best timepoints post LPS stimulation to accommodate the gene and protein expression profiles of the cytokines tested (Figure 3.1B). These gene and protein expression analyses provided the experimental conditions for subsequent gene and protein arrays with samples collected at 4 h- and 24 h-post treatment, respectively.

While the greatest care was taken to establish and optimise a robust *in vitro* inflammatory model, there are a number of limitations to this model. Firstly, this model is a monoculture of immortalised macrophages taken out of the context of the tissue microenvironment. It is well-documented that inflammation relies on bidirectional communication between many different cell types (including numerous specialised innate and adaptive immune cells, fibroblasts and epithelial cells) and their environment¹⁹¹. Future work should make use of co-culture experiments with different cell types to better simulate the inflammatory microenvironment. One such study co-cultured murine peritoneal macrophages with B16 melanoma cells, and showed that allicin treatment increased the tumouricidal activities of these macrophages¹³². Secondly, LPS stimulation of macrophages is representative of the acute inflammatory response and not chronic inflammation which is the driving force of cancer development and progression. It is, however, difficult to study chronic inflammation *in vitro*, as macrophages are known to become tolerant and hence unresponsive to inflammatory stimuli when exposed for extended periods of time^{175,195}. Thirdly, the concentrations of the garlic OSCs used in the *in vitro* experiments may not be biologically relevant to *in vivo* experiments. For example, unpublished

animal studies conducted in our laboratory where naïve BALB/c mice were fed garlic OSC gavage showed that allicin and Z-ajoene had a stronger immunomodulatory effects in proximal gastrointestinal tract organs such as the stomach and duodenum, where absorption of dietary material occurs, with little or no effect on the colon. In these experiments, different concentrations and secondary metabolites reach different parts of the gastrointestinal tract and may not necessarily reflect the concentrations used for the *in vitro* model presented in this thesis.

While this model has its limitations, it provides the necessary groundwork and proof-of-concept required for an ethics application to study the effects of garlic OSC gavage on inflammation in a BALB/c mouse colitis-model.

4.2. Experiments investigating immune and inflammatory responses

In order to determine the effect of allicin and Z-ajoene treatment on LPS-induced inflammation, inflammatory cytokines (*Il1b*/IL1B, *Il6*/IL6, *Il12b*/IL12B, *Il10*/IL10 and *Tnf*/TNF), enzymes (*Cox2*/COX2 and *Nos2*) and the pro-apoptotic mediator *Trail*/TRAIL, all of which are associated with inflammation and inflammation-based cancer, were selected for initial gene and protein expression analyses. Based on these findings, gene and protein profiler arrays were conducted to obtain a broader indication of the effects of garlic OSC treatment on LPS-induced inflammation. It must be noted that as the expression data from the Proteome Profiler Array was performed in duplicate, we consider these results to be more reliable and statistically significant than those of the RT² Profiler PCR Array which is representative of a single qPCR experiment.

Major findings from the gene and protein expression analyses include the effect of allicin and Z-ajoene treatment on LPS-induced gene and protein expression of interleukins, chemokines, inflammatory enzymes and the TNF ligand superfamily.

4.2.1. Allicin and Z-ajoene regulate interleukins to prevent inflammation

In this study the pro-inflammatory interleukins *Il1b*/IL1B, *Il6*/IL6 and *Il12b*/IL12B (a subunit of the IL12 and IL23 interleukin) and the anti-inflammatory interleukin *Il10*/IL10 were selected for gene and protein expression analysis in initial experiments. The pro-inflammatory interleukins have previously been shown to be upregulated during chronic inflammation and cancer, while IL10 can act as either an anti-inflammatory or immunosuppressive cytokine in these processes^{10,19,59,196}.

qPCR gene and ELISA protein expression data indicated that LPS-induced expression of *Il1b*/IL1B, *Il6*/IL6 and *Il12b*/IL12B was decreased by allicin and Z-ajoene treatment, whereas allicin generally had

a more pronounced immunomodulatory effect (Figures 3.4-3.6). Interestingly, *IL6/IL6* gene expression was initially upregulated by allicin treatment after 4 h in both the qPCR (Figure 3.5A) and the RT² Profiler PCR Array (Table 3.3), but decreased after 8 h (Figure 3.5A). This downregulation was reflected at the protein level, where allicin treatment significantly decreased LPS-induced *IL6/IL6* protein after 24 h by both ELISA (Figure 3.5B) and the Proteome Profiler Array (Figure 3.17 and Table 3.5). The data for allicin immunomodulation of *IL6/IL6* was thus reproducible across all experimental gene and protein expression analysis methods. Additionally, the RT² Profiler PCR Array revealed that allicin also downregulated the gene expression of pro-inflammatory *IL22* (a member of the IL10 family of cytokines) (Table 3.3), while the Proteome Profiler Array showed that both Z-ajoene and allicin treatment downregulated the protein expression of IL1A and IL27 (a member of the IL6 family of cytokines) (Figure 3.17 and Table 3.5). In addition, the LPS-induced expression of the receptor antagonist *IL1RN/IL1RN*, which is structurally related to IL1A and IL1B, was downregulated by Z-ajoene treatment at both the gene (Table 3.4) and protein level and by allicin treatment at the protein level (Figure 3.17 and Table 3.5). The expression of LPS-induced *IL10/IL10*, on the other hand, was significantly increased by allicin treatment at 4 h and 8 h (gene expression), and 8 h and 24 h (protein expression) (Figure 3.7A and B), and this was supported by the result from the RT² Profiler PCR Array (Table 3.3). It must be noted that protein expression of IL10, IL1B and IL12 (full protein), included in the Proteome Profiler Array, was not detected for either the LPS-treated or the garlic OSC-LPS-treated samples, which suggests differences in sensitivity between the ELISAs versus the Proteome Profiler Array.

In support of these findings, studies investigating the effect of garlic OSCs on LPS-stimulated RAW264.7 macrophages found that DATS decreased IL6 and IL12 (full protein) expression¹³⁹; DAS decreased IL1B and IL6 expression¹⁴⁰ and E/Z-ajoene decreased IL1B and IL6 expression¹⁴³ (Table 1.1). In addition, LPS-stimulated CD4⁺ monocytes (isolated from human whole blood) treated with garlic extract showed a decrease in the expression of LPS-induced IL1A, IL2, IL6 and IL12 (full protein)⁸⁴. Reports on the effect of garlic OSC treatment on IL10 expression are contradictory; while DAS and DADS treated LPS-stimulated RAW264.7 macrophages showed a decrease in IL10 expression, allyl methyl sulfide (AMS) increased IL10 expression¹⁴⁰. Another study also looking at LPS-stimulated RAW264.7 macrophages showed that DATS decreased IL10 expression¹³⁹. Conversely, LPS-stimulated CD4⁺ monocytes treated with garlic extract were shown to have increased IL10 levels when treated with garlic extract⁸⁴.

In general, allicin and Z-ajoene downregulated the LPS-induced expression of pro-inflammatory cytokines IL1A, *IL1b/IL1B*, *IL6/IL6*, *IL12b/IL12B*, *IL22* and IL27 while upregulating the anti-inflammatory cytokine *IL10/IL10*. As *IL10* is known to play a dual role in cancer development (it can downregulate

inflammatory responses and promote tissue homeostasis and return to normal immune surveillance, or it can promote immunosuppression and thereby facilitate tumourigenesis and cancer progression^{55,59}), future work should aim to distinguish between the anti-inflammatory and immunosuppressive functions of IL10, which are often context-dependent. As previously mentioned, LPS stimulation of macrophages simulates an acute inflammatory response and therefore the overall effect on LPS-induced interleukin expression by allicin and Z-ajoene treatment is anti-inflammatory.

4.2.2. Allicin and Z-ajoene differentially modulate chemokine expression

Chemokines, or chemoattractant cytokines, are low molecular weight proteins (7-15kDa) involved in the recruitment and activation of innate and adaptive immune cells to sites of injury or inflammation²⁴. In addition to regulating leukocyte adhesion and migration, chemokines also regulate inflammation and wound healing processes including reactive oxygen species (ROS) release, angiogenesis and tissue remodelling²¹.

Analysis of the RT² Profiler PCR Array and the Proteome Profiler Array showed that allicin and Z-ajoene differentially modulated the expression of the chemokines selected for further analysis. A 4 h treatment with allicin generally had strong upregulating effects on the LPS-induced chemokine gene expression, while Z-ajoene showed a modest downregulatory effect on fewer chemokines (Table 3.3 and 3.4). In contrast, and more importantly, the Proteome Profiler Array, performed on samples collected after 24 h, showed that Z-ajoene significantly decreased the LPS-induced expression of all eight chemokines that were affected by LPS treatment, while allicin significantly upregulated the LPS-induced expression of only two of these chemokines (Figure 3.17 and Table 3.5).

Z-ajoene was found to mediate the downregulation of the LPS-induced proteins CCL2 and CXCL1 (Table 3.5) which is in agreement with the study conducted by You et al. (2013) which showed that treatment of LPS-stimulated RAW264.7 macrophages with DATS for 12 h resulted in a dose-dependent decrease in these same proteins¹³⁹. Another study looking at the effects of allicin treatment in *TNF*-stimulated colorectal adenocarcinoma cancer HT-29 and Caco-2 cells showed a dose-dependent decrease in protein expression of CXCL8 (also IL8), CXCL9 and CXCL10, after 24 h¹³⁷. Similarly, in our study, allicin and Z-ajoene decreased the LPS-induced expression of CXCL10 (Table 3.5).

Taken together, the gene expression data suggests that allicin upregulates the expression of many chemokines after 4 h while Z-ajoene has weaker downregulatory effects. More importantly, however, Z-ajoene exerts a strong downregulatory effect on LPS-induced protein expression of chemokines after 24 h, while allicin has mixed upregulatory- and downregulatory effects. This data suggests that allicin rapidly exerts its effects in the cells, while the effects of Z-ajoene treatment last for a longer

period of time. This is in line with the compounds' reactivity, as allicin is a more reactive compound which readily interacts with proteins or other molecules¹²⁰, while Z-ajoene is a more stable compound and has longer-lasting effects. The observed changes in expression over time add another layer of complexity to understanding the immunomodulatory effects of these garlic OSCs. Future experiments should investigate the effects of allicin treatment on protein expression at earlier timepoints to determine whether the strong pro-inflammatory effects of allicin treatment on LPS-induced gene expression are seen at a protein level.

4.2.3. Differential effects on inflammatory enzymes

COX2/PTGS2 and NOS2 are inflammatory enzymes which regulate the production of inflammatory prostaglandins and NO (an inflammatory signalling molecule), respectively. Significantly, NSAIDs and a number of naturally-occurring compounds with anti-inflammatory properties have been shown to have protective effects against cancer by either inhibiting COX2 enzyme activity or downregulating pro-inflammatory enzyme expression^{74,82}.

Surprisingly, gene and protein expression of *Cox2*/COX2 was found to be upregulated by both allicin and Z-ajoene treatment determined by qPCR and ELISA analysis, respectively (Figure 3.9 and Table 3.2). *Cox2* gene expression was also shown to be upregulated by allicin treatment in the RT² Profiler PCR Array (Table 3.3). In contrast, three studies (summarised in Table 1.2) investigating the effect of garlic OSC treatment on LPS-stimulated macrophages showed a decrease in COX2 expression for 10 μ M DAS¹⁴⁸, 100-200 μ M DATS¹³⁹ and 20 μ M *E/Z*-ajoene¹⁴³. These studies, however, used much higher treatment concentrations of these garlic OSCs (we report IC₅₀ values for DATS of 4.59 ± 1.66 μ M and *E*- and *Z*-ajoene between 2.71-4.39 μ M after 24 h (Table 3.1) and higher LPS concentrations for shorter periods of time. In addition, all of these studies showed that treatment with the relevant garlic OSC downregulated PGE2 expression. In support of our findings, however, a study conducted by Dirsch and Vollmar (2001) showed that treatment of LPS (1 μ g/ml)-stimulated RAW264.7 macrophages with 10 μ M of *E/Z*-ajoene for 2-8 h increased COX2 protein expression. The production of PGE2, however, was decreased by *E/Z*-ajoene treatment in a dose-dependent fashion, indicating that while COX2 expression was increased, COX2 enzyme activity was inhibited¹⁴⁷. In this way, the *E/Z*-ajoene mixture has NSAID-like properties¹⁴⁷. In this thesis, COX2 enzyme activity was not measured due to time constraints. Similarities in experimental design between the Dirsch and Vollmar (2001) study and this thesis suggest that COX2 enzyme activity may be similarly inhibited in our *in vitro* inflammatory model. Further experimentation is necessary to test this theory.

With respect to LPS-induced *Nos2* gene expression, modest increasing trends for allicin and decreasing trends for Z-ajoene were seen although these effects were not statistically significant (Figure 3.11).

The effects of allicin and Z-ajoene on LPS-induced NOS2 and NO protein expression, however, were not determined due to time limitations. Previous studies report that allicin¹⁴⁶, DAS¹⁴⁸, DADS¹⁴⁸, DATS¹³⁹ and *E/Z*-ajoene^{143,146} decreased NOS2 expression and NO levels in LPS-stimulated RAW264.7 macrophages. Again, the LPS and garlic OSC concentrations of allicin and *E/Z*-ajoene used for these studies was much higher than used in our research. For example, Dirsch et al. (1998), , showed that treatment of LPS-stimulated (1µg/ml) RAW264.7 macrophages with 10 µM *E/Z*-ajoene or 50 µM allicin for 12 h significantly decreased NOS2 enzyme activity¹⁴⁶. It thus appears that the sub-toxic (½ IC₅₀) concentrations used in our study had only subtle effects on NOS2 expression.

Taken together, both allicin and Z-ajoene increase the gene and protein expression of *Cox2*/COX2, but have no significant effect on *Nos2* gene expression. Future work should investigate the effects of garlic OSC treatment on PGE2 and NO expression in order to determine whether these garlic OSCs modulate COX2 and NOS2 enzyme activity.

4.2.4. Effects on TNF and TNF ligand superfamily cytokines

The TNF ligand superfamily (TNFSF) consists of 19 structurally-related proteins which bind to TNF ligand superfamily receptors (also known as death receptors)^{197–199}. These membrane-bound or soluble trimer ligands regulate immune functions including inflammation, cell growth, cell survival and cell death. Binding of soluble or membrane-bound TNFSF ligands can induce inflammatory signalling including activation of NF-κB pathways and/or caspase signalling which induces apoptosis. TNF (also known as TNFSF2), CD40L/TNFSF5 and lymphotoxin-α (LTA/TNFSF1) and -β (LTB/TNFSF3) generally promote survival and inflammatory signalling, while FASL/TNFSF6 and TRAIL/TNFSF10 stimulate caspase-mediated cell death^{197,198}. In addition, CD40L/TNFSF5 and TNFSF14 have been shown to regulate immune responses by mediating communication between immune cells and non-immune cells^{197,198}. To date, there are five clinically approved drugs which target TNF or LTA for the treatment of autoimmune and inflammatory disorders. In addition, a number of cancer therapeutic drugs targeting TNFSF ligands and receptors are in clinical trials (see Croft et al. (2013) for a comprehensive review)¹⁹⁷.

Significantly, a number of studies have shown that garlic OSCs activate caspase signalling and apoptosis in cancer cells^{124,125,127}. In addition, DATS has also been shown to increase the expression of death receptors and enhance cancer-cell sensitivity to *TRAIL*-mediated apoptosis, suggesting that pro-apoptotic activities of garlic OSCs can be mediated through *TNFSF*-family and death-receptor signalling¹²⁴.

In this thesis the LPS-induced gene and protein expression of *Tnf*/TNF, a well-known pro-inflammatory cytokine, was shown to be upregulated by allicin treatment in qPCR gene expression analysis, as well as ELISA and Proteome Profiler Array protein expression analyses (Figure 3.8A and B, Table 3.2, Figure 3.17 and Table 3.5). In contrast, Z-ajoene was found to have a modest downregulatory effect on LPS-induced *Tnf* gene expression after 4 h (Figure 3.8C and Table 3.2), while a significant decrease in protein expression was seen after 24 h in the Proteome Profiler Array (Figure 3.17 and Table 3.5). In contrast, no significant change was seen in the ELISA analysis at the same timepoint (Figure 3.8D and Table 3.2). In general, however, allicin upregulated, while Z-ajoene downregulated *TNF* gene and protein expression. In support of these findings, Kang et al. (2001) found that allicin treatment increased the expression of TNF in thioglycollate-induced peritoneal macrophages¹³², while Lee et al. (2012) found that *E/Z*-ajoene decreased TNF expression in LPS-induced RAW264.7 macrophages¹⁴³.

Moreover, qPCR experiments showed that both allicin and Z-ajoene significantly increased the LPS-induced gene expression of *Trail/Tnfsf10* (Figure 3.10 and Table 3.2). However, when cell culture supernatants were analysed for soluble TRAIL/TNFSF10 protein, none was detected (data not shown). TRAIL/TNFSF10 belongs to the TNF ligand superfamily of type II transmembrane ligands, and can be cleaved by metalloproteases to release a soluble protein/ligand²⁰⁰. The absence of soluble TRAIL/TNFSF10 in cell culture supernatants could therefore be a result of no metalloprotease cleavage of transmembrane TRAIL/TNFSF10. Further analysis using protein lysates needs to be conducted to test this theory.

The RT² Profiler PCR array identified four additional TNFSF members whose expression is affected by either allicin or Z-ajoene treatment following stimulation with LPS. Significantly, the downregulatory effect of LPS treatment on *Fasl/Tnfsf6* and *Light/Tnfsf14* gene expression was further decreased in allicin-LPS treated cells (Table 3.3). It is also interesting to note that allicin treatment alone resulted in a large decrease in expression of *Fasl/Tnfsf6*, but an increase in *Light/Tnfsf14* expression. In contrast, Z-ajoene treatment alone did not alter the endogenous expression levels of *Ltb/Tnfsf3* or *Cd40l/Tnfsf5*, but did downregulate the LPS-induced increase in expression of these genes back to endogenous expression levels (Table 3.4).

Taken together, allicin and Z-ajoene were shown to affect the gene expression levels of six TNFSF ligands as well as the protein expression of TNF/TNFSF2. Future work is needed to confirm the effect of these garlic OSCs on protein expression levels of these TNFSF ligands as well as the effect on associated signalling pathways.

4.3. Garlic OSCs may affect STAT3 phosphorylation and activity through posttranslational modification of cysteine residues

NF- κ B and STAT3 are transcription factors which regulate diverse aspects of the immune response^{31,38,201}. The dysregulation of these two transcription factors is associated with chronic inflammation and immunosuppression which can facilitate tumourigenesis and cancer progression^{30–32}. In addition, research has shown that these transcription factors co-operate to selectively transcribe pro-inflammatory and immunosuppressive genes that have binding sites for both transcription factors³⁵.

In this thesis, many of the cytokines, chemokines and growth factors whose LPS-induced expression was modulated by garlic OSC treatment are known to target NF- κ B and/or STAT3 target genes such as *Il1b*, *Il6*, *Il10*, *Nos2*, *Cox2/Ptgs2* and *Cxcl10*. While there are many reports showing that garlic OSC treatment affects NF- κ B signalling and activity^{85,99,124,137,139,142}, there is only one study investigating the effects of garlic OSC treatment on STAT3 signalling and activation¹⁵⁰. That study showed that 20–40 μ M DATS decreased *IL6*-stimulated Tyr705 STAT3 phosphorylation and hence activation in LNCaP prostate cancer cells and downregulated levels of constitutively active Tyr705 phosphorylated STAT3 in DU145 prostate cancer cells¹⁵⁰. To date, however, no study has reported the effects of garlic OSC treatment of STAT3 Tyr705 phosphorylation in immune cells.

To this end, we investigated the effect of allicin and Z-ajoene treatment on LPS-induced STAT3 Tyr705 phosphorylation by Western blot in RAW264.7 murine macrophages. Western blot analysis showed that allicin treatment caused a spike in the LPS-induced STAT3 phosphorylation after 6 h, which returned to basal levels (i.e. LPS alone) after 8 h (Figure 3.19 and 3.20). Z-ajoene treatment, however, resulted in a sustained 2.5-fold decrease in LPS-induced STAT3 Tyr705 phosphorylation between 6 and 24 h (Figure 3.19 and 3.20).

In support of these findings, a number of gene targets that possess both NF- κ B and STAT3 binding sites and are preferentially transcribed in the presence of both of these transcription factors were shown to be modulated by allicin or Z-ajoene treatment (Table 4.1). The increase (or increasing trend) in the LPS-induced gene expression of *Cox2*, *Cxcl2*, *IL6*, *Nos2*, *Sele*, *Ccl5* and *Cxcl10* after 4 h of treatment with allicin, corresponds with the observed peak in LPS-induced STAT3 phosphorylation seen for allicin treatment after 6 h. After 24 h, when LPS- and allicin-LPS-treated cells have similar levels of phosphorylated STAT3, allicin treatment had both up- and downregulatory effects on the LPS-induced protein expression of the listed inflammatory mediators. In contrast, Z-ajoene treatment had little effect on gene expression after 4 h, when STAT3 phosphorylation levels were similar to that of LPS-only treated cells. However, the sustained downregulation in STAT3 phosphorylation by Z-ajoene

treatment was found to occur between 6 and 24 h (Figure 3.20) which correlates with the general decrease in protein expression of STAT3 and NF- κ B gene targets listed in Table 4.1.

Table 4.1: Summary of the effects of allicin or Z-ajoene treatment on the LPS-induced gene or protein expression of NF- κ B and STAT3 target genes in RAW264.7 murine macrophages. Genes containing both NF- κ B and STAT3 binding sites are often preferentially upregulated in immune and cancer cells in the tumour microenvironment over genes containing only NF- κ B binding sites. Gene or protein upregulation is shown by red upward arrows, while downregulated gene or protein expression is shown as green downward arrows. *Table adapted from supplementary Tables 3 and 4 from Lee et al. (2011)³⁵.*

| Gene Target | Gene Symbol | NF- κ B Binding site | STAT3 Binding site | STAT3-dependent gene expression | Effect of garlic OSCs on LPS-induced gene and/or protein expression | | | |
|---------------------------------|-------------------|-----------------------------|--------------------|---------------------------------|---|---------------------------|-----------------------|---------------------------|
| | | | | | Allicin | | Z-ajoene | |
| | | | | | Gene expression (4 h) | Protein Expression (24 h) | Gene Expression (4 h) | Protein Expression (24 h) |
| Chemokine C-C motif Ligand 2 | <i>Ccl2</i> | Yes | Yes | ↑ | Not detected | No change | Not detected | ↓ |
| Cyclooxygenase 2 | <i>Cox2/Ptgs2</i> | Yes | Yes | ↑ | ↑ | ↑ | ↑ | ↑ |
| Chemokine C-X-C motif Ligand 2 | <i>Cxcl2</i> | Yes | Yes | ↑ | ↑ | ↑ | Not detected | ↓ |
| Intercellular Adhesion Molecule | <i>Icam1</i> | Yes | Yes | ↑ | Not measured | No change | Not measured | ↓ |
| Interleukin-1 β | <i>Il1b</i> | Yes | Yes | ↑ | No change | ↓ | ↓ | ↓ |
| Interleukin-6 | <i>Il6</i> | Yes | Yes | ↑ | ↑ | ↓ | No change | ↓ (trend) |
| Nitric Oxide Synthase 2 | <i>Nos2</i> | Yes | Yes | ↑ | ↑ (trend) | Not measured | ↓ (trend) | Not measured |
| E-selectin | <i>Sele</i> | Yes | Yes | ↑ | ↑ | Not measured | Not detected | Not measured |
| Chemokine C-C motif Ligand 5 | <i>Ccl5</i> | Yes | Not reported | ↓ | ↑ (trend) | ↓ | Not detected | ↓ |
| Chemokine C-X-C motif Ligand 10 | <i>Cxcl10</i> | Yes | Not reported | ↓ | ↑ | ↓ (trend) | Not detected | ↓ |
| Interferon- γ | <i>Ifng</i> | Yes | Not reported | ↓ | Not detected | No change | Not detected | ↓ (trend) |

Based on the decreased STAT3 phosphorylation and decreased gene and protein expression levels of many of the gene targets listed in Table 4.1, we hypothesised that Z-ajoene may downregulate LPS-induced STAT3 phosphorylation by directly interacting with STAT3 cysteines via a thiol-disulfide exchange reaction analogous to S-glutathionylation. Significantly, Xie *et al.* (2009) showed that STAT3 is susceptible to S-glutathionylation, and this is associated with decreased Tyr705 phosphorylation, loss of STAT3 nuclear accumulation and the impaired expression of STAT3 target genes¹⁶¹. In addition, the alkylating agent National Cancer Institute (NCI) compound NSC-368262 (C48) was shown to interact with Cys468 of STAT3¹⁸⁸, while Stattic (an irreversible STAT3 inhibitor) alkylates STAT3 cysteines 251, 259, 367 and 426²⁰². In addition, a recent study by Sobotta *et al.* (2015) showed that STAT3 cysteines in the DNA-binding domain (DBD) and the trans-activating domain (TAD) are targets of peroxiredoxin-2-mediated oxidation, which results in the formation of mixed disulfide bridges between STAT3 oligomers and attenuates the transcriptional activity of STAT3²⁰³. Figure 4.1 shows the relative positions of the 14 cysteines in full length human STAT3. It is important to note that the STAT3 amino acid sequence is highly conserved between *Mus musculus* and *Homo sapiens*, only differing in one amino acid (a Glu760 in the human sequence is substituted for Asp760 in the mouse sequence)²⁰⁴, allowing for direct comparison between human and mouse STAT3. As shown in these papers, alkylation of cysteines in the TAD can affect STAT3 phosphorylation, dimerization and nuclear translocation, while alkylation of cysteines in the DBD can affect STAT3 DNA binding and hence transcriptional activity^{188,202}. In addition, the modification of STAT3 by C48 and Stattic has been shown to induce apoptosis in tumour cells^{188,205,206}.

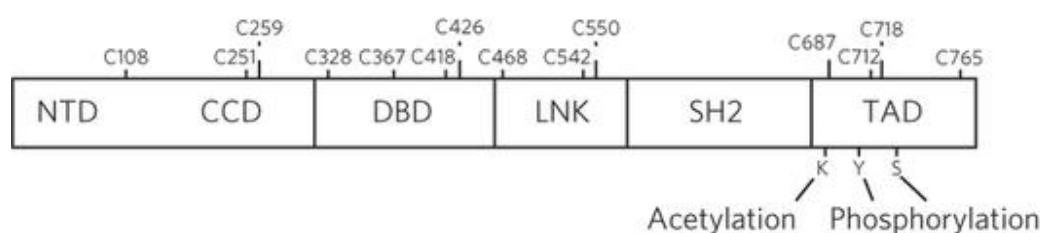


Figure 4.1: The relative position of the 14 cysteine residues with respect to the structural domains in full length human STAT3. NTD, N-terminal domain; CCD, coiled-coil domain; DBD, DNA-binding domain; LNK, linker domain; SH2, SH2-binding domain; TAD, trans-activating domain. Reproduced with permission from Sobotta *et al.* (2015)²⁰³.

In this thesis we found that *E/Z*-ajoene does indeed reversibly alkylate STAT3 *in vitro* (Figure 3.22). This is the first report that a garlic OSC directly interacts with and modify STAT3. While we did not test whether *E/Z*-ajoene-mediated alkylation influences STAT3 transcriptional activity directly, the decrease in LPS-induced STAT3 phosphorylation (Figure 3.19B and 3.20), and the decreased

expression of LPS-induced STAT3 target genes (Table 4.1) by Z-ajoene treatment, suggests that STAT3 activity is affected. We did not test whether STAT3 is alkylated by allicin, but the more pro-inflammatory effects seen on LPS-induced gene expression of STAT3 targets after 4 h, and the short peak in STAT3 phosphorylation occurring at 6 h, suggests that allicin rather facilitates LPS-induced STAT3 phosphorylation and transcriptional activity at early timepoints. Therefore, if both allicin and Z-ajoene alkylate STAT3, the cysteine targets are not likely to be the same.

Future work should determine whether allicin alkylates STAT3 and if so, the STAT3 cysteine targets for allicin and Z-ajoene should be identified by proteomic analysis. In addition, *E/Z*-ajoene alkylation of STAT3 and the resulting effects on STAT3 activity must be confirmed in cell culture and *in vivo*. Possible experimental approaches include the use of immunofluorescence imaging-labelling to determine whether *E/Z*-ajoene affects STAT3 nuclear translocation, and the use of STAT3 reporter constructs to determine the effect of *E/Z*-ajoene alkylation of STAT3 on transcriptional activity. As STAT3 and NF- κ B have been shown to directly interact and this interaction regulates the transcription profile in inflammation and cancer³⁵, it would also be of interest to determine whether NF- κ B is alkylated by garlic OSCs, especially because there are a number of reports in the literature which show that NF- κ B subunits are targets of *S*-glutathionylation^{158,160}. Further, if both STAT3 and NF- κ B are targets of garlic OSC alkylation it would be interesting to ascertain whether alkylation of these transcription factors can modulate transcription factor interactions and transcriptional activity.

4.4. Potential garlic OSC-target proteins in inflammatory signalling pathways

In this thesis we hypothesised that garlic OSCs reversibly alkylate redox-sensitive cysteine thiols in proteins, which are also targets of *S*-glutathionylation. We found that STAT3, a known target of *S*-glutathionylation, can be reversibly alkylated by *E/Z*-ajoene. In addition, Western blot analysis of STAT3 phosphorylation and gene and protein expression analyses suggest that this alkylation may affect the LPS-induced expression of STAT3 target genes. There are, however, many signalling proteins and transcription factors involved in inflammatory signalling pathways that are known targets of *S*-glutathionylation. Figure 4.2 summarises the literature reporting the effects of garlic OSC or garlic extract treatment on inflammatory signalling pathways (taken from Table 1.3). In order to identify potential garlic OSC targets, the Database of Cysteine *S*-glutathionylation (dbGSH) (<http://csb.cse.yzu.edu.tw/dbGSH/index.php>)²⁰⁷ was used to identify signalling proteins and transcription factors susceptible to *S*-glutathionylation (shown in blue in Figure 4.2). Based on Figure 4.2, it is clear that garlic OSCs affect many aspects of inflammatory signalling pathways, and that many proteins involved in these pathways are targets of *S*-glutathionylation. We hypothesise that garlic

OSCs exert these effects by alkylating these S-glutathionylation target proteins. Future work should focus on determining whether these proteins are indeed garlic OSC targets and whether alkylation by garlic OSCs affects protein function and thereby inflammatory signalling.

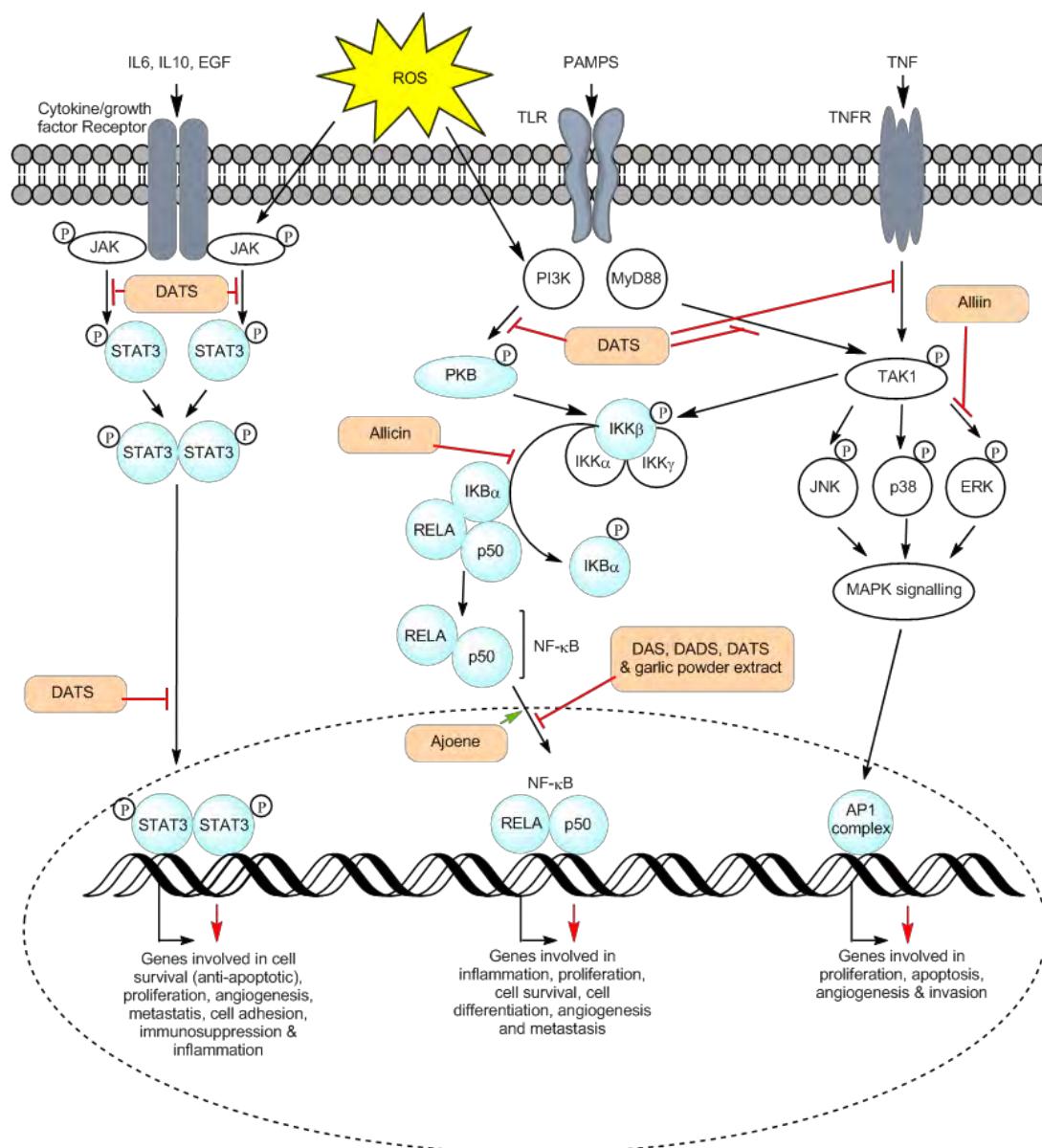


Figure 4.2: Visual representation of the effects of garlic OSC or garlic extract treatment on inflammatory signalling pathways and transcription factors based on the literature collated in Table 1.3. As redox sensitive cysteines are known to be targets of S-glutathionylation, The Database of Cysteine S-glutathionylation (dbGSH) (<http://csb.cse.yzu.edu.tw/dbGSH/index.php>) was used to identify signalling proteins depicted in Figure 1.5. Proteins susceptible to S-glutathionylation, and therefore likely targets of garlic OSCs, are shown in blue. The red arrows above the description of the transcription factor gene targets indicate the overall downregulatory effect of the garlic OSCs on these signalling pathways. Note that the NF-κB signalling pathway is representative of both canonical and non-canonical NF-κB signalling. Protein symbols can be found in the list of Abbreviations and Symbols.

Conclusion

In this study we established a well-defined *in vitro* inflammatory model in cultured murine RAW264.7 macrophage cells in order to measure the effects of the pure garlic OSCs allicin and Z-ajoene on the LPS-induced inflammatory response. We found that allicin had a short-lived pro-inflammatory-effect, initially upregulating LPS-induced *IL6* gene expression, while *IL6* protein was significantly downregulated by allicin treatment after 24 h. Allicin also upregulated the LPS-induced gene and protein expression of the anti-inflammatory cytokine *IL10*. Z-ajoene, on the other hand, was found to have longer-lasting anti-inflammatory effect on LPS-induced gene and protein expression as it downregulated the expression of *IL1b*/IL1B as well as eight chemokines affected by LPS treatment. Preliminary gene array experiments also showed that these garlic OSCs modulated the gene expression of a number of TNF ligand superfamily members, an observation that has not been previously reported in the literature.

We also investigated the effect of allicin and Z-ajoene on the LPS-induced phosphorylation, and hence activation, of the transcription factor STAT3. While allicin facilitated and caused a spike in STAT3 phosphorylation at 6 h, Z-ajoene was found to downregulate STAT3 phosphorylation between 6 and 24 h. In addition, using a cell-free system, we showed that *E/Z*-ajoene reversibly alkylated recombinant STAT3 protein. This is the first report of a garlic OSC directly interacting with the STAT3 protein and coincides with the observed downregulation of LPS-induced STAT3 target genes by Z-ajoene. Future work will focus on whether this interaction occurs *in vivo* and if *E/Z*-ajoene-mediated alkylation affects STAT3 activity as suggested by the observed decrease in the LPS-induced expression of STAT3 target genes and STAT3 phosphorylation.

Together, these observations suggest that the garlic OSCs allicin and Z-ajoene differentially modulate inflammatory gene and protein expression; where allicin has a short-lived pro-inflammatory effect and Z-ajoene has a longer-lasting anti-inflammatory effect. These effects may be a result of garlic OSC interactions with the transcription factor STAT3. Our findings therefore support the use of dietary garlic containing Z-ajoene and allicin as an immunomodulatory agent which may have implications in the prevention of inflammatory diseases.

Appendix A Reagent Recipes

| | |
|------------------------------------|---|
| Lidocaine/EDTA | 10 mM lidocaine HCl (Sigma-Aldrich) and 10 mM EDTA in 1x PBS, pH8 |
| MTT Reagent | 5mg/ml MTT (3-[4,5-dimethylthiazol-2-yl]-2,5-diphenyltetrazolium bromide, Cat. No. M2128, Sigma-Aldrich) in 1x PBS, pH7.4 |
| Solubilisation Reagent | 10 % w/v sodium dodecyl sulfate, 0.01M HCl |
| 3 % Agarose gel | 3 % w/v agarose in 1x TAE buffer |
| 10x Tris-acetate-EDTA (TAE) Buffer | 0.4M Tris, 0.04M acetate, 0.01M EDTA |
| ELISA Wash Buffer 1 | 1x PBS (pH7.4), 0.5 % v/v Tween-20 |
| ELISA Wash Buffer 2 | 1x PBS (pH7.4), 0.1 % v/v Tween-20 |
| 3 % SDS-PAGE Stacking Gel | 0.05 % (w/v) ammonium persulfate; 0.1 % (w/v) SDS, 0.2 % (v/v) N,N,N',N'-tetramethylethylenediamine; 3 % (v/v) Acrylamide/bis-acrylamide; 125 mM Tris, pH6.8 |
| 10 % SDS-PAGE Resolving Gel | 0.05 % (w/v) ammonium persulfate; 0.1 % (w/v) SDS; 0.1 % (v/v) N,N,N',N'-tetramethylethylenediamine; 10 % (v/v) Acrylamide/bis-acrylamide (Bio-Rad); 375 mM Tris, pH8.8 |
| 10x SDS-PAGE Running Buffer | 0.1 % (w/v) SDS; 25 mM Tris; 90 mM glycine |
| 10x SDS-PAGE Transfer Buffer | 25 mM Tris; 90 mM glycine; 20 % (v/v) methanol (added immediately before use) |
| Ponceau Stain | 0.1 % (w/v) Ponceau-S Sodium Salt; 5 % (v/v) acetic acid |

10x Phosphate-Buffered Saline (PBS) 1.37M NaCl; 14 mM KH_2PO_4 ; 27 mM KCl; 43 mM Na_2HPO_4

10x Tris-Buffered Saline (TBS) 0.2M Tris, 5M NaCl, pH7.4

Appendix B Literature Review Supplementary Tables

Supplementary Table B1: A summary of the literature reporting the effects of garlic OSC and garlic extract treatment on cell proliferation and apoptosis. All abbreviations and symbols used in this table can be found in the list of Abbreviations and Symbols.

| Functional Component | Concentration | Experimental System | Reported effect | Ref |
|----------------------|---|--|---|-----|
| <i>E/Z</i> -ajoene | 5-40 μ M | Human promyeloleukemic cells | Apoptosis induced by stimulated NF- κ B activation and peroxide production. | 99 |
| Garlic extract | 10-1000 μ g/ml | Placenta and pre-eclampsic placenta explants | Anti-inflammatory effect but no change in apoptotic rate. Increased soluble <i>TRAIL</i> at 1000 μ g/ml. | 86 |
| DATS | 20-40 μ M | <i>IL6</i> -stimulated DU145 and LNCaP prostate cancer cells | Inhibition of STAT3 phosphorylation resulted in apoptosis. | 150 |
| <i>Z</i> -ajoene | <i>In vitro</i> : 1-80 μ M <i>In vivo</i> : 2-8 mg/kg/day x 12 days | <i>In vitro</i> : Cancer cell lines; MCF-7, HL60, HeLa, Bel-7402, HCT, BGC-823 and normal marsupial kidney (PtK2) cells <i>In vivo</i> : Kunming mice implanted with hepatocarcinoma 22 & sarcoma 180 cells | <i>In vitro</i> : Increased cytotoxicity seen in cancer cells as opposed to normal cells. Induced microtubule network disassembly associated with G2/M cell cycle arrest. <i>In vivo</i> : Inhibited tumour growth . | 208 |
| DAS, DADS, DATS | 1-100 μ M | Human colon cancer HCT-1 and DLD-1 cells | DATS oxidised β -tubulin cysteines by mixed disulfide bond formation affecting β -tubulin function causing G2/M cell cycle arrest, increased caspase 3 activity and apoptosis. | 127 |
| Allicin | 1-20 μ M | Human gastric carcinoma cells | Increase in mitochondrial Bax and Cytochrome C release. Caspase-independent apoptosis. | 209 |
| Allicin | 1-100 μ M | SiHa and Hela human cervical cancer cells, murine fibrosarcoma cells (L-929) and human colon cancer cells (SW480) | Inhibition of cancer cell growth. Induced formation of apoptosis bodies, DNA fragmentation and activation of caspase-3, -8 and -9. | 125 |
| DATS | <i>In vitro</i> : 0-40 μ M/L <i>In vivo</i> : 40 mg/kg x 5 days per week | <i>In vitro</i> : PC-3 and LNCaP human prostate cancer cells <i>In vivo</i> : Orthotopically implanted PC-3 cells in nude BALB/c mice | Enhanced apoptosis-inducing potential of <i>TRAIL</i> . <i>In vitro</i> : Increased expression of death receptors and pro-apoptotic <i>BCL2</i> proteins. Inhibited expression of anti-apoptotic <i>BCL2</i> proteins. Inhibited cell proliferation and induced apoptosis by inducing caspase-3 and -9. <i>In vivo</i> : Inhibited tumour cell proliferation, angiogenesis and metastasis and induced apoptosis. | 124 |
| Allicin | 1-100 ng/ml | B16 melanoma cells & thioglycolate-induced murine peritoneal macrophages | Increased tumouricidal activity of macrophages against B16 melanoma cells. | 132 |

Supplementary Table B2: A summary of the literature reporting the effects of garlic OSC and garlic extract treatment on antioxidant enzymes. All abbreviations and symbols used in this table can be found in the list of Abbreviations and Symbols.

| Functional Component | Concentration | Experimental System | Reported effect | Ref |
|-----------------------|---|--|--|-----|
| E/Z-ajoene | 5-40 µM | Human promyeloleukemic cells | Apoptosis induced by increased peroxide production and NF-κB activation. | 99 |
| AGE, S-allyl cysteine | 0.1-5g/L, 0.1-20 mmol/L | Oxidative-LDL induced injury of epithelial cells | Prevention of membrane damage, lipid peroxidation and cell viability via prevention of GSH depletion. | 210 |
| DADS | 100mg/kg | Ethanol-induced gastric ulceration in Sprague-Dawley rats | Increased GR, GPX and CAT enzyme activity. | 149 |
| DAS | 15 µM | TNF- or histamine-stimulated A7r5 aortic smooth rat muscle cells | Decreased ROS and ROS-induced signalling by activating the antioxidant NRF2 transcription factor and increasing the expression antioxidant enzymes. | 142 |
| DAS, DADS, DATS | 100 µM/kg/day x 14 days | CCl ₄ -induced liver injury in rats | DATS reduced Liver injury by suppressing LDH and AST enzyme activity. DADS and DATS increased antioxidant enzyme activity of GST and QR. | 211 |
| DATS | 100-200 µM | LPS-stimulated RAW264.7 macrophages | Stimulated expression of HO1& NQO1. | 139 |
| AGE | 100-200mg/kg | Indomethacin-induced gastric inflammation in male albino rats | Increased GSH levels and SOD and CAT enzyme activity. | 212 |
| DAS | 150mg/kg x 6 days | Gentamicin-induced nephrotoxicity in Wistar rats | Prevented gentamicin-induced decrease in antioxidant enzymes SOD, GPx, CAT, NQO1, GST and GR via activation of NRF2. Prevented LPS-induced lipid peroxidation and kidney damage. | 95 |
| Garlic powder, DADS | 5% garlic powder- or 3.4 mmol/kg DADS-supplemented diet x 14 days | Male Wistar rats | Increased levels and activity of CYP1A2. Increased activity of GST and UDP and decreased activity of CYP2E1. | 213 |
| Garlic Powder | 0-5% garlic powder-supplemented diet x 8 weeks | Diethylnitrosamine (DEN)-stimulated hepatocellular carcinoma in male Sprague-Dawley rats | Decreased activity expression levels of CYP2E1. Decreased GST foci (a marker for DEN-induced lesions). | 214 |

Appendix C MIQE Guidelines Checklist and qPCR Optimisation and Quality Control

Supplementary Table C1: A checklist for the Minimum Information for Publication of Quantitative Real-Time PCR Experiments (MIQE) guidelines¹⁶⁸. The listed items are designated as either E, essential or D, desirable.

| ITEM TO CHECK | IMPORTANCE | CHECKLIST | COMMENTS |
|--|------------|-----------|--|
| EXPERIMENTAL DESIGN | | | |
| Definition of experimental and control groups | E | YES | Section 2.5, Table 2.1 |
| Number within each group | E | YES | Section 2.5 |
| Assay carried out by core lab or investigator's lab? | D | YES | Core lab |
| Acknowledgement of authors' contributions | D | YES | All experiments performed by author |
| SAMPLE | | | |
| Description | E | YES | Section 2.5 |
| Volume/mass of sample processed | D | YES | 4 x 10 ⁵ cells plated and cultured for 52 h |
| Microdissection or macrodissection | E | N/A | Not tissue (N/A) |
| Processing procedure | E | N/A | |
| If frozen - how and how quickly? | E | N/A | |
| If fixed - with what, how quickly? | E | N/A | |
| Sample storage conditions and duration | E | YES | RNA samples stored at -80°C |
| NUCLEIC ACID EXTRACTION | | | |
| Procedure and/or instrumentation | E | YES | Section 2.7.1 |
| Name of kit and details of any modifications | E | YES | GeneJET™ RNA Purification kit (Thermo Scientific) |
| Source of additional reagents used | D | YES | Section 2.7.1 |
| Details of DNase or RNase treatment | E | YES | Section 2.7.2 |
| Contamination assessment (DNA or RNA) | E | YES | RT-negative control |
| Nucleic acid quantification | E | YES | Section 2.7.1-2.7.3 |
| Instrument and method | E | YES | Section 2.7.1 |
| Purity (A260/A280) | D | YES | 2.7.3 |
| Yield | D | YES | Section 2.7.1-2.7.3 |
| RNA integrity method/instrument | E | YES | Section 2.7.4 |
| RIN/RQI or Cq of 3' and 5' transcripts | E | YES | Section 2.7.4 |
| Electrophoresis traces | D | NO | |
| Inhibition testing (Cq dilutions, spike or other) | E | YES | Serial dilution |
| REVERSE TRANSCRIPTION | | | |
| Complete reaction conditions | E | YES | Section 2.7.5 |
| Amount of RNA and reaction volume | E | YES | Section 2.7.5 |

| | | | |
|---|---|-----|--|
| Priming oligonucleotide (if using GSP) and concentration | E | NO | Section 2.7.5 |
| Reverse transcriptase and concentration | E | YES | Section 2.7.5 |
| Temperature and time | E | YES | Section 2.7.5 |
| Manufacturer of reagents and catalogue numbers | D | YES | Section 2.7.5 |
| Cqs with and without RT | D | YES | RT negative control |
| Storage conditions of cDNA | D | YES | Section 2.7.5 |
| qPCR TARGET INFORMATION | | | |
| If multiplex, efficiency and LOD of each assay. | E | N/A | Not multiplex |
| Sequence accession number | E | YES | Table 2.2 |
| Location of amplicon | D | YES | Supplementary Table C2, Appendix C |
| Amplicon length | E | YES | Table 2.2 |
| <i>In silico</i> specificity screen (BLAST, etc.) | E | YES | NCBI BLAST, Supplementary Table C2, Appendix C |
| Pseudogenes, retropseudogenes or other homologs? | D | NO | |
| Sequence alignment | D | YES | Supplementary Table C2, Appendix |
| Secondary structure analysis of amplicon | D | YES | Maximum Tm of secondary structures, Supplementary Table C2, Appendix C |
| Location of each primer by exon or intron (if applicable) | E | YES | Supplementary Table C2, Appendix C |
| What splice variants are targeted? | E | Y | Supplementary Table C2, Appendix C |
| qPCR OLIGONUCLEOTIDES | | | |
| Primer sequences | E | YES | Table 2.2 |
| RTPrimerDB Identification Number | D | YES | Table 2.2 |
| Probe sequences | D | N/A | No probes used |
| Location and identity of any modifications | E | N/A | No modifications |
| Manufacturer of oligonucleotides | D | YES | Section 2.7.6.1 |
| Purification method | D | YES | Direct precipitation with butanol |
| qPCR PROTOCOL | | | |
| Complete reaction conditions | E | YES | Table 2.3, Section 2.7.6.3 |
| Reaction volume and amount of cDNA/DNA | E | YES | Section 2.7.6.3 |
| Primer, (probe), Mg++ and dNTP concentrations | E | YES | Section 2.7.6.3 |

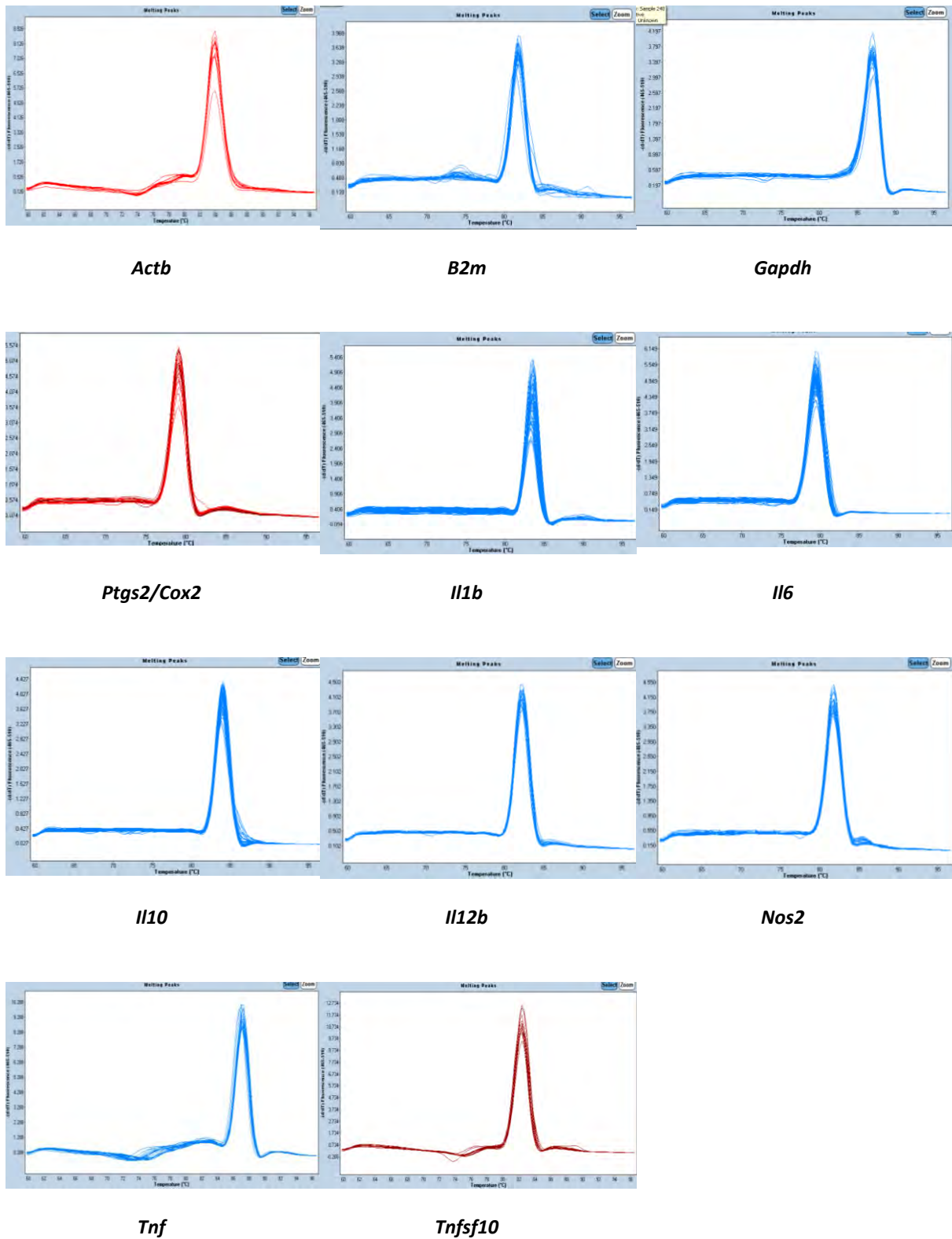
| | | | |
|--|---|-----|---|
| Polymerase identity and concentration | E | YES | SensiMix™ SYBR®-No-ROX Kit (BioLine), hot-start DNA polymerase |
| Buffer/kit identity and manufacturer | E | YES | SensiMix™ SYBR®-No-ROX Kit (BioLine) |
| Exact chemical constitution of the buffer | D | NO | Information not provided by kit |
| Additives (SYBR Green I, DMSO, etc.) | E | YES | No additives were used |
| Manufacturer of plates/tubes and catalogue number | D | YES | White LightCycler® 480 Multi well Plate 384 (Cat. No. 04 729 749 001, Roche) & 96 (Cat. No. 04 729 692 001, Roche) & Hard-Shell® 96-Well PCR Plates (Cat. No. HSP9655, Bio-Rad Laboratories, Inc) |
| Complete thermocycling parameters | E | YES | Table 2.3, Section 2.7.6.3 |
| Reaction setup (manual/robotic) | D | YES | Manual |
| Manufacturer of qPCR instrument | E | YES | Roche LightCycler® 480II |
| qPCR VALIDATION | | | |
| Evidence of optimisation (from gradients) | D | YES | Optimised for specificity based on annealing temperature gradients, Supplementary Figure 3C, Appendix C |
| Specificity (gel, sequence, melt, or digest) | E | YES | Supplementary Figure 3A and B, Appendix C |
| For SYBR Green I, Cq of the NTC | E | YES | NTC is >5 cycles from experimental samples |
| Standard curves with slope and y-intercept | E | YES | Performed, amplification efficiency reported Supplementary Table C2 |
| PCR efficiency calculated from slope | E | YES | Supplementary Table C2 |
| Confidence interval for PCR efficiency or standard error | D | NO | |
| r2 of standard curve | E | NO | Performed but not reported |
| Linear dynamic range | E | NO | Performed but not reported |
| Cq variation at lower limit | E | NO | |
| Confidence intervals throughout range | D | NO | |
| Evidence for limit of detection | E | NO | |
| If multiplex, efficiency and LOD of each assay. | E | N/A | |
| DATA ANALYSIS | | | |
| qPCR analysis program (source, version) | E | YES | Biogazelle qbase+ version 2.6.1 |
| Cq method determination | E | YES | Target and run specific amplification efficiency standards curves were determined using qBase plus software |

| | | | |
|---|---|-----|---|
| Outlier identification and disposition | E | YES | Cq value cut-off 0.5 difference between samples |
| Results of NTCs | E | YES | NTC is >5 cycles from experimental samples |
| Justification of number and choice of reference genes | E | YES | Section 2.7.6.6 |
| Description of normalisation method | E | YES | Section 2.7.6.6 |
| Number and concordance of biological replicates | D | YES | 3 biological repeats with 2 technical repeats performed for each sample |
| Number and stage (RT or qPCR) of technical replicates | E | YES | 2 qPCR technical repeats |
| Repeatability (intra-assay variation) | E | NO | |
| Reproducibility (inter-assay variation, %CV) | D | NO | |
| Power analysis | D | NO | |
| Statistical methods for result significance | E | YES | Section 2.12, 1-way ANOVA, Tukey's HSD test |
| Software (source, version) | E | YES | GraphPad Prism 5.00 (GraphPad Software, http://www.graphpad.com) |
| Cq or raw data submission using RDML | D | NO | |

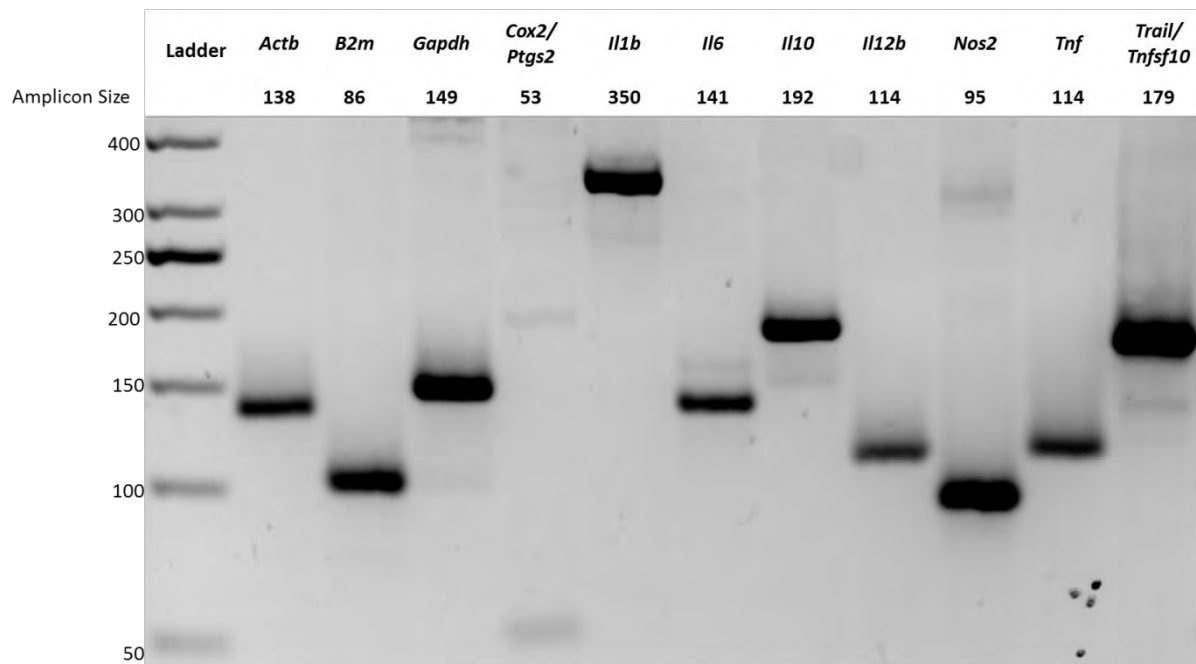
Supplementary Table C2: Primer oligonucleotide design supplementary information to Table 2.2. Primer amplification efficiency was determined by qBase plus software (Biogazelle) using a standard curve obtained from a serial dilution of pooled cDNA. *In silico* analysis of primer melting temperature (T_m); the maximum T_m of the amplicon secondary structure and the Gibbs Free energy (Delta G kcal/mol) for the homo- and heterodimers was obtained using the OligoAnalyzer 3.1 software (Integrated DNA Technologies, Inc). The spontaneity of the oligonucleotide binding to its perfect complement was always -30 kcal/mol more spontaneous than any other structure. Analysis of primer exon location and amplicon position on the coding sequence was determined using the RTPrimerDB *In silico* analysis tool. *In silico* NCBI Primer BLASTs were performed to verify primer targets and transcript variants.

| Gene Symbol | Primer amplification efficiency | Exon /s | Primer Tm | Max Tm Amplicon secondary structure | Amplicon position on coding sequence | Primer Blast Results | Transcript variants recognised | Perfect Complement Max kcal/mol | Most spontaneous homodimer kcal/mol | Difference: Perfect complement - homodimer | Perfect complement Max kcal/mol | Most spontaneous heterodimer kcal/mol | Difference: Perfect complement – heterodimer kcal/mol |
|-------------|---------------------------------|---|-----------|-------------------------------------|--------------------------------------|----------------------|--------------------------------|---------------------------------|-------------------------------------|--|---------------------------------|---------------------------------------|---|
| Actb | 100.5 | 3 | 67.1 | 50.1 | 692-830 | NM_007 | | -39.29 | -3.61 | -36 | -40 | -4.67 | -35.33 |
| | | 3 | 66.9 | 393.3 | | -40 | | -9.28 | -31 | | | | |
| B2m | 199.5 | 2 | 67.7 | 53.3 | 338-403 | NM_009 | | -38.63 | -3.53 | -35 | -38.63 | -4.89 | -33.74 |
| | | 2 & 3 | 65.6 | 735.3 | | -37.52 | | -6.76 | -31 | | | | |
| Gapdh | 102.2 | 4 | 68.7 | 48.3 | 756-905 | NM_001289726.1 | Transcript variant 1 | -42.41 | -5.02 | -37 | -42.41 | -4.87 | -37.54 |
| | | 5 | 67.6 | NM_008084.3 | | -41.05 | | -5.24 | -36 | | | | |
| Ptgs2/Cox2 | 106.6 | 5 | 67.4 | 38.8 | 663 - 716 | NM_011 | | -39.45 | -3.14 | -36 | -39.52 | -4.74 | -34.78 |
| | | 5 | 67.7 | 198.3 | | -39.52 | | -4.67 | -35 | | | | |
| Il1b | 99.1 | 3 | 66.5 | Too long for analysis | 248 - 597 | XM_006498795.1 | Transcript variant X1 | -36.85 | -3.14 | -34 | -38.89 | -6.21 | -32.68 |
| | | 5 | 65.3 | | | NM_008361.3 | | -38.89 | -9.28 | -30 | | | |
| Il6 | 106.3 | 2 | 67.9 | 40.6 | 139 - 280 | NM_031 | | -42.05 | -4.64 | -37 | -42.05 | -5.24 | -36.81 |
| | | 3 | 65.8 | 168.1 | | -41.38 | | -7.05 | -34 | | | | |
| Il10 | 102.9 | 3 | 67.4 | 48.1 | 308 - 500 | NM_010 | | -42.03 | -3.9 | -38 | -42.03 | -5.05 | -36.98 |
| | | 4 | 71.3 | 548.2 | | -40.64 | | -3.14 | -38 | | | | |
| Il12b | 107.5 | Purchased from Qiagen Cat. No. 330001 PPM03020E | | | | | | | | | | | |
| Nos2 | 107..8 | 16 | 67.6 | 50.5 | 2174 - 2269 | NM_010927.3 | | -40.52 | -10.24 | -30 | -41.1 | -5.23 | -35.87 |
| | | 17 | 64.8 | XM_006532440.1 | | -41.1 | | -3.61 | -37 | | | | |
| Tnf | 106.2 | 3 | 64.8 | 49.9 | 408 - 522 | NM_013 | Transcript variant 1 | -41.04 | -6.76 | -34 | -41.04 | -6.21 | -34.83 |
| | | 4 | 65.9 | 693.3 | | -37.52 | | -6.21 | -31 | | | | |
| | 91.6 | 2 | 65 | 51 | 296 - 475 | | | -36.73 | -3.55 | -33 | -38.44 | -3.55 | -34.89 |

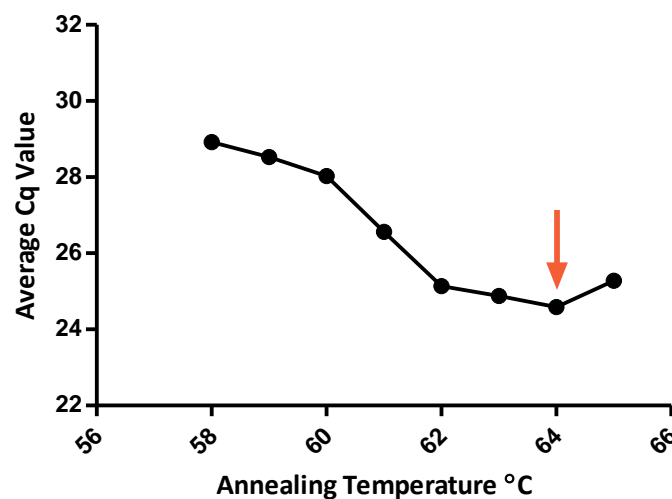
| | | | | | | |
|---------------------------------|---|------|-----------------|--------|-------|-----|
| <i>Tnfsf10/</i> <i>Trail</i> | 4 | 64.7 | NM_009 425.2 | -38.44 | -4.62 | -34 |
|---------------------------------|---|------|-----------------|--------|-------|-----|



Supplementary Figure C1: Confirmation of primer oligonucleotide specificity determined by qPCR melt-curve analysis. Melt curve analysis was performed after every qPCR run using default settings on the Roche LightCycler 480II thermal cycler. A single peak is indicative of a single amplicon product. All gene symbols are listed in the Abbreviations and Symbols section.



Supplementary Figure C2: Confirmation of primer oligonucleotide specificity analysed by agarose gel electrophoresis. In order to verify primer oligonucleotide specificity, qPCR samples and 5 µl O'GeneRuler 50bp DNA Ladder (Thermo Scientific) were loaded onto a 3% agarose gel and subjected to gel electrophoresis in 1x TBE for 2 h at 100 V to separate products by size. The expected amplicon sizes listed correspond with the band size. As these samples were used for qPCR analysis and subjected to 45 thermal cycles and melt curve analysis, we expect some product degradation. All gene symbols are listed in the Abbreviations and Symbols section.



Supplementary Figure C3: Optimisation of qPCR annealing temperature. A temperature gradient qPCR was performed using the CFX96 Touch™ Real-Time PCR System (Bio-Rad Laboratories, Inc) gradient PCR thermal cycler, with the following reaction conditions; 95°C for 10 min, 45 cycles of (95°C for 30 s, gradient annealing temperature (58-65°C) for 30 s, 72°C for 90 s (extension and fluorescence acquisition)), followed by melt curve analysis. The mean Cq value was determined by averaging the Cq values determined for all target genes including; *Actb*, *B2m*, *Gapdh*, *Il1b*, *Il6*, *Il10*, *Tnf*, *Trail/Tnfsf10*, *Cox2/Ptgs2* and *Nos2*. The optimal annealing temperature is defined as the temperature that yields the lowest average Cq value, which is 64°C (highlighted by the red arrow).

References

1. Hanahan, D. & Weinberg, R. A. The Hallmarks of Cancer. *Cell* **100**, 57–70 (2000).
2. Hanahan, D. & Weinberg, R. A. Hallmarks of Cancer : The Next Generation. *Cell* **144**, 646–674 (2011).
3. Cancer: Factsheet number 297. *World Health Organization* (2013). at <<http://www.who.int/mediacentre/factsheets/fs297/en/#>>
4. World Health Organisation: Global Action Against Cancer. (2013). at <http://www.who.int/cancer/publications/action_against_cancer/en/>
5. Ngoma, T. World Health Organization cancer priorities in developing countries. *Ann. Oncol.* **17**, viii9–viii14 (2006).
6. Anand, P. *et al.* Cancer is a preventable disease that requires major lifestyle changes. *Pharm. Res.* **25**, 2097–2116 (2008).
7. Murphy, K. in *Janeway's Immunobiology* 1–75 (Garland Science, 2012). at <<http://www.ncbi.nlm.nih.gov/books/NBK27090/>>
8. Male, D. in *Immunology: An Illustrated Outline* (eds. Toledo, M., Lucas, G. & Goatley, B.) 52–107 (Garland Science, 2014).
9. Male, D. in *Immunology* (eds. Ozols, I. & Cook, L.) 127–145 (Elsevier Ltd, 2006).
10. Baniyash, M. Chronic inflammation , immunosuppression and cancer: New insights and outlook. *Semin. Cancer Biol.* **16**, 80–88 (2006).
11. Federico, A., Morgillo, F., Tuccillo, C., Ciardiello, F. & Loguercio, C. Chronic inflammation and oxidative stress in human carcinogenesis. *Int. J. Cancer* **121**, 2381–2386 (2007).
12. Grivennikov, S. I., Greten, F. R. & Karin, M. Immunity, inflammation, and cancer. *Cell* **140**, 883–899 (2010).
13. Qian, B. Z. & Pollard, J. W. Macrophage Diversity Enhances Tumor Progression and Metastasis. *Cell* **141**, 39–51 (2010).
14. Pikarsky, E. & Ben-Neriah, Y. NF-kappaB inhibition: A double-edged sword in cancer? *Eur. J. Cancer* **42**, 779–784 (2006).
15. Dvorak, H. F. Tumors: wounds that do not heal. Similarities between tumor stroma generation and wound healing. *N. Engl. J. Med.* **315**, 1650–1659 (1986).
16. Bingle, L., Brown, N. J. & Lewis, C. E. The role of tumour-associated macrophages in tumour progression: implications for new anticancer therapies. *J. Pathol.* **196**, 254–265 (2002).
17. Wesolowski, R., Markowitz, J. & Carson, W. E. Myeloid derived suppressor cells – a new therapeutic target in the treatment of cancer. *J. Immunother. Cancer* **1**, (2013).

18. Shime, H. *et al.* Toll-like receptor 3 signaling converts tumor-supporting myeloid cells to tumoricidal effectors. *Proc. Natl. Acad. Sci.* **109**, 2066–2071 (2012).
19. Cavaillon, J. M. Pro- versus anti-inflammatory cytokines: myth or reality. *Cell. Mol. Biol.* **47**, 695–702 (2001).
20. Tincani, a, Andreoli, L., Bazzani, C., Bosiso, D. & Sozzani, S. Inflammatory molecules: a target for treatment of systemic autoimmune diseases. *Autoimmun. Rev.* **7**, 1–7 (2007).
21. Neurath, M. F. Cytokines in inflammatory bowel disease. *Nat. Rev. Immunol.* **14**, 329–342 (2014).
22. Waldner, M. J. & Neurath, M. F. Master regulator of intestinal disease: IL-6 in chronic inflammation and cancer development. *Semin. Immunol.* **26**, 75–79 (2014).
23. Berg, D. J. *et al.* Enterocolitis and colon cancer in interleukin-10-deficient mice are associated with aberrant cytokine production and CD4⁺ Th1-like responses. *J. Clin. Invest.* **98**, 1010–1020 (1996).
24. Atreya, R. & Neurath, M. F. Chemokines in inflammatory bowel diseases. *Dig. Dis.* **28**, 386–394 (2010).
25. Biswas, S. K. *et al.* A distinct and unique transcriptional program expressed by A distinct and unique transcriptional program expressed by tumor-associated macrophages (defective NF- κ B and enhanced IRF-3 / STAT1 activation). *Blood* **107**, 2112–2122 (2006).
26. Ricciotti, E. & FitzGerald, G. a. Prostaglandins and inflammation. *Arterioscler. Thromb. Vasc. Biol.* **31**, 986–1000 (2011).
27. Wallace, J. L. Prostaglandins, NSAIDs, and gastric mucosal protection: why doesn't the stomach digest itself? *Physiol. Rev.* **88**, 1547–1565 (2008).
28. Kim, Y. J., Kim, E.-H. & Hahm, K. B. Oxidative stress in inflammation-based gastrointestinal tract diseases: challenges and opportunities. *J. Gastroenterol. Hepatol.* **27**, 1004–1010 (2012).
29. Kim, K. M. *et al.* Differential regulation of NO availability from macrophages and endothelial cells by the garlic component S-allyl cysteine. *Free Radic. Biol. Med.* **30**, 747–756 (2001).
30. Grivennikov, S. I. & Karin, M. Dangerous liaisons: STAT3 and NF- κ B collaboration and crosstalk in cancer. *Cytokine Growth Factor Rev.* **21**, 11–19 (2010).
31. Yu, H., Pardoll, D. & Jove, R. STATs in cancer inflammation and immunity: a leading role for STAT3. *Nat. Rev. Cancer* **9**, 798–809 (2009).
32. Dolcet, X., Llobet, D., Pallares, J. & Matias-guiu, X. NF- κ B in development and progression of human cancer. *Virchows Arch.* **446**, 475–482 (2005).
33. Yu, Z. & Kone, B. C. The STAT3 DNA-binding domain mediates interaction with NF- κ B p65 and iuducible nitric oxide synthase transrepression in mesangial cells. *J. Am. Soc. Nephrol.* **15**, 585–591 (2004).

34. Lee, H. *et al.* Persistently Activated Stat3 Maintains Constitutive NF- κ B Activity in Tumors. *Cancer Cell* **15**, 283–293 (2009).
35. Lee, H. *et al.* A requirement of STAT3 DNA binding precludes Th-1 immunostimulatory gene expression by NF- κ B in tumors. *Cancer Res.* **71**, 3772–3780 (2011).
36. Lam, L. T. *et al.* Cooperative signalling through the signal transducer and activator of transcription 3 and nuclear factor- κ B pathways in subtypes of diffuse large B-cell lymphoma. *Blood* **117**, 1851–1860 (2010).
37. Aggarwal, B. B., Vijayalekshmi, R. V & Sung, B. Targeting inflammatory pathways for prevention and therapy of cancer: short-term friend, long-term foe. *Clin. Cancer Res.* **15**, 425–430 (2009).
38. Karin, M. NF- κ B as a Critical Link Between Inflammation and Cancer. *Cold Spring Harb. Perspect. Biol.* **1**, a000141 (2009).
39. Pikarsky, E. *et al.* NF- κ B functions as a tumour promoter in inflammation-associated cancer. *Nature* **431**, 461–466 (2004).
40. Sen, R. & Baltimore, D. Inducibility of κ immunoglobulin enhancer-binding protein NF- κ B by a posttranslational mechanism. *Cell* **47**, 921–928 (1986).
41. Karin, M. Nuclear factor-kappaB in cancer development and progression. *Nature* **441**, 431–436 (2006).
42. Ghosh, S., May, M. J. & Kopp, E. B. NF- κ B and Rel proteins: evolutionarily conserved mediators of immune responses. *Annu. Rev. Immunol.* **16**, 225–260 (1998).
43. Pahl, H. L. Activators and target genes of Rel/NF- κ B transcription factors. *Oncogene* **18**, 6853–6866 (1999).
44. DiDonato, J. a, Mercurio, F. & Karin, M. NF- κ B and the link between inflammation and cancer. *Immunol. Rev.* **246**, 379–400 (2012).
45. Yu, H., Kortylewski, M. & Pardoll, D. Crosstalk between cancer and immune cells: role of STAT3 in the tumour microenvironment. *Nat. Rev. Immunol.* **7**, 41–51 (2007).
46. Mohr, A. *et al.* Dynamics and non-canonical aspects of JAK/STAT signalling. *Eur. J. Cell Biol.* **91**, 524–532 (2012).
47. Aggarwal, B. B. *et al.* Signal transducer and activator of transcription-3, inflammation, and cancer: how intimate is the relationship?. *Ann. N. Y. Acad. Sci.* **1171**, 59–76 (2009).
48. Dauer, D. J. *et al.* Stat3 regulates genes common to both wound healing and cancer. *Oncogene* **24**, 3397–3408 (2005).
49. Choi, J. H. *et al.* Phospho-Stat3 expression and correlation with VEGF, p53, and Bcl-2 in gastric carcinoma using tissue microarray. *APMIS* **114**, 619–625 (2006).
50. Sinibaldi, D. *et al.* Induction of p21WAF1/CIP1 and cyclin D1 expression by the Src oncoprotein in mouse fibroblasts: role of activated STAT3 signaling. *Oncogene* **19**, 5419–5427 (2000).

51. Braun, D. a, Fribourg, M. & Sealfon, S. C. Cytokine response is determined by duration of receptor and signal transducers and activators of transcription 3 (STAT3) activation. *J. Biol. Chem.* **288**, 2986–2993 (2013).
52. Groner, B. Determinants of the extent and duration of STAT3 signaling. *JAK-STAT* **1**, 211–215 (2012).
53. Grivennikov, S. *et al.* IL-6 and Stat3 Are Required for Survival of Intestinal Epithelial Cells and Development of Colitis-Associated Cancer. *Cancer Cell* **15**, 103–113 (2009).
54. Alonzi, T. *et al.* Induced somatic inactivation of STAT3 in mice triggers the development of a fulminant form of enterocolitis. *Cytokine* **26**, 45–56 (2004).
55. Kühn, R., Löhler, J., Rennick, D., Rajewsky, K. & Müller, W. Interleukin-10-deficient mice develop chronic enterocolitis. *Cell* **75**, 263–274 (1993).
56. Welte, T. *et al.* STAT3 deletion during hematopoiesis causes Crohn’s disease-like pathogenesis and lethality: a critical role of STAT3 in innate immunity. *Proc. Natl. Acad. Sci. U. S. A.* **100**, 1879–1884 (2003).
57. Duchmann, R., Schmitt, E., Knolle, P., Meyer zum Büschenfelde, K. H. & Neurath, M. Tolerance towards resident intestinal flora in mice is abrogated in experimental colitis and restored by treatment with interleukin-10 or antibodies to interleukin-12. *Eur. J. Immunol.* **26**, 934–938 (1996).
58. Yanagawa, H. *et al.* Presence and potent immunosuppressive role of interleukin-10 in malignant pleural effusion due to lung cancer. *Cancer Lett.* **136**, 27–32 (1999).
59. Jarnicki, A., Putoczki, T. & Ernst, M. Stat3: linking inflammation to epithelial cancer - more than a ‘gut’ feeling? *Cell Div.* **5**, (2010).
60. Karin, M., Cao, Y., Greten, F. R. & Li, Z.-W. NF- κ B in cancer: from innocent bystander to major culprit. *Nat. Rev. Cancer* **2**, 301–310 (2002).
61. Shen, C. & Stavnezer, J. Transcription Interaction of Stat6 and NF- κ B: Direct Association and Synergistic Activation of Interleukin-4-Induced Transcription. *Mol. Cell. Biol.* **18**, 3395–3404 (1998).
62. Yu, Z., Zhang, W. & Kone, B. C. Signal transducers and activators of transcription 3 (STAT3) inhibits transcription of the inducible nitric oxide synthase gene by interacting with nuclear factor kappaB. *Biochem. J.* **367**, 97–105 (2002).
63. Niu, G. *et al.* Role of Stat3 in Regulating p53 Expression and Function. *Mol. Cell. Biol.* **25**, 7432–7440 (2005).
64. Greten, F. R. *et al.* IKK β Links Inflammation and Tumorigenesis in a Mouse Model of Colitis-Associated Cancer. *Cell* **118**, 285–296 (2004).
65. Budunova, I. V *et al.* Increased expression of p50-NF-kappaB and constitutive activation of NF-kappaB transcription factors during mouse skin carcinogenesis. *Oncogene* **18**, 7423–7431 (1999).

66. Judd, L. M. *et al.* Inhibition of the JAK2/STAT3 pathway reduces gastric cancer growth in vitro and in vivo. *PLoS One* **9**, e95993 (2014).
67. Fuke, H. *et al.* Jak inhibitor induces S phase cell-cycle arrest and augments TRAIL-induced apoptosis in human hepatocellular carcinoma cells. *Biochem. Biophys. Res. Commun.* **363**, 738–744 (2007).
68. Kusaba, M. *et al.* Abrogation of constitutive STAT3 activity sensitizes human hepatoma cells to TRAIL-mediated apoptosis. *J. Hepatol.* **47**, 546–555 (2007).
69. Wei, D. *et al.* Stat3 activation regulates the expression of vascular endothelial growth factor and human pancreatic cancer angiogenesis and metastasis. *Oncogene* **22**, 319–329 (2003).
70. Kortylewski, M. *et al.* Inhibiting Stat3 signaling in the hematopoietic system elicits multicomponent antitumor immunity. *Nat. Med.* **11**, 1314–1321 (2005).
71. Maeda, S., Kamata, H., Luo, J. L., Leffert, H. & Karin, M. IKK β Couples Hepatocyte Death to Cytokine-Driven Compensatory Proliferation that Promotes Chemical Hepatocarcinogenesis. *Cell* **121**, 977–990 (2005).
72. Van Hogerlinden, M., Rozell, B. L., Ahrlund-Richter, L. & Toftgård, R. Squamous cell carcinomas and increased apoptosis in skin with inhibited Rel/nuclear factor- κ B signaling. *Cancer Res.* **59**, 3299–3303 (1999).
73. Takeda, K. *et al.* Enhanced Th1 Activity and Development of Chronic Enterocolitis in Mice Devoid of Stat3 in Macrophages and Neutrophils. *Immunity* **10**, 39–49 (1999).
74. Ulrich, C. M., Bigler, J. & Potter, J. D. Non-steroidal anti-inflammatory drugs for cancer prevention: promise, perils and pharmacogenetics. *Nat. Rev. Cancer* **6**, 130–140 (2006).
75. Thun, M. J., Henley, S. J. & Patrono, C. Nonsteroidal Anti-inflammatory Drugs as Anticancer Agents: Mechanistic, Pharmacologic, and Clinical Issues. *J. Natl. Cancer Inst.* **94**, 252–266 (2002).
76. Tayal, V. & Kalra, B. S. Cytokines and anti-cytokines as therapeutics--an update. *Eur. J. Pharmacol.* **579**, 1–12 (2008).
77. Liekens, S., Schols, D. & Hatse, S. CXCL12-CXCR4 axis in Angiogenesis, Metastasis and Stem Cell Mobilization. *Curr. Pharm. Des.* **16**, 3903–3920 (2010).
78. Algra, A. M. & Rothwell, P. M. Effects of regular aspirin on long-term cancer incidence and metastasis: a systematic comparison of evidence from observational studies versus randomised trials. *Lancet. Oncol.* **13**, 518–527 (2012).
79. Huang, E. S., Strate, L. L., Ho, W. W., Lee, S. S. & Chan, A. T. Long-term use of aspirin and the risk of gastrointestinal bleeding. *Am. J. Med.* **124**, 426–433 (2011).
80. Silverstein, F. E. *et al.* Gastrointestinal Toxicity With Celecoxib vs Nonsteroidal Anti-Inflammatory Drugs for Osteoarthritis and Rheumatoid Arthritis. *J. Am. Med. Assoc.* **284**, 1247–1255 (2000).

81. Bessone, F. Non-steroidal anti-inflammatory drugs: What is the actual risk of liver damage? *World J. Gastroenterol.* **16**, 5651–5661 (2010).
82. Pan, M.-H., Lai, C.-S., Dushenkov, S. & Ho, C.-T. Modulation of Inflammatory Genes by Natural Dietary Bioactive Compounds. *J. Agric. Food Chem.* **57**, 4467–4477 (2009).
83. Aboelsoud, N. H. Herbal medicine in ancient Egypt. *J. Med. Plants Res.* **4**, 82–86 (2010).
84. Hodge, G., Hodge, S. & Han, P. *Allium sativum* (Garlic) Suppresses Leukocyte Inflammatory Cytokine Production In Vitro: Potential Therapeutic Use in the Treatment of Inflammatory Bowel Disease. *Cytometry* **48**, 209–215 (2002).
85. Keiss, H. *et al.* Garlic (*Allium sativum* L.) Modulates Cytokine Expression in Lipopolysaccharide-Activated Human Blood Thereby Inhibiting NF- κ B Activity. *J. Nutr.* **133**, 2171–2175 (2003).
86. Makris, A., Thornton, C. E., Xu, B. & Hennessy, A. Garlic increases IL-10 and inhibits TNF α and IL-6 production in Endotoxin-stimulated Human Placental Explants. *Placenta* **26**, 828–834 (2005).
87. Cavallito, C. J., Bailey, J. H. & Buck, J. S. The Antibacterial Principle of *Allium sativum*. III. Its Precursor and 'Essential Oil of Garlic'. *J. Am. Chem. Soc.* **67**, 1032–1033 (1945).
88. Kim, J. W., Kim, Y. S. & Kyung, K. H. Inhibitory Activity of Essential Oils of Garlic and Onion against Bacteria and Yeasts. *J. Food Prot.* **67**, 499–504 (2004).
89. Sivam, G. P. Protection against *Helicobacter pylori* and Other Bacterial Infections by Garlic. *J. Nutr.* **131**, 1106–1108 (2001).
90. Lanzotti, V., Barile, E., Antignani, V., Bonanomi, G. & Scala, F. Antifungal saponins from bulbs of garlic, *Allium sativum* L. var. *Voghiera*. *Phytochemistry* **78**, 126–134 (2012).
91. Iwalokun, B. a, Ogunledun, A., Ogbolu, D. O., Bamiro, S. B. & Jimi-Omojola, J. In Vitro Antimicrobial Properties of Aqueous Garlic Extract Against Multidrug-Resistant Bacteria and *Candida* Species from Nigeria. *J. Med. Food* **7**, 327–333 (2004).
92. Tsai, Y. *et al.* Antiviral properties of garlic: in vitro effects on influenza B, herpes simplex and coxsackie viruses. *Planta Med.* **51**, 460–461 (1985).
93. Block, E. *et al.* (E,Z)-Ajoene: a potent antithrombotic agent from garlic. *J. Am. Chem. Soc.* **106**, 8295–8296 (1984).
94. Augusti, K. T. & Mathew, P. T. Lipid lowering effect of allicin (diallyl disulphide-oxide) on long term feeding to normal rats. *Experientia* **30**, 468–470 (1974).
95. Kalayarasan, S. *et al.* Diallyl sulfide enhances antioxidants and inhibits inflammation through the activation of Nrf2 against gentamicin-induced nephrotoxicity in Wistar rats. *Eur. J. Pharmacol.* **606**, 162–171 (2009).
96. El-Bayoumy, K., Sinha, R., Pinto, J. T. & Rivlin, R. S. Cancer Chemoprevention by Garlic and Garlic-Containing Sulfur and Selenium Compounds. *J. Nutr.* **136**, 864S–869S (2006).

97. Shukla, Y. & Kalra, N. Cancer chemoprevention with garlic and its constituents. *Cancer Lett.* **247**, 167–181 (2007).
98. Fleischauer, A. T., Poole, C. & Arab, L. Garlic consumption and cancer prevention: meta-analyses of colorectal and stomach cancers. *Am. J. Clin. Nutr.* **72**, 1047–1052 (2000).
99. Dirsch, V. M., Gerbes, A. L. & Vollmar, A. M. Ajoene, a Compound of Garlic, Induces Apoptosis in Human Promyeloleukemic Cells, Accompanied by Generation of Reactive Oxygen Species and Activation of Nuclear Factor κ B. *Mol. Pharmacol.* **53**, 402–407 (1998).
100. Steinmetz, K. A., Kushi, L. H., Bostick, R. M., Folsom, A. R. & Potter, J. D. Vegetables, Fruit, and Colon Cancer in the Iowa Women's Health Study. *Am. J. Epidemiol.* **160**, 825–841 (1994).
101. Hsing, A. W. *et al.* Allium Vegetables and Risk of Prostate Cancer: A Population-Based Study. *J. Natl. Cancer Inst.* **94**, 1648–1651 (2002).
102. Gao, C. M., Takezaki, T., Ding, J. H., Li, M. S. & Tajima, K. Protective effect of allium vegetables against both esophageal and stomach cancer: a simultaneous case-referent study of a high-epidemic area in Jiangsu Province, China. *Jpn. J. Cancer Res.* **90**, 614–621 (1999).
103. You, W. *et al.* Allium Vegetables and Reduced Risk of Stomach Cancer. *J. Natl. Cancer Inst.* **81**, 162–164 (1989).
104. Kodali, R. T. & Eslick, G. D. Meta-Analysis: Does Garlic Intake Reduce Risk of Gastric Cancer? *Nutr. Cancer* **67**, 1–11 (2015).
105. Zhou, Y. *et al.* Consumption of large amounts of Allium vegetables reduces risk for gastric cancer in a meta-analysis. *Gastroenterology* **141**, 80–89 (2011).
106. Fleischauer, A. T. & Arab, L. Garlic and Cancer: A Critical Review of the Epidemiologic Literature. *J. Nutr.* **131**, 1032–1040 (2001).
107. Kim, J. Y. & Kwon, O. Garlic intake and cancer risk: an analysis using the Food and Drug Administration's evidence-based review system for the scientific evaluation of health claims. *Am. J. Clin. Nutr.* **89**, 257–264 (2009).
108. Ngo, S. N. T., Williams, D. B., Cobiac, L. & Head, R. J. Does Garlic Reduce Risk of Colorectal Cancer? A Systematic Review. *J. Nutirtion* **137**, 2264–2269 (2007).
109. Hu, J.-Y. *et al.* Consumption of garlic and risk of colorectal cancer: an updated meta-analysis of prospective studies. *World J. Gastroenterol.* **20**, 15413–15422 (2014).
110. Zhu, B., Zou, L., Qi, L., Zhong, R. & Miao, X. Allium Vegetables and Garlic Supplements Do Not Reduce Risk of Colorectal Cancer, Based on Meta-analysis of Prospective Studies. *Clin. Gastroenterol. Hepatol.* **12**, 1991–2001 (2014).
111. Dong, Q., Sugiura, T., Toyohira, Y. & Yoshida, Y. Stimulation of IFN- γ production by garlic lectin in mouse spleen cells: Involvement of IL-12 via activation of p38 MAPK and ERK in macrophages. *Phytomedicine* **18**, 309–316 (2011).

112. Berginc, K., Milisav, I. & Kristl, A. Garlic flavonoids and organosulfur compounds: impact on the hepatic pharmacokinetics of saquinavir and darunavir. *Drug Metab. Pharmacokinet.* **25**, 521–530 (2010).
113. Amagase, H. Clarifying the Real Bioactive Constituents of Garlic. *J. Nutr.* 716–725 (2006).
114. Stoll, A. & Seebeck, E. Chemical investigations on alliin, the specific principle of garlic. *Adv. Enzymol. Relat. Subj. Biochem.* **11**, 377–400 (1951).
115. Borlinghaus, J., Albrecht, F., Gruhlke, M. C. H., Nwachukwu, I. D. & Slusarenko, A. J. Allicin: Chemistry and Biological Properties. *Molecules* **19**, 12591–12618 (2014).
116. Block, E., Ahmad, S., Catalfamo, J. L., Jain, M. K. & Apitz-Castro, R. Antithrombotic organosulfur compounds from garlic: structural, mechanistic, and synthetic studies. *J. Am. Chem. Soc.* **108**, 7045–7055 (1986).
117. Schäfer, G. & Kaschula, C. H. The Immunomodulation and Anti-Inflammatory Effects of Garlic Organosulfur Compounds in Cancer Chemoprevention. *Anticancer. Agents Med. Chem.* **14**, 233–240 (2014).
118. Block, E. Fifty years of smelling sulfur. *J. Sulfur Chem.* **34**, 158–207 (2013).
119. Taucher, J., Hansel, A., Jordan, A. & Lindinger, W. Analysis of Compounds in Human Breath after Ingestion of Garlic Using Proton-Transfer-Reaction Mass Spectrometry. *J. Agric. Food Chem.* **44**, 3778–3782 (1996).
120. Rosen, R. T. *et al.* Determination of Allicin, S-Allylcysteine and Volatile Metabolites of Garlic in Breath, Plasma or Simulated Gastric Fluids. *J. Nutr.* **131**, 968–971 (2001).
121. Biswas, S., Chida, A. S. & Rahman, I. Redox modifications of protein-thiols: emerging roles in cell signaling. *Biochem. Pharmacol.* **71**, 551–564 (2006).
122. Miron, T., Rabinkov, A., Mirelman, D., Wilchek, M. & Weiner, L. The mode of action of allicin: Its ready permeability through phospholipid membranes may contribute to its biological activity. *Biochim. Biophys. Acta* **1463**, 20–30 (2000).
123. Xiao, D. *et al.* Diallyl Trisulfide Selectively Causes Bax and Bak Mediated Apoptosis in Human Lung Cancer Cells. *Environ. Mol. Mutagen.* **50**, 201–212 (2009).
124. Shankar, S., Chen, Q., Ganapathy, S., Singh, K. P. & Srivastava, R. K. Diallyl trisulfide increases the effectiveness of TRAIL and inhibits prostate cancer growth in an orthotopic model: molecular mechanisms. *Mol. Cancer Ther.* **7**, 2328–2338 (2008).
125. Oommen, S., Anto, R. J., Srinivas, G. & Karunakaran, D. Allicin (from garlic) induces caspase-mediated apoptosis in cancer cells. *Eur. J. Pharmacol.* **485**, 97–103 (2004).
126. Park, S. J., Lee, S. C., Hong, S. H. & Kim, H. M. Degradation of IkappaBalpha in activated RAW264.7 cells is blocked by the phosphatidylinositol 3-kinase inhibitor LY294002. *Cell Biol. Toxicol.* **18**, 121–130 (2002).

127. Hosono, T. *et al.* Diallyl trisulfide suppresses the proliferation and induces apoptosis of human colon cancer cells through oxidative modification of beta-tubulin. *J. Biol. Chem.* **280**, 41487–41493 (2005).
128. Yang, C. S., Chhabra, S. K., Hong, J.-Y. & Smith, T. J. Mechanisms of Inhibition of Chemical Toxicity and Carcinogenesis by Diallyl Sulfide (DAS) and Related Compounds from Garlic. *J. Nutr.* **131**, 1041–1045 (2001).
129. Yu, F. L., Bender, W., Fang, Q., Ludeke, A. & Welch, B. Prevention of chemical carcinogen DNA binding and inhibition of nuclear RNA polymerase activity by organosulfur compounds as the possible mechanisms for their anticancer initiation and proliferation effects. *Cancer Detect. Prev.* **27**, 370–379 (2003).
130. Dirsch, V. M., Keiss, H.-P. & Vollmar, A. M. Garlic metabolites fail to inhibit the activation of the transcription factor NF-kappaB and subsequent expression of the adhesion molecule E-selectin in human endothelial cells. *Eur. J. Nutr.* **43**, 55–59 (2004).
131. Tsai, C., Chen, H., Sheen, L. & Lii, C. Garlic: Health benefits and actions. *BioMedicine* **2**, 17–29 (2012).
132. Kang, N. S., Moon, E. Y., Cho, C. G. & Pyo, S. Immunomodulating effect of garlic component , allicin , on murine peritoneal macrophages. *Nutr. Res.* **21**, 617–226 (2001).
133. Powolny, A. A. & Singh, S. V. Multitargeted prevention and therapy of cancer by diallyl trisulfide and related Allium vegetable-derived organosulfur compounds. *Cancer Lett.* **269**, 305–314 (2008).
134. Trio, P. Z. *et al.* Chemopreventive functions and molecular mechanisms of garlic organosulfur compounds. *Food Funct.* **5**, 833–844 (2014).
135. Salman, H., Bergman, M., Bessler, H., Punskey, I. & Djaldetti, M. Effect of a garlic derivative (alliin) on peripheral blood cell immune responses. *Int. J. Immunopharmacol.* **21**, 589–597 (1999).
136. Ghazanfari, T., Hassan, Z. M., Ebtekar, M. & Ahmadiani, A. Garlic Induces a Shift in Cytokine Pattern in Leishmania major- Infected BALB/c Mice. *Scand. J. Immunol.* **52**, 491–495 (2000).
137. Lang, A. *et al.* Allicin inhibits spontaneous and TNF- α induced secretion of proinflammatory cytokines and chemokines from intestinal epithelial cells. *Clin. Nutr.* **23**, 1199–1208 (2004).
138. Quintero-Fabián, S., Ortuño-Sahagún, D., Vázquez-Carrera, M. & López-Roa, R. I. Alliin, a garlic (*Allium sativum*) compound, prevents LPS-induced inflammation in 3T3-L1 adipocytes. *Mediators Inflamm.* **2013**, ID381815 (2013).
139. You, S. *et al.* Inhibitory effects and molecular mechanisms of garlic organosulfur compounds on the production of inflammatory mediators. *Mol. Nutr. Food Res.* **57**, 2049–2060 (2013).
140. Chang, H.-P., Huang, S.-Y. & Chen, Y.-H. Modulation of Cytokine Secretion by Garlic Oil Derivatives Is Associated with Suppressed Nitric Oxide Production in Stimulated Macrophages. *J. Agric. Food Chem.* **53**, 2530–2534 (2005).

141. Bauer, D. *et al.* Diallyl Disulfide Inhibits TNF α -induced CCL2 Release by MDA-MB-231 Cells. *Anticancer Res.* **34**, 2763–2770 (2014).
142. Ho, C.-Y. *et al.* Diallyl sulfide as a potential dietary agent to reduce TNF- α - and histamine-induced proinflammatory responses in A7r5 cells. *Mol. Nutr. Food Res.* **58**, 1069–1078 (2014).
143. Lee, D. Y. *et al.* Anti-inflammatory activity of sulfur-containing compounds from garlic. *J. Med. Food* **15**, 992–999 (2012).
144. Alma, E., Eken, A., Ercil, H. & Daglioglu, N. The Effect of Garlic Powder on Human Urinary Cytokine Excretion. *Urol. J.* **11**, 1308–1315 (2014).
145. Zare, A. *et al.* Purified Aged Garlic Extract Modulates Allergic Airway Inflammation in Balb/c Mice. *Iran. J. Allergy, Asthma Immunol.* **7**, 133–141 (2008).
146. Dirsch, V. M., Kiemer, A. K., Wagner, H. & Vollmar, A. M. Effect of allicin and ajoene, two compounds of garlic, on inducible nitric oxide synthase. *Atherosclerosis* **139**, 333–339 (1998).
147. Dirsch, V. M. & Vollmar, A. M. Ajoene, a natural product with non-steroidal anti-inflammatory drug (NSAID)-like properties ? *Biochem. Pharmacol.* **61**, 587–593 (2001).
148. Chang, H.-P. & Chen, Y.-H. Differential effects of organosulfur compounds from garlic oil on nitric oxide and prostaglandin E2 in stimulated macrophages. *Nutrition* **21**, 530–536 (2005).
149. Lee, I.-C. *et al.* Effect of diallyl disulfide on acute gastric mucosal damage induced by alcohol in rats. *Hum. Exp. Toxicol.* 1–13 (2014). doi:10.1177/0960327114537095
150. Chandra-Kuntal, K. & Singh, S. V. Diallyl trisulfide inhibits activation of signal transducer and activator of transcription 3 in prostate cancer cells in culture and in vivo. *Cancer Prev. Res.* **3**, 1473–1483 (2010).
151. Dalle-Donne, I., Rossi, R., Giustarini, D., Colombo, R. & Milzani, A. S-glutathionylation in protein redox regulation. *Free Radic. Biol. Med.* **43**, 883–898 (2007).
152. Klatt, P. & Lamas, S. Regulation of protein function by S-glutathiolation in response to oxidative and nitrosative stress. *Eur. J. Biochem.* **267**, 4928–4944 (2000).
153. Sun, M. *et al.* RedoxDB--a curated database for experimentally verified protein oxidative modification. *Bioinformatics* **28**, 2551–2552 (2012).
154. Pan, S. & Berk, B. C. Glutathiolation Regulates Tumor Necrosis Factor- α -Induced Caspase-3 Cleavage and Apoptosis: Key Role for Glutaredoxin in the Death Pathway. *Circ. Res.* **100**, 213–219 (2007).
155. Anathy, V. *et al.* Redox amplification of apoptosis by caspase-dependent cleavage of glutaredoxin 1 and S-glutathionylation of Fas. *J. Cell Biol.* **184**, 241–252 (2009).
156. Landino, L. M., Moynihan, K. L., Todd, J. V & Kennett, K. L. Modulation of the redox state of tubulin by the glutathione/glutaredoxin reductase system. *Biochem. Biophys. Res. Commun.* **314**, 555–560 (2004).

157. Wang, J. *et al.* Reversible Glutathionylation Regulates Actin Polymerization in A431 Cells. *J. Biol. Chem.* **276**, 47763–47766 (2001).
158. Pineda-Molina, E. *et al.* Glutathionylation of the p50 Subunit of NF- κ B: a Mechanism for Redox-Induced Inhibition of DNA Binding. *Biochemistry* **40**, 14134–14142 (2001).
159. Qanungo, S., Starke, D. W., Pai, H. V, Mieyal, J. J. & Nieminen, A.-L. Glutathione supplementation potentiates hypoxic apoptosis by S-glutathionylation of p65-NF κ B. *J. Biol. Chem.* **282**, 18427–18436 (2007).
160. Reynaert, N. L. *et al.* Dynamic redox control of NF- κ B through glutaredoxin-regulated S-glutathionylation of inhibitory κ B kinase β . *Proc. Natl. Acad. Sci. U. S. A.* **103**, 13086–13091 (2006).
161. Xie, Y., Kole, S., Precht, P., Pazin, M. J. & Bernier, M. S-glutathionylation impairs signal transducer and activator of transcription 3 activation and signaling. *Endocrinology* **150**, 1122–1131 (2009).
162. Pastore, A. & Piemonte, F. S-Glutathionylation signaling in cell biology: progress and prospects. *Eur. J. Pharm. Sci.* **46**, 279–292 (2012).
163. Pinto, J. T., Krasnikov, B. F. & Cooper, A. J. L. Redox-Sensitive Proteins Are Potential Targets of Garlic-Derived Mercaptocysteine Derivatives. *J. Nutr.* **136**, 835–841 (2006).
164. Rabinkov, A. *et al.* The mode of action of allicin: Trapping of radicals and interaction with thiol containing proteins. *Biochim. Biophys. Acta* **1379**, 233–244 (1998).
165. Gallwitz, H. *et al.* Ajoene is an inhibitor and subversive substrate of human glutathione reductase and Trypanosoma cruzi trypanothione reductase: Crystallographic, kinetic, and spectroscopic studies. *J. Med. Chem.* **42**, 364–372 (1999).
166. White, J. *et al.* Guidelines for Human Gene Nomenclature. *Genomics* **45**, 464–468 (1997).
167. Blake, J., Bult, C., Eppig, J., Kadin, J. & Richardson, J. The Mouse Genome Database: integration of and access to knowledge about the laboratory mouse. *Nucleic Acids Res.* **42**, D810–D817 (2014).
168. Bustin, S. a *et al.* The MIQE guidelines: minimum information for publication of quantitative real-time PCR experiments. *Clin. Chem.* **55**, 611–622 (2009).
169. Untergasser, A. *et al.* Primer3Plus, an enhanced web interface to Primer3. *Nucleic Acids Res.* **35**, W71–W74 (2007).
170. Lefever, S., Vandesompele, J., Speleman, F. & Pattyn, F. RTPrimerDB: the portal for real-time PCR primers and probes. *Nucleic Acids Res.* **37**, D942–D945 (2009).
171. Pfaffl, M. W. A new mathematical model for relative quantification in real-time RT – PCR. *Nucleic Acids Res.* **29**, 16–21 (2001).

172. Hellemans, J., Mortier, G., De Paepe, A., Speleman, F. & Vandesompele, J. qBase relative quantification framework and software for management and automated analysis of real-time quantitative PCR data. *Genome Biol.* **8**, (2007).
173. Vandesompele, J. *et al.* Accurate normalization of real-time quantitative RT-PCR data by geometric averaging of multiple internal control genes. *Genome Biol.* **3**, research0034.1–0034.11 (2002).
174. Weinberg, Sharon Lawner, N. Y. U. & Abramowitz, Sarah Knapp, D. U. in *Statistics with SPSS, An Integrative Approach* 321–322 (2008).
175. Nomura, F. *et al.* Cutting edge: endotoxin tolerance in mouse peritoneal macrophages correlates with down-regulation of surface toll-like receptor 4 expression. *J. Immunol.* **164**, 3476–3479 (2000).
176. Kumar, H., Kawai, T. & Akira, S. Pathogen recognition by the innate immune system. *Int. Rev. Immunol.* **30**, 16–34 (2011).
177. Mukherjee, S. *et al.* LPS-driven Th2 cytokine production in macrophages is regulated by both MyD88 and TRAM. *J. Biol. Chem.* **284**, 29391–8 (2009).
178. Sharif, O., Bolshakov, V. N., Raines, S., Newham, P. & Perkins, N. D. Transcriptional profiling of the LPS induced NF- κ B response in macrophages. *BMC Immunol.* **8**, (2007).
179. Liu, D. & Yang, P. S. Minocycline hydrochloride nanoliposomes inhibit the production of TNF- α in LPS-stimulated macrophages. *Int. J. Nanomedicine* **7**, 4769–4775 (2012).
180. Li, S. *et al.* IL-21 modulates release of proinflammatory cytokines in LPS-stimulated macrophages through distinct signaling pathways. *Mediators Inflamm.* **2013**, 548073 (2013).
181. Zhong, W. *et al.* Regulation of Cytokine mRNA Expression in Lipopolysaccharide-Stimulated Human Macrophages. *Arch. Surg.* **128**, 158–164 (1993).
182. Szekanecz, Z. *et al.* Temporal expression of inflammatory cytokines and chemokines in rat adjuvant-induced arthritis. *Arthritis Rheum.* **43**, 1266–1277 (2000).
183. Lopes, M. *et al.* Temporal profiling of cytokine-induced genes in pancreatic β -cells by meta-analysis and network inference. *Genomics* **103**, 264–275 (2014).
184. Lopez-Castejon, G. & Brough, D. Understanding the mechanism of IL-1B secretion. *Cytokine Growth Factor Rev.* **22**, 189–195 (2011).
185. Münchberg, U., Anwar, A., Mecklenburg, S. & Jacob, C. Polysulfides as biologically active ingredients of garlic. *Org. Biomol. Chem.* **5**, 1505–1518 (2007).
186. Happel, K. I. *et al.* Divergent roles of IL-23 and IL-12 in host defense against *Klebsiella pneumoniae*. *J. Exp. Med.* **202**, 761–769 (2005).
187. Hatzimanikatis, V., Choe, L. H. & Lee, K. H. Proteomics: Theoretical and experimental considerations. *Biotechnol. Prog.* **15**, 312–318 (1999).

188. Buettner, R. *et al.* Alkylation of cysteine 468 in Stat3 defines a novel site for therapeutic development. *Am. Chem. Soc. Chem. Biol.* **6**, 432–443 (2012).
189. Lin, W. & Karin, M. A cytokine-mediated link between innate immunity , inflammation, and cancer. *J. Clin. Invest.* **117**, 1175–1183 (2007).
190. Vasto, S. *et al.* Inflammation, ageing and cancer. *Mech. Ageing Dev.* **130**, 40–45 (2009).
191. Schultz, G. S., Davidson, J. M., Kirsner, R. S., Bornstein, P. & Herman, I. M. Dynamic reciprocity in the wound microenvironment. *Wound Repair Regen.* **19**, 134–148 (2011).
192. Balkwill, F. & Mantovani, A. Inflammation and cancer: back to Virchow? *Lancet* **357**, 539–545 (2001).
193. Mantovani, A., Allavena, P., Sica, A. & Balkwill, F. Cancer-related inflammation. *Nature* **454**, 436–444 (2008).
194. Santhosha, S. G., Jamuna, P. & Prabhavathi, S. N. Bioactive components of garlic and their physiological role in health maintenance: A review. *Food Biosci.* **3**, 59–74 (2013).
195. Xiang, Q. *et al.* Endotoxin tolerance of RAW264.7 correlates with p38-dependent up-regulation of scavenger receptor-A. *J. Int. Med. Res.* **37**, 491–502 (2009).
196. Aggarwal, B. B., Shishodia, S., Sandur, S. K., Pandey, M. K. & Sethi, G. Inflammation and cancer: How hot is the link? *Biochem. Pharmacol.* **72**, 1605–1621 (2006).
197. Croft, M., Benedict, C. a & Ware, C. F. Clinical targeting of the TNF and TNFR superfamilies. *Nat. Rev. Drug Discov.* **12**, 147–168 (2013).
198. Croft, M. *et al.* TNF superfamily in inflammatory disease: translating basic insights. *Trends Immunol.* **33**, 144–152 (2012).
199. Locksley, R. M., Killeen, N. & Lenardo, M. J. The TNF and TNF receptor superfamilies: Integrating mammalian biology. *Cell* **104**, 487–501 (2001).
200. Shinnoh, M. *et al.* Clostridium butyricum MIYAIRI 588 shows antitumor effects by enhancing the release of TRAIL from neutrophils through MMP-8. *Int. J. Oncol.* **42**, 903–911 (2013).
201. Cheng, F. *et al.* A critical role for Stat3 signaling in immune tolerance. *Immunity* **19**, 425–436 (2003).
202. Heidelberger, S. *et al.* Investigation of the protein alkylation sites of the STAT3:STAT3 inhibitor Stattic by mass spectrometry. *Bioorganic Med. Chem. Lett.* **23**, 4719–22 (2013).
203. Sobotta, M. C. *et al.* Peroxiredoxin-2 and STAT3 form a redox relay for H₂O₂ signaling. *Nature. Chem. Biol.* **11**, 64–71 (2015).
204. Pietra, L. D., Bressan, A., Pezzotti, A. R. & Serlupi-Crescenzi, O. Highly conserved amino-acid sequence between murine STAT3 and a revised human STAT3 sequence. *Gene* **213**, 119–124 (1998).

205. Schust, J., Sperl, B., Hollis, A., Mayer, T. U. & Berg, T. Stattic: A Small-Molecule Inhibitor of STAT3 Activation and Dimerization. *Chem. Biol.* **13**, 1235–1242 (2006).
206. Song, H., Wang, R., Wang, S. & Lin, J. A low-molecular-weight compound discovered through virtual database screening inhibits Stat3 function in breast cancer cells. *Proc. Natl. Acad. Sci. U. S. A.* **102**, 4700–4705 (2005).
207. Chen, Y.-J., Lu, C.-T., Lee, T.-Y. & Chen, Y.-J. dbGSH: a database of S-glutathionylation. *Bioinformatics* **30**, 2386–2388 (2014).
208. Li, M. *et al.* Antitumor activity of Z-ajoene, a natural compound purified from garlic : antimitotic and microtubule-interaction properties. *Carcinogenesis* **23**, 573–579 (2002).
209. Park, S.-Y. *et al.* Caspase-independent cell death by allicin in human epithelial carcinoma cells: involvement of PKA. *Cancer Lett.* **224**, 123–132 (2005).
210. Ide, N. & Lau, B. H. S. Garlic Compounds Minimize Intracellular Oxidative Stress and Inhibit Nuclear Factor- κ B Activation. *J. Nutr.* **131**, 1020–1026 (2001).
211. Fukao, T., Hosono, T., Misawa, S., Seki, T. & Ariga, T. Chemoprotective effect of diallyl trisulfide from garlic against carbon tetrachloride-induced acute liver injury of rats. *BioFactors* **21**, 171–174 (2004).
212. Badr, G. M. & Al-Mulhim, J. A. The protective effect of aged garlic extract on nonsteroidal anti-inflammatory drug-induced gastric inflammations in male albino rats. *Evidence-Based Complement. Altern. Med.* **2014**, 1–9 (2014).
213. Le Bon, A. M. *et al.* Effects of Garlic Powders with Varying Alliin Contents on Hepatic Drug Metabolizing Enzymes in Rats. *J. Agric. Food Chem.* **51**, 7617–7623 (2003).
214. Park, K.-A., Kweon, S. & Choi, H. Anticarcinogenic effect and modification of cytochrome P450 2E1 by dietary garlic powder in diethylnitrosamine-initiated rat hepatocarcinogenesis. *J. Biochem. Mol. Biol.* **35**, 615–622 (2002).